On the Application of Bandlimitation and Sampling Theory to Quantum Field Theory

by

Jason Pye

A thesis
presented to the University of Waterloo
in fulfillment of the
thesis requirement for the degree of
Doctor of Philosophy
in
Applied Mathematics (Quantum Information)

Waterloo, Ontario, Canada, 2020

Examining Committee Membership

The following served on the Examining Committee for this thesis. The decision of the Examining Committee is by majority vote.

External Examiner:	Dr. Stefano Liberati Professor Department of Physics Scuola Internazionale Superiore di Studi Avanzati (SISSA)
Supervisor:	Dr. Achim Kempf Professor Department of Applied Mathematics University of Waterloo
Internal Members:	Dr. Eduardo Martin-Martinez Associate Professor Department of Applied Mathematics University of Waterloo
	Dr. Florian Girelli Associate Professor Department of Applied Mathematics University of Waterloo
Internal-External Member:	Dr. Robert Mann Professor Department of Physics and Astronomy University of Waterloo

Author's Declaration

This thesis consists of material all of which I authored or co-authored: see Statement of Contributions included in the thesis. This is a true copy of the thesis, including any required final revisions, as accepted by my examiners.

I understand that my thesis may be made electronically available to the public.

Statement of Contributions

Chapters 1-4 of this thesis mainly consist of background material, apart from certain insights based on papers that I co-authored. The work included here that is based on these papers has been entirely rewritten by me. The specific sections including this work are as follows. Sections 3.1 and 5.1 contain content based on my Master's work published in a paper [102] (co-authored by Dr. William Donnelly and Prof. Achim Kempf) as well as my Master's thesis [100], although this content is not considered to be original results of the present thesis. Figures in this thesis which are adapted from these publications include citations in their captions. Section 3.1 also contains work based on the paper [96], which I co-authored with a fellow graduate student, Maria Papageorgiou. Both authors contributed equally to the research and writing of this publication.

The original results of this thesis are presented in Section 5.2 and Chapters 6-9. Chapters 7 and 8 contain an expanded version of material from a single-authored paper written by me [101]. Section 5.2 and Chapters 6 and 9 consist of unpublished work done solely by me and originally presented in this thesis.

Abstract

It is widely believed that combining the uncertainty principle with gravity will lead to an effective minimum length scale. A particular challenge is to specify this scale in a coordinate-independent manner so that covariance is not broken. Here we will consider bandlimitation and sampling theory as a means to model Planck-scale modifications to spacetime within quantum field theory. Two different cases will be considered.

The first is the case of Euclidean-bandlimitation, which imposes a notion of minimal length while preserving Euclidean symmetries. This leads to a sampling theory where one can represent fields as equivalently living on either continuous space or on lattices. We will discuss how this leads to a regulation of the information density in quantum fields. We then proceed to quantify notions of localization and density of degrees of freedom within these fields.

We then turn to the case of Lorentzian-bandlimitation. Quantum fields bandlimited in this way have reconstruction properties which are qualitatively different than the Euclidean case. Nevertheless, here we will examine what impacts this has on the structure of quantum field theory with such a bandlimit imposed. In particular, we will investigate which quantities are and are not regulated by the Lorentzian bandlimit in both free and interacting field theories.

Acknowledgements

I would first like to thank my supervisor Prof. Achim Kempf for the endless generosity and support he has provided throughout my years as a graduate student. I would also like to thank Prof. Eduardo Martin-Martinez for his mentorship and support.

I am indebted to all of the following people for the countless invaluable interactions we have had during my time as a Ph.D. student: Aida Ahmadzadegan, Michael Broughton, Yangang Chen, Ding Jia, Robert Jonsson, Henry Ho, David Layden, Marco Letizia, Mikhail Panine, Maria Papageorgiou, Atmn Patel, Jose de Ramon, Nitica Sakharwade, Turner Silverthorne, Barbara Soda, Nadine Stritzelberger, Paul Tiede, and Guillaume Verdon.

I would also be remiss if I did not thank Dorion de Gobeo, Jennifer Fernick, Nolan Finkelstein, Afsheen Ghorashy, Angela Kim, Louie Mansour, and Paul van der Vecht for their continuing support and friendship.

I also must thank my family for their neverending encouragement. Perhaps most importantly, I thank my partner Katelyn Battista (and Charlie, of course) for her support of me during the writing of this thesis while being quarantined together in the midst of a global pandemic.

Finally, I thank the University of Waterloo, the Ontario Ministry of Training, Colleges and Universities (MTCU), as well as the Natural Sciences and Engineering Research Council (NSERC) of Canada for financial support during the course of this work.

Table of Contents

List of Figures

Chapter 1

Introduction

The idea that there may be a limit to our classical notions regarding the continuity of spacetime goes back to [25]. Therein, it was suggested that there should be a fundamental limit to the precision of gravitational field measurements. Ensuing thought experiments have indicated that in the presence of gravity, there should generally be a limitation to measurements of distance, in the form of a lower bound on the uncertainty, given by the Planck length [41, 54, 89]:

$$\Delta X \geq \ell_P := \sqrt{\frac{\hbar G}{c^3}} \sim 10^{-35}\text{m}. \tag{1.1}$$

Indeed, this concept is a feature of many approaches to quantum gravity [41, 54, 128].

Intuitively, the presence of a minimum length suggests that spacetime may be fundamentally discrete, rather than continuous. The simplest picture of a discrete space is analogous to a crystal lattice, but such a scenario would imply a breakdown of continuous spacetime symmetries. For example, any length scale introduced into a model would be subject to contraction under a Lorentz transformation. Therefore, a naive introduction of such a length scale would be observer-dependent. There are more sophisticated approaches where notions of minimum length scales can be introduced without picking out preferred frames [20, 22], or alternatives where one considers deforming spacetime symmetries near the Planck scale [7, 8, 44, 82, 113]. At the present time, there has been no experimental evidence for violations of Lorentz invariance [1, 3, 77, 88].

Apart from experimental signatures, it is interesting to consider the role of such a minimal length on fundamental questions in quantum field theory (QFT). For example, in interacting field theories it is common to introduce regulators that are occasionally loosely

motivated by a Planck-scale cutoff, but one would like a better sense of exactly how this might occur [31, 32].

There is also currently much interest in entanglement in quantum field theory and its role in black hole thermodynamics and the holographic principle [4–6, 12, 21, 48, 62, 97, 114, 115, 117, 121]. There are also ideas about how the structure of spacetime may emerge from quantum entanglement in some sense [18, 26, 52, 60, 61, 125]. However, in these studies one must introduce a cutoff to regulate the entanglement of quantum fields. It would be desirable to obtain a more precise picture of how one could implement such a regulator in a manner that does not conflict with the structure of the underlying spacetime. This is especially important for these considerations since the spacetime structure plays a fundamental role.

Therefore, our motivation for this work is how one can have a notion of minimal length and/or spacetime discreteness without the breaking of continuous symmetries. Furthermore, to what extent would such discreteness act as a regulator for entanglement, interactions, and other quantities of interest in quantum field theory. The particular approach we will be examining in this work is that of bandlimitation and sampling theory.

Our hope is that this will complement other models of Planck-scale modifications of spacetime. Here, the approach is to begin in the well-established territory of ordinary quantum field theory, and modify it in a conservative manner so that it exhibits some of the features one may expect from Planck-scale effects. One could then attempt to match it with low-energy limits of some quantum gravity approaches, or perhaps it may give some insight by connecting it to other low-energy approaches.

The idea of applying bandlimitation to quantum field theory began with considerations of deforming the uncertainty principle of quantum mechanics to qualitatively match expected modifications due to gravity [65, 73]. In particular, one would expect that a large uncertainty in momentum would produce a large uncertainty in the spacetime geometry through the gravitational field equations. This uncertainty in the spacetime geometry would then feed back to produce large uncertainties in distance measurements. Schematically, this would look like Figure 1.1, where we have drawn the boundaries of the allowable region of position and momentum uncertainty (the dashed line being the undeformed Heisenberg uncertainty principle). One can achieve this qualitative behaviour through a modification to the uncertainty principle of the kind:

$$\Delta x \Delta p \geq \tfrac{1}{2}(1 + \ell_P^2 \Delta P^2), \tag{1.2}$$

called a *Generalized Uncertainty Principle* [65, 73]. (Note that hereafter we will be setting $\hbar = c = 1$.) It is simple to show that the above inequality implies a finite lower bound to the position uncertainty, $\Delta x \geq \ell_P$.

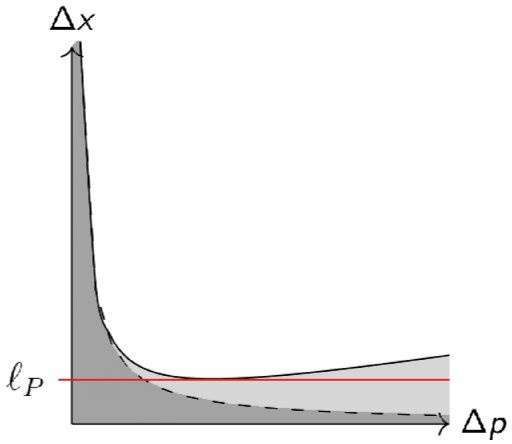

Figure 1.1: Qualitative modification of the allowable region of position and momentum uncertainty due to gravitational effects at the Planck scale. The dashed line corresponds to the boundary of the region according to the ordinary Heisenberg uncertainty principle. The solid black line denotes the boundary according to the Generalized Uncertainty Principle. The red line demonstrates that there is a minimum to the uncertainty in position for the modified region.

It was later noted that this is formally equivalent to simply implementing an ultraviolet cutoff in the usual momentum space [68]. However, such a cutoff does not simply imply a lattice theory. Rather, this connects to a well-studied branch of information theory called *sampling theory*. Sampling theory is a set of tools used throughout communications engineering for representing continuous bandlimited signals *exactly* by a set of values that the function takes at a discrete set of points. The central result in sampling theory is the Shannon sampling formula, which holds for any signal, $\phi(t)$, whose Fourier transform has support in the interval $[-W, W]$:

$$\phi(t) = \sum_n \text{sinc}[W(t - t_n)]\phi(t_n), \tag{1.3}$$

where $\{t_n = n\pi/W\}_{n\in\mathbb{Z}}$ is a discrete set of sample points, and $\text{sinc}(x) := \sin(x)/x$ [93, 110, 111]. Because these functions can be equivalently represented on both the continuum and a lattice, sampling theory blurs the distinction between continuous and discrete space.

One can show that this space of bandlimited functions continues to exhibit translation invariance. Indeed, we have not removed the underlying space simply because these functions can be represented on a lattice. It is simply that by restricting the space of functions one is considering, it is possible to specify one of these functions by a discrete set of infor-

mation. Therefore, sampling theory provides a model for how one can have discreteness without symmetry breaking.

Sampling theory can also be generalized to higher dimensions. There are also natural extensions to Riemannian manifolds [71, 74]. Further, one can also generalize bandlimitation to pseudo-Riemannian manifolds [27, 69, 72].

In this thesis, we are going to examine various aspects of bandlimitation and sampling theory applied to quantum field theory in both the Euclidean- and Lorentzian-signature cases. The outline is as follows.

We will begin in Chapter 2 by reviewing sampling theory. This will include the traditional sampling theory of Shannon, as well as some discussion of the generalization to Riemannian and pseudo-Riemannian manifolds. We will then review how bandlimitation and sampling theory can be introduced to quantum field theory in Chapter 3. Some of this review will consist of previous work done by the author [100, 102], as well as some further insights achieved in some more recent work [96].

Chapters 4-6 will be focused on developing a notion of subsystem localization for Euclidean-bandlimited quantum fields. The aim of this is to quantify exactly how one can think of sampling theory as imposing a limit to the density of degrees of freedom despite the fact that the theory exhibits full translation invariance.

Although the Euclidean case may not be fundamentally intriguing for the purposes of modelling Planck-scale physics, sampling theory is ubiquitous in classical communications engineering, and so one would anticipate that it will also be a crucial tool for quantum communication through quantum fields. For example, this could arise in cavities which only support electromagnetic modes up to a certain wavenumber, or simply in cases where the instruments one is using can only probe frequencies up to some scale. It is then worth exploring Euclidean-bandlimited quantum field theory for these purposes as well. Also, some of our investigation here, although motivated by questions in quantum field theory, is fundamentally only about classically bandlimited fields. Therefore, perhaps some of this study would be insightful for the classical case as well.

For the Lorentzian case, in Chapter 7 we will first examine in detail how one can reconnect the idea of Lorentzian bandlimitation back to a type of Generalized Uncertainty Principle. We will then proceed in Chapters 8 and 9 examine how it affects the structure of quantum field theory. Specifically, Chapter 8 will examine free fields and Chapter 9 will examine interacting theories.

Of course, ultimately one would also like to look for manifestations of Lorentzian bandlimitation in experiments. Some work that has been done towards this is determining how

Lorentzian bandlimitation in cosmological spacetime may be imprinted in the fluctuations of the cosmic microwave background (CMB) [27, 72]. Here our aim is to further develop theory for Lorentzian-bandlimited quantum fields in order to eventually pursue other ideas for how they could be probed.

Chapters 7 and 8 are based on a publication [101] by the author. New contributions of this thesis consist of the contents of Chapters 5-9, except for some interspersed background material which is clearly indicated.

Chapter 2

Background on sampling theory

The aim of sampling theory is to find discrete representations of continuous signals. For the purposes of quantum field theory, we are interested in finding discrete space or spacetime representations which also preserve the underlying symmetries of the manifold. In this chapter, we will review the basics of sampling theory, beginning with the traditional cases for the circle and the line, and then extensions to arbitrary Riemannian and pseudo-Riemannian manifolds.

2.1 Prelude: sampling on a circle

Consider a circle S^1 of length L, with coordinates $x \in [0, L)$. On the circle, we have a plane wave basis for the space of square-integrable functions: $\frac{1}{\sqrt{L}} e^{ik_m x}$ with $k_m \equiv \frac{2\pi m}{L}$, $m \in \mathbb{Z}$. Now let us consider the subspace of functions that only have nonzero Fourier coefficients in the range $m \in [-M, M]$ (i.e., an ultraviolet cutoff $|k_m| \leq k_M$). These so-called *bandlimited* functions are of the form

$$\phi(x) = \frac{1}{\sqrt{L}} \sum_{m=-M}^{M} \phi_m e^{ik_m x}. \tag{2.1}$$

This is a finite dimensional function space. Since there are $2M+1$ degrees of freedom, is a function in this subspace fixed by its values at $2M+1$ positions? Suppose we fix $2M+1$ "sample points" $\{x_n\}_{n=1}^{2M+1}$. Now let us evaluate an arbitrary function in the bandlimited subspace at these sample points,

$$\phi(x_n) = \frac{1}{\sqrt{L}} \sum_{m=-M}^{M} \phi_m e^{ik_m x_n}. \tag{2.2}$$

This is stating that the $2M+1$ Fourier coefficients are mapped to the $2M+1$ sample points by the square matrix $\frac{1}{\sqrt{L}}e^{ik_m x_n}$.

Generically, this matrix will be invertible [67], which allows us to express the Fourier coefficients in terms of the sample values. We can then insert this expression for the Fourier coefficients back into the original Fourier series (2.1) to write $\phi(x)$ (i.e., the value of the bandlimited function at an arbitrary x) in terms of the values at the $2M+1$ sample points x_n. For example, suppose we choose the sample points equidistantly at $x_n = \frac{n-1}{2M+1}L$. It is simple to show that the inverse of (2.2) in this case is

$$\phi_m = \frac{\sqrt{L}}{2M+1}\sum_{n=1}^{2M+1}\phi(x_n)e^{-ik_m x_n}. \tag{2.3}$$

Then inserting these into (2.1),

$$\begin{aligned}\phi(x) &= \frac{1}{\sqrt{L}}\sum_{m=-M}^{M}\left(\frac{\sqrt{L}}{2M+1}\sum_{n=1}^{2M+1}\phi(x_n)e^{-ik_m x_n}\right)e^{ik_m x} \\ &= \sum_{n=1}^{2M+1}K(x,x_n)\phi(x_n),\end{aligned}$$

where K is the Dirichlet kernel

$$\begin{aligned}K(x,x_n) &:= \frac{1}{2M+1}\sum_{m=-M}^{M}e^{ik_m(x-x_n)} \\ &= \frac{\sin[(2M+1)(x-x_n)\frac{\pi}{L}]}{(2M+1)\sin[(x-x_n)\frac{\pi}{L}]}\end{aligned}$$

Hence, we see that the value of a bandlimited function at the sample points $x_n = \frac{n-1}{2M+1}L$ fixes the value of the function everywhere on the circle.

This form of K is dependent on the fact that we chose the sampling lattice $x_n = \frac{n-1}{2M+1}L$. But one can see that as long as we choose the samples points so that (2.2) is invertible, one will arrive at an analogous sampling kernel K. One does not have to choose x_n equidistantly spaced either, can actually choose a generic set of points, as long as there are enough. Note that the invertibility of (2.2) and form of K depends only on the choice of sample points x_n, and not on the particular function we want to reconstruct.

Note also that one needs the same number of samples as the number of Fourier modes. If we examine a subspace of functions with a larger bandlimit, we will require more sample points.

We have imposed an ultraviolet cutoff, which is a restriction to a bandlimited subspace of $L^2(S^1)$. Although these functions can be represented by their values on a sampling lattice, we have not eliminated the underlying continuous manifold nor the associated continuous translation covariance. Thus, we have discreteness without symmetry breaking, which is only possible since none of the lattices are preferred.

Shannon sampling theory is essentially a demonstration that this also occurs for bandlimited functions on $\mathbb{R}$.

2.2 Shannon's sampling theorem

Define bandlimited functions on $\mathbb{R}$, with bandlimit Λ, as a subspace of $L^2(\mathbb{R})$ where the support of the Fourier transform of these functions lies within the interval $[-\Lambda, \Lambda]$:

$$\phi(x) = \int_{-\Lambda}^{\Lambda} \frac{dk}{2\pi} \tilde{\phi}(k) e^{ikx}. \tag{2.4}$$

We are looking for a reconstruction from samples of the form

$$\phi(x) = \sum_n K(x, x_n)\phi(x_n), \tag{2.5}$$

for some discrete set of sample points $\{x_n\}_n \subset \mathbb{R}$ and some reconstruction kernel K.

There is a potential point of confusion as to what we mean by $\phi(x_n)$, which also occurs in the S^1 case. Recall that the elements of $L^2(\mathbb{R})$ are equivalence classes of (square integrable) functions, which only differ on sets of measure zero. However, a discrete set of points $\{x_n\}$ will have zero measure. If we were to change the values of ϕ on this set, it would still be considered the same function in $L^2(\mathbb{R})$, yet the reconstruction would yield a function in a completely different equivalence class. So let us be a bit more precise about what we mean by such a reconstruction formula.

A simple way to do this is to first recognize that bandlimited functions are entire (analytic everywhere), which for $\phi \in L^2(\mathbb{R})$ means that ϕ is equal to an entire function almost everywhere (i.e., differ only on a set of measure zero) [104]. Therefore, each equivalence class of bandlimited functions in $L^2(\mathbb{R})$ contains a representative that is entire, so by a sample $\phi(x_n)$, we mean the value of the entire function in the equivalence class containing ϕ at the point x_n. Also note that convergence of the above series will be in the sense of the $L^2(\mathbb{R})$ norm.

In the S^1 case, the insight that led us to the sampling formula was that, since the bandlimited function space was finite dimensional, we should be able to specify a function from specifying finitely many sample values. In the case of $\mathbb{R}$, it is less clear that this can be done, since the bandlimited function space is still an infinite dimensional subspace. There are many ways to proceed to show that a sampling theorem still holds. We will demonstrate via a functional analytic approach developed in [68], through a study of the spectrum of a position (i.e., multiplication) operator on $L^2(\mathbb{R})$. The key idea is that we know that we are guaranteed from the spectral theorem for self-adjoint operators that an element in the relevant Hilbert space can be expanded in a complete basis of eigenvectors of that operator. If we can show that a position operator has a discrete basis, then a function can be expanded in terms of sample points on a discrete lattice. But how we can use this to reconstruct the function anywhere in the continuous background space requires some subtle issues in the functional analysis of the position operator.

For $\phi \in L^2(\mathbb{R})$, define a *position operator*, X, by $(X\phi)(x) = x\phi(x)$. Of course, if we take $L^2(\mathbb{R})$ as the Hilbert space in which X acts, then X has a continuous spectrum consisting of all of $\mathbb{R}$. The (approximate) eigenvectors form a basis for this space, in the sense that for any ϕ, we have $|\phi) = \int_{\mathbb{R}} dx |x)(x|\phi)$. It will be useful to start using braket notation, for example $|\phi)$ will be an element of $L^2(\mathbb{R})$ represented by a function $\phi(x) \equiv (x|\phi)$.[1]

If we restrict our attention to the Hilbert space of bandlimited functions, this situation changes. Bandlimited functions in Fourier space lie in the Hilbert space $L^2[-\Lambda, \Lambda]$. Let us denote this Hilbert space abstractly by $B(\Lambda)$. In Fourier space operator X is represented as a derivative operator id/dk. What is the spectrum of X? Notice that this situation is mathematically analogous to the quantum mechanical problem of a particle in an infinite potential well. In that case, the momentum and energy operators exhibit discrete spectra. Here, the roles of position and momenta are flipped, and so we should expect the position operator X to have a discrete spectrum, despite the fact that bandlimited functions were defined to have a continuous spatial representation (2.4). Below we will return to this latter point.

First, note that X will have a spectrum if it is self-adjoint. Is it symmetric? Only after

[1] In the next chapter, we will be discussing the quantum field theory one obtains by choosing the space of classical field configurations to be the Hilbert space of bandlimited functions. This differs from the Hilbert space of quantum states (Fock space) of the quantum field. To avoid confusion, throughout this thesis we will be using angular brackets $|\cdot\rangle$ to denote quantum states, and round brackets $|\cdot)$ to denote elements in the Hilbert space of classical field configurations, or, in other words, a space of "c-number" functions.

imposing boundary conditions:

$$(\phi|X\psi) - (X\phi|\psi) = \int_{-\Lambda}^{\Lambda} \frac{dk}{2\pi} \left(\tilde{\phi}^*(k) i \frac{d\tilde{\psi}(k)}{dk} - (-i) \frac{d\tilde{\phi}^*(k)}{dk} \tilde{\psi}(k) \right)$$
$$= \frac{i}{2\pi} \left(\tilde{\phi}^*(\Lambda)\tilde{\psi}(\Lambda) - \tilde{\phi}^*(-\Lambda)\tilde{\psi}(-\Lambda) \right).$$

We need this expression to vanish in order for X to be symmetric. In the analogous quantum mechanical problem, the physics dictates Dirichlet boundary conditions. Here, imposing $\tilde{\phi}(\pm\Lambda) = 0$ and $\tilde{\psi}(\pm\Lambda) = 0$ would suffice to make X symmetric. However it will not be self-adjoint, which is required for the spectral decomposition we are seeking.

To see this, we must analyze more carefully the domain of X, denoted $D(X)$. First, note that we cannot simply take $D(X)$ to be the entire Hilbert space $B(\Lambda)$. That is because X is unbounded, in which case this follows from the Hellinger-Toeplitz theorem. This theorem states that any symmetric linear operator defined on all of a complex Hilbert space is necessarily bounded [78]. We require X to be an operator from $D(X) \subset B(\Lambda)$ to $B(\Lambda)$, i.e., X is restricted to act on functions such that the output is square integrable and bandlimited. Let us also impose Dirichlet boundary conditions in Fourier space so that X is symmetric, and then let us see what occurs. Let

$$D(X) = \{\tilde{\phi} \in L^2[-\Lambda, \Lambda] | (X\tilde{\phi}) = i\tilde{\phi}' \in L^2[-\Lambda, \Lambda], \tilde{\phi}(\pm\Lambda) = 0\}. \tag{2.6}$$

Now recall the definition of the adjoint of X [2, 78],

Definition 1 (Adjoint) *Consider a (densely defined) linear operator X acting on a Hilbert space $\mathcal{H}$. For a given $|\phi) \in \mathcal{H}$, suppose there exists an element $|\chi) \in \mathcal{H}$ such that*

$$(\phi|X\psi) = (\chi|\psi) \tag{2.7}$$

*for all $|\psi) \in \mathcal{H}$. The **adjoint** of X, denoted $X^\dagger$, is defined by the map $X^\dagger|\phi) := |\chi)$.*

Note: if X not densely defined, then $X^\dagger$ is not well-defined. An operator is *self-adjoint* if it is symmetric, i.e., $(\phi|X\psi) = (X\phi|\psi)$ for all $\phi, \psi \in D(X)$, and if $D(X) = D(X^\dagger)$. In the case where we choose functions in $D(X)$ to obey Dirichlet boundary conditions in Fourier space, we see that $X^\dagger$ is not only defined for elements in $D(X)$, but also includes functions with no particular boundary conditions, i.e.,

$$D(X^\dagger) = \{\tilde{\phi} \in L^2[-\Lambda, \Lambda] | (X\tilde{\phi}) = i\tilde{\phi}' \in L^2[-\Lambda, \Lambda]\}. \tag{2.8}$$

The point is that once we choose $D(X)$, the domain $D(X^\dagger)$ is fixed by the definition of $X^\dagger$. Even if X is symmetric, these may not always coincide.

Therefore, we must choose a different set of boundary conditions so that $D(X^\dagger) = D(X)$. One can verify that this can be achieved by choosing $D(X)$ to contain functions that are periodic up to a phase. Let us fix some $\alpha \in [0, 1)$, then let

$$D(X_\alpha) = \{\tilde{\phi} \in L^2[-\Lambda, \Lambda] | (X\tilde{\phi}) = i\tilde{\phi}' \in L^2[-\Lambda, \Lambda], \tilde{\phi}(\Lambda) = e^{-2\pi i\alpha}\tilde{\phi}(-\Lambda)\}. \tag{2.9}$$

There is a story here about self-adjoint extensions of symmetric operators [2], but we will not need to elaborate upon this here.

We then have a one-parameter family of self-adjoint position operators, X_α, each represented formally in Fourier space as $i\frac{d}{dk}$, but have different domains, $D(X_\alpha)$. Formally the eigenfunctions of each X_α are of the form e^{-ikx} in Fourier space, and with the respective boundary conditions we have that X_α has a discrete spectrum:

$$x_n^{(\alpha)} = \frac{\pi}{\Lambda}(n + \alpha), \quad n \in \mathbb{Z} \tag{2.10}$$

and corresponding eigenvectors

$$(k|x_n^{(\alpha)}) = e^{-ikx_n^{(\alpha)}}, \quad \text{with} \quad \frac{\pi}{\Lambda}\sum_{n\in\mathbb{Z}} |x_n^{(\alpha)})(x_n^{(\alpha)}| = 1_{D(X_\alpha)}. \tag{2.11}$$

So we see that if we fix some α, and hence a particular position operator, then we have a discrete position-space representation for the functions in $D(X_\alpha)$. However, we began by considering bandlimited functions to be a subspace of the set of square integrable functions on the full space $\mathbb{R}$ (i.e., (2.4)). Where did this continuous representation go?

Let us return to the set of functions obeying Dirichlet boundary conditions in Fourier space. The key insight is to notice that these are contained in $D(X_\alpha)$ for each choice of α. Therefore, we could choose any of these bases to represent one of these functions. Notice also that the union of the spectra of these operators covers the full line $\mathbb{R}$ exactly once, i.e., for each $x \in \mathbb{R}$ we can find an $n \in \mathbb{Z}$ and $\alpha \in [0, 1)$ such that $x_n^{(\alpha)} = x$. Therefore, in the intersection $\cap_{\alpha\in[0,1)} D(X_\alpha)$, which is in fact equal to the space of Dirichlet functions, we can write

$$\int_{\mathbb{R}} dx\, |x)(x| = \int_0^1 \frac{\pi}{\Lambda} d\alpha \sum_{n\in\mathbb{Z}} |x_n^{(\alpha)})(x_n^{(\alpha)}| = 1_{\cap_{\alpha\in[0,1)} D(X_\alpha)}, \tag{2.12}$$

where the π/Λ factor in front of α is due to the fact that α appears in $x_n^{(\alpha)}$ as $\frac{\pi}{\Lambda}(n+\alpha)$ (see also the next section, where this resolution of identity is built in a more abstract manner).

This allows us to make sense of representing a bandlimited function in the continuum as $\phi(x) = (x|\phi)$ for $x \in \mathbb{R}$, since $|x)$ will be an eigenvector of one of the position operators X_α. Note, however, the $|x)$'s are not orthogonal:

$$(x|x') = \frac{\Lambda}{\pi}\,\mathrm{sinc}[\Lambda(x - x')]. \tag{2.13}$$

The set $\{|x)\}_{x\in\mathbb{R}}$ is an overcomplete basis.The crucial observation was that we do not need to fix a choice of α (i.e., choice of lattice), and this democracy of lattices allows us to restore the continuum. This is in distinction from, for example, a crystal lattice where there is a preferred choice of α.

However, we can still choose to represent these functions on one of the lattices $x_n^{(\alpha)}$. Since $|x_n^{(\alpha)})$ is a basis, the function is completely specified by its values at these points. With these tools, we can now establish Shannon's sampling formula [110, 111]:

$$\begin{aligned}\phi(x) = (x|\phi) &= \frac{\pi}{\Lambda}\sum_{n\in\mathbb{Z}}(x|x_n^{(\alpha)})(x_n^{(\alpha)}|\phi)\\ &= \sum_{n\in\mathbb{Z}}\mathrm{sinc}[\Lambda(x - x_n^{(\alpha)})]\phi(x_n^{(\alpha)}).\end{aligned}$$

Similar to the case of S^1, one can also derive analogous reconstruction formulas by picking a discrete set of non-orthogonal $|x)$'s. The only requirement is that the average sample density is greater than the *Nyquist density* Λ/π [93]. The case of equidistantly-spaced lattice points corresponding to an orthogonal basis in the Hilbert space will be referred to as *Nyquist lattices*.

In the general case, for non-uniform sampling on $\mathbb{R}^n$, it is known that it is necessary that the density of sample points required for reconstruction is bounded below by the volume of momentum space (divided by $(2\pi)^n$, where n is the dimension of space) [79] (see also, e.g., [72]).

2.3 Functional analysis of sampling on S^1

Is there a way to think of the sampling theorem for bandlimited functions on S^1 in terms of the spectra of a collection of position operators? We will see this not a natural way to frame the problem in S^1, but examining common elements between the sampling theories for S^1 and $\mathbb{R}$ will indicate a way to think about it that will be useful for generalizations.

Let us frame the discussion for $\mathbb{R}$ from the previous section a little differently. Start with a Hilbert space $\mathcal{H} = L^2(\mathbb{R})$, with position and momentum operators satisfying $[X, K] = i$. Momentum eigenvectors are $(x|k) = e^{ikx}$, with $\int \frac{dk}{2\pi}|k)(k| = 1$. Now consider a bandlimited projector, $P_\Lambda := \int_{-\Lambda}^{\Lambda} \frac{dk}{2\pi}|k)(k|$, which projects elements of $\mathcal{H}$ down to the bandlimited subspace $B(\Lambda) := P_\Lambda \mathcal{H}$. Then we wanted to consider the spectral decomposition of X restricted to this subspace. Since $B(\Lambda)$ is itself a Hilbert space, the Hellinger-Toeplitz theorem implies that the domain of X cannot be all of $B(\Lambda)$. There is a one-parameter family of densely defined domains in $B(\Lambda)$ on which X is self-adjoint. This collection of self-adjoint operators provides a one-parameter family of bases with which one can decompose any function lying in the intersection of the domains (for example, functions obeying Dirichlet boundary conditions in Fourier space). The set of bases can be combined to recover a notion of the continuous functions. The picture is then that each basis can be thought of as corresponding to a particular sampling lattice in the continuum. But now phrasing the problem as the restriction of X to $B(\Lambda) \subset L^2(\mathbb{R})$, we notice that we have two different constructions of continuous position representations. On one hand, the eigenvectors of X in $L^2(\mathbb{R})$ form a basis, and hence for $\phi \in B(\Lambda) \subset L^2(\mathbb{R})$ we can write $\phi(x) = (x|\phi)$ using these eigenvectors. On the other hand, we had $|x) = |x_n^{(\alpha)}) \in D(X_\alpha)$ for some n and α, and identified $\phi(x) = (x|\phi)$. Are these two $|x)$'s the same? Indeed, we can think of the latter as simply the former after being projected onto the bandlimited subspace, i.e., equal to $P_\Lambda|x)$. This can be seen, for example, by equality of their Fourier space representations,

$$(k|P_\Lambda|x) = \begin{cases} e^{ikx}, & \text{for } k \in [-\Lambda, \Lambda] \\ 0, & \text{otherwise.} \end{cases} \tag{2.14}$$

Then we have that $\{P_\Lambda|x_n^{(\alpha)})\}$ forms a basis for $D(X_\alpha)$, where $|x_n^{(\alpha)})$ is identified with an eigenvector of X on $L^2(\mathbb{R})$. The sampling theorem for $\phi \in \cap_{\alpha\in[0,1)} D(X_\alpha) \subset B(\Lambda)$ is then

$$(x|\phi) = \frac{\pi}{\Lambda} \sum_{n\in\mathbb{Z}} (x|P_\Lambda|x_n^{(\alpha)})(x_n^{(\alpha)}|P_\Lambda|\phi) = \sum_{n\in\mathbb{Z}} \text{sinc}[\Lambda(x - x_n^{(\alpha)})]\phi(x_n^{(\alpha)}). \tag{2.15}$$

We see that the important objects are the bandlimited projector P_Λ and the position eigenvectors $|x)$ in the original (non-bandlimited) ambient space $L^2(\mathbb{R})$. The elements $P_\Lambda|x_n^{(\alpha)})$ are eigenvectors of X restricted to the domain $D(X_\alpha)$, which coincide with $P_\Lambda|x)$ for some x (note this is the reverse of how we were thinking about it in the previous section). Examining these family of spectra of the position operator X restricted to the bandlimited subspace $B(\Lambda)$ was useful in order to establish that a discrete subset of the projected position eigenvectors, $P_\Lambda|x)$ (which coincide with the eigenvectors of X for particular values

of x), would suffice to form a basis, i.e., to establish $\frac{\pi}{\Lambda}\sum_{n\in\mathbb{Z}} P_\Lambda|x_n^{(\alpha)})(x_n^{(\alpha)}|P_\Lambda = P_\Lambda$ (at least on a dense subset).

However, by re-examining the case of sampling on S^1, we will see that focusing on the position operator restricted to a subspace may not be the most useful way forward in general. Let us consider an analogous setup. We now have the Hilbert space $\mathcal{H} = L^2(S^1)$, with position and momentum operators satisfying $[X, K] = i$. Let us focus on functions that are continuous on S^1, hence obey periodic boundary conditions for $x \in [0, L)$. The normalized eigenvectors of K are then $(x|k_m) = \frac{1}{\sqrt{L}} e^{ik_m x}$ with $k_m = \frac{2\pi m}{L}$ and $m \in \mathbb{Z}$, and $(k_m|k_{m'}) = \delta_{mm'}$. Resolution of identity is $\int_0^L |x)(x| = \sum_{m\in\mathbb{Z}} |k_m)(k_m| = 1$. Now introduce the bandlimited projector $P_M := \sum_{m=-M}^{M} |k_m)(k_m|$. In analogy with the $\mathbb{R}$ case, let us examine the position operator X restricted to the bandlimited subspace $B(M) := P_M\mathcal{H}$.

The first thing to note is that X does not map $B(M)$ back into itself. In the previous case for $\mathbb{R}$, we had to define X on a dense subset $D(X)$ of $B(\Lambda)$ so that X acting on $D(X)$ remained in $B(\Lambda)$. The case of S^1 is quite different. Can we restrict X to some subspace of $B(M)$ so that it maps back into $B(M)$? It is easy to check that generally this only occurs for the zero vector. Consider the representation of X in momentum space,

$$\begin{aligned} X_{mm'} \equiv (k_m|X|k_{m'}) &= \frac{1}{L}\int_0^L dx\; x\; e^{-\frac{2\pi i}{L}(m-m')x} \\ &= \begin{cases} \frac{L}{2} & \text{if } m = m' \\ \frac{-L}{2\pi i(m-m')} & \text{if } m \neq m'. \end{cases} \end{aligned}$$

Now we would like to find a subspace of $\tilde{\phi}_m \equiv \tilde{\phi}(k_m)$ in $B(M)$ which are mapped back into $B(M)$ by $X_{mm'}$. Suppose we chose a simple example of $M = 1$. It is simple to verify numerically that the block of $X_{mm'}$ with $m = 2, 3, 4$ and $m' = -1, 0, 1$ is invertible, which implies that if we want $(X\phi)_m = 0$ for $m = 2, 3, 4$ (which is outside the bandlimit), then we have to require $\phi \equiv 0$. Hence, in general, the only element of $B(M)$ which X maps back into $B(M)$ is the zero vector.

If we want to force X to map back into $B(M)$, we can of course manually apply projectors and examine the self-adjoint operator $\tilde{X} := P_M X P_M$. Now $\tilde{X}$ will of course have a discrete spectrum, since it is simple a $(2M+1)\times(2M+1)$ matrix, and its eigenvectors will certainly form a basis for $B(M)$. But, if $|\tilde{x})$ is an eigenvector of $\tilde{X}$, can the coefficient $(\tilde{x}|\phi)$ be interpreted as a sample point? Again, one can find simple numerical examples that demonstrate that generally $(k_m|\tilde{x})$ is not proportional to $e^{-ik_m\tilde{x}}$ for any $\tilde{x}$. Hence the transformation between momentum space and the space in which $\tilde{X}$ is diagonal is not a Fourier transform, and so $(\tilde{x}|\phi)$ cannot be interpreted as a sample value of ϕ in the position

representation. (We can also see that $\tilde{X}$ and X do not share eigenvectors since $[\tilde{X}, X] \neq 0$. This can be argued, for example, by recalling that X does not map a bandlimited ϕ into $B(M)$. Therefore, $XP_MXP_M\phi$ is not bandlimited, but $P_MXP_MX\phi$ is, so $XP_MXP_M \neq P_MXP_MX$ on the bandlimited subspace. One can also show $[\tilde{X}, \tilde{K}] \neq iP_M$. Although P_M commutes with $\tilde{K}$, it is not true that $P_MKXP_M = P_MKP_MXP_M$, i.e., $\tilde{K}\tilde{X} \neq \tilde{K}\tilde{X}$.)

Of course, the operator $\tilde{X}$ provides us with a finite basis, but any basis for this space must have dimension $\dim B(M) = 2M+1$. Although it provides a discrete representation, remember the aim of sampling theory is to determine whether there are discrete position representations.

So how can we arrive at the sampling formula for bandlimited functions on S^1 in this functional analytic language? Recall that the key is that we want to find a discrete subset of $P_M|x)$'s that form a basis. If we examine,

$$(x|P_M|x') = \frac{1}{L}\frac{\sin[(2M+1)(x-x')\frac{\pi}{L}]}{\sin[(x-x')\frac{\pi}{L}]}, \tag{2.16}$$

we notice that if we choose $x_n = \frac{n-1}{2M+1}L$ for $n = 1, \ldots, 2M+1$, then $(x_n|P_M|x_{n'}) = \frac{2M+1}{L}\delta_{nn'}$. Hence it is easy to see that $\{P_M|x_n)\}_{n=1}^{2M+1}$ forms a basis for $B(M)$, and therefore one has

$$\begin{aligned}\phi(x) = (x|\phi) &= \frac{L}{2M+1}\sum_{n=1}^{2M+1}(x|P_M|x_n)(x_n|P_M|\phi) \\ &= \sum_{n=1}^{2M+1}\frac{\sin[(2M+1)(x-x_n)\frac{\pi}{L}]}{(2M+1)\sin[(x-x_n)\frac{\pi}{L}]}\phi(x_n)\end{aligned}$$

To summarize, we see that although a careful analysis of a restricted position operator helped in the case of $\mathbb{R}$ to establish $\{P_\Lambda|x_n^{(\alpha)})\}_{n\in\mathbb{Z}}$ (fixed α) as a basis for bandlimited functions (obeying Dirichlet BCs), this is not how we should approach tackling the problem in general, i.e., we should not always focus on the restricted position operator. The general way we will think about the sampling problem is this: given a Hilbert space $\mathcal{H}$, a position operator X, and a projector P_Λ, can we find a discrete subset of $P_\Lambda|x)$'s that form a basis for a (dense subset) of $P_\Lambda\mathcal{H}$. Indeed, this is perhaps the notion closest to what we intuitively mean by a sampling theorem, since it would imply a reconstruction formula for $\phi \in P_\Lambda\mathcal{H}$ (or perhaps only in some dense subset) of the form

$$\phi(x) \equiv (x|\phi) \sim \sum_n (x|P_\Lambda|x_n)\phi(x_n). \tag{2.17}$$

However, it turns out to be useful to loosen this idea a bit more, because sometimes it can be difficult to explicitly find a discrete orthonormal basis that has a resolution of the identity $\sum_n P_\Lambda|x_n)(x_n|P_\Lambda \sim P_\Lambda$ that can be used to establish a sampling formula. The notion of frames will provide a useful set of tools for thinking about the more general problem of how to find reconstruction formulas of the kind $\phi(x) = \sum_n K(x, x_n)\phi(x_n)$ for some kernel K. This still gives us a discrete representation of the continuous function $\phi(x)$ in terms of its values at sample points. We will see that when we have an orthonormal basis as above, it is, in a sense, an efficient reconstruction of the continuous function. One can then think of the techniques for $\mathbb{R}$ and S^1 as a means for finding these efficient sampling lattices. However, finding these efficient lattices can be difficult/impossible in general, so we want to still have a way to talk about sampling. I.e., in cases where we can't work out self-adjoint extensions of X restricted to some subspace or explicitly find a discrete set $\{P_\Lambda|x_n)\}$ satisfying $(x_n|P_\Lambda|x_{n'}) \sim \delta_{nn'}$. An appropriate relaxation of the efficiency leads to a way of thinking about sampling that will be useful in the following chapters, where we don't care so much about finding the most efficient lattices and instead focus our attention on other issues (e.g., localization and subsystem size).

Concretely, a sequence $\{|x_n)\}_n$ is a *frame* for a general Hilbert space $\mathcal{H}$ if there exists constants $A, B > 0$ such that

$$A(\phi|\phi) \leq \sum_n |(x_n|\phi)|^2 \leq B(\phi|\phi) \tag{2.18}$$

for all $|\phi) \in \mathcal{H}$ [15, 129]. For a frame $\{|x_n)\}_n$, the *frame operator*, $S := \sum_n |x_n)(x_n|$ is invertible, and can be used to generate a reconstruction formula of the form [15, 129]:

$$|\phi) = \sum_n (x_n|\phi)S^{-1}|x_n). \tag{2.19}$$

That is, the element $|\phi) \in \mathcal{H}$ is completely specified by its coefficients $(x_n|\phi)$.

2.4 Sampling on a general Riemannian manifold

Is there an analogue of bandlimitation and sampling on curved manifolds? Well, if we think of momentum space as being labelled by eigenvalues of the momentum operator, then in other spaces one can try to analogously find an operator, or set of operators, upon which a restriction of the spectrum could correspond to a kind of bandlimitation. We would particularly be interested in a definition that respects symmetries. So let us choose an operator whose spectrum is invariant with respect to whatever symmetries.

For a Riemannian manifold, the idea [68, 70, 74] is to pick a covariant differential operator, such as the Laplace-Beltrami operator

$$\Box_g = \frac{1}{\sqrt{|g|}}\partial_\mu \left(\sqrt{|g|}g^{\mu\nu}\partial_\nu \cdot\right). \tag{2.20}$$

The space of bandlimited functions will be square integrable functions spanned by eigenfunctions with corresponding eigenvalues less than some chosen cutoff Λ^2. Although in this thesis we will focus on this operator acting on scalar functions, one could also study the Laplace-Beltrami operator on tensors, the Laplace-de Rham operator on differential forms, or the Dirac operator on spinors.

For a compact manifold, this will be a finite dimensional function space. Hence, one can generically find a finite set of points that can be used as sample points to specify a function in this space. For non-compact manifold, one will have a finite density of sample points, in analogy with the flat Euclidean case [69, 71, 86].

2.5 Lorentzian-signature bandlimitation

In analogy with the case of the curved manifold, one can also define a version of bandlimitation when the metric is of Lorentzian signature [69]. This allows for a kind of bandlimitation respecting (local) Lorentz symmetry. The corresponding sampling theory, however, turns out to be qualitatively different in character. We will explain briefly here some of the observations that have been previously made for this kind of bandlimitation, and then we will further discuss consequences in Chapters 7 and 9.

Previous work has been done for two examples: flat Minkowski spacetime and certain cosmological spacetimes [27, 69, 72]. We will only review the case of flat spacetime here, and refer the interested reader to [27, 72] for the cosmological cases. For $(n+1)$-dimensional Minkowski spacetime, we examine the d'Alembertian operator $\Box = \partial_t^2 - \nabla^2$. The eigenvectors are plane waves, $e^{ik\cdot x}$, with eigenvalue $-k^2 = -k_0^2 + \vec{k}^2$. Bandlimited subspace will likewise be square integrable functions spanned by plane waves with eigenvalues $|k^2| < \Lambda^2$ for some cutoff Λ. So the bandlimited functions are those with $(4d)$ Fourier transforms restricted to the region in momentum space depicted in Figure 2.1. This region has infinite volume, which by the density theorem stated before implies that one requires an infinite sample density for reconstruction of functions in this bandlimited subspace [79].

In the Riemannian case, we know from the Weyl law, stating that, for an n-dimensional Riemannian manifold $\mathcal{M}$, the number of eigenvalues of the Laplace-Beltrami operator less

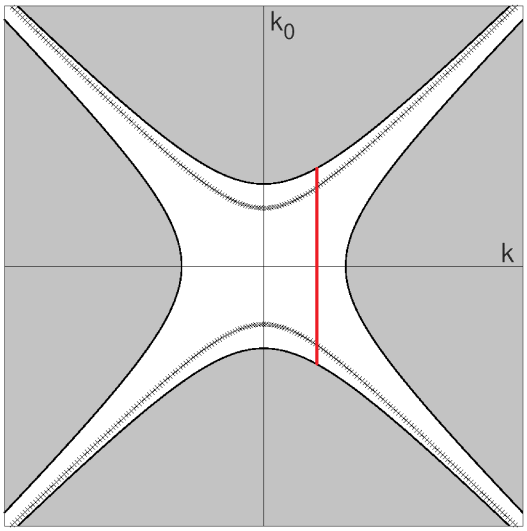

Figure 2.1: Illustration of the region $|k_0^2 - \vec{k}^2| < \Lambda^2$ in 1+1 dimensions. A mass shell is shown as a series of $\times$'s. The vertical red line indicates a surface of fixed $\vec{k}$.

than Λ^2 obeys

$$\lim_{\Lambda\to\infty} \frac{N(\Lambda)}{\Lambda^n} = \frac{1}{(2\pi)^n} V_n \mathrm{vol}(\mathcal{M}), \tag{2.21}$$

where V_n is the volume of the unit n-ball. (The intuition here is that high-frequency modes are not significantly influenced by lower-frequency curvature modulations.) So we see that if the cutoff Λ is fixed, but large, then the number of sample points needed scales with the volume, $N \sim \Lambda^n \mathrm{vol}(\mathcal{M})$ [71]. Then in the limit of infinite volume, we expect the sample density, $N/\mathrm{vol}(\mathcal{M})$, to remain finite. For example, for the case of S^1, we saw that for a cutoff $|k_m| = \left|\frac{2\pi m}{L}\right| \leq \Lambda$, we required $2M+1$ samples, where $M = \lfloor \frac{L\Lambda}{2\pi} \rfloor$. In the limit $L \to \infty$ (in units of Λ if you like), the sample density $(2M+1)/L = \frac{1}{L}\left(2\lfloor \frac{L\Lambda}{2\pi} \rfloor + 1\right) \to \frac{\Lambda}{\pi}$, which is precisely the Nyquist density for sampling on $\mathbb{R}$.

However, this does not happen in the pseudo-Riemannian case, at least for Minkowski spacetime. Even on a compact manifold, the bandlimited subspace is infinite dimensional. For example, consider T^2 with $(t, x) \in [0, L) \times [0, L)$ with flat Minkowski metric $g = -dt^2 + dx^2$. Consider the space of square integrable functions obeying periodic boundary conditions. The eigenvalues of the d'Alembertian are $\left(\frac{2\pi}{L}\right)^2 (n^2 - m^2)$ for $n, m \in \mathbb{Z}$. For any cutoff $\Lambda > 0$, the bandlimited function space will be infinite dimensional, since, for example, the kernel is infinitely degenerate (there are infinitely many solutions to $n^2 = m^2$

in $\mathbb{Z}^2$). Even if we eliminate the kernel by modifying the geometry to $(t, x) \in [0, L) \times [0, L')$ with $\frac{L}{L'} \in \mathbb{R} \setminus \mathbb{Q}$, then the Dirichlet approximation theorem guarantees that there are still infinitely many solutions in $\mathbb{Z}^2$ to

$$\left| \frac{n^2}{m^2} - \frac{L^2}{L'^2} \right| < \frac{1}{m^2} \frac{\Lambda^2 L^2}{(2\pi)^2}, \tag{2.22}$$

assuming $\Lambda L/(2\pi) > 1$, which is appropriate for the physical scenario where ΛL is the time interval in units of Planck time. The picture here is that there are infinitely many integer pairs $\mathbb{Z}^2$ in the region bounded by the hyperbolas in Figure 2.1. In higher dimensions, we argued that the volume of the region where either $|k^0| > \Lambda$ or $|\vec{k}| > \Lambda$ is even larger, and hence it will be easier to find infinitely many integer solutions, regardless of the lengths chosen. Indeed, it is clear that there are two-dimensional slices of the region $|k^2| < \Lambda^2$ that reduce to the $(1 + 1)$-dimensional case.

Hence, because the bandlimited subspace is infinite dimensional, there is no possibility to specify a function within it by finitely many sample points. Of course, any (uniformly) discrete lattice on $[0, L)^n$ will only contain finitely many points. Therefore, the reconstruction of a Lorentzian bandlimited function on this space will require an infinite density of samples. One would then expect this to persist in the limit of infinite volume.

Therefore, it seems we cannot represent a Lorentzian-bandlimited function on a discrete lattice of sampling points in spacetime. However, there is a sense in which one requires fewer degrees of freedom after the restriction to a Lorentzian-bandlimited subspace. First consider a fixed spatial mode $\vec{k}$, and hence functions of the form $\phi(x) = \psi(t)e^{i\vec{k}\cdot\vec{x}}$. Then in order for $|k^2| < \Lambda^2$, the temporal frequencies of $\psi(t)$ must lie in the range

$$|k_0^2 - \vec{k}^2| < \Lambda^2 \iff \max\{0, \vec{k}^2 - \Lambda^2\} < k_0^2 < \vec{k}^2 + \Lambda^2, \tag{2.23}$$

or, writing $r_\pm(\vec{k}) \equiv \sqrt{\vec{k}^2 \pm \Lambda^2}$

$$k_0 \in I(\vec{k}) := \begin{cases} [-r_+(\vec{k}), r_+(\vec{k})], & \text{if } |\vec{k}| \leq \Lambda \\ [-r_+(\vec{k}), -r_-(\vec{k})] \cup [r_-(\vec{k}), r_+(\vec{k})], & \text{if } |\vec{k}| > \Lambda. \end{cases} \tag{2.24}$$

Then we see each spatial mode $\vec{k}$ has a finite temporal bandwidth. This can be visualized in Figure 2.1. So we expect that we should be able to reconstruct such a fixed spatial mode from sampling at a discrete set of points in time. For the modes $|\vec{k}| \leq \Lambda$, the bandlimited interval in time is, $[-r_+(\vec{k}), r_+(\vec{k})]$, analogous to the one-dimensional case. Therefore, these

modes can be reconstructed using the same one-dimensional reconstruction formula using $r_+(\vec{k}) = \sqrt{\vec{k}^2 + \Lambda^2}$ as the bandlimit:

$$\phi(x) = \psi(t)e^{i\vec{k}\cdot\vec{x}} = \sum_{n\in\mathbb{Z}} \mathrm{sinc}[r_+(\vec{k})(t - t_n^{(\alpha)})]\psi(t_n^{(\alpha)})e^{i\vec{k}\cdot\vec{x}}, \tag{2.25}$$

where $t_n^{(\alpha)} = \pi(n+\alpha)/\Lambda$, for some fixed $\alpha \in [0, 1)$. Or one could use a nonequidistantly-spaced lattice, similar to before. For, modes $|\vec{k}| > \Lambda$, we can also reconstruct using this formula with $r_+(\vec{k})$ as the bandlimit (which goes to ∞ as $|\vec{k}| \to \infty$). However, these modes do not have support on the full interval $[-r_+(\vec{k}), r_+(\vec{k})]$, but rather a much smaller interval, which has a vanishing volume, $2(r_+(\vec{k}) - r_-(\vec{k})) \to 0$, as $|\vec{k}| \to \infty$. Therefore, from the density arguments, we expect to be able to reconstruct from a much coarser lattice, with samples taken at a rate of roughly $(r_+(\vec{k}) - r_-(\vec{k}))/\pi$. Indeed, such so-called "band-pass" signals can be reconstructed using a more complex formula. We will not be needing its explicit form, so we will refer the interested reader to [64, 72].

We see that for each mode the spatial dependence is fixed, and we are simply applying the reconstruction for the amplitude which may change in time. Is there a way to combine these modes to recover a reconstruction formula for a general function? Notice that since the bandwidth of mode $\vec{k}$ vanishes as $|\vec{k}| \to \infty$, there will be some $\vec{k}$ such that the temporal bandwidth is largest. It is easy to see, e.g., from Figure 2.1, that this occurs for modes $|\vec{k}| = \Lambda$, which have a bandwidth of $\sqrt{2}\Lambda$. Therefore, we should be able to reconstruct every spatial mode on a temporal lattice of density $\sqrt{2}\Lambda/\pi$. For the spatial modes with a smaller temporal bandwidth, this would simply correspond to an oversampling. Each mode $\vec{k}$ will have a different reconstruction kernel, but all of the sample points can be taken on the lattice $\{t_n = \pi n/\sqrt{2}\Lambda\}_{n\in\mathbb{Z}}$. Formally, this will look like

$$\begin{aligned}
\phi(x) &= \int \frac{d\vec{k}}{(2\pi)^N} \tilde{\phi}(t, \vec{k}) e^{i\vec{k}\cdot\vec{x}} \\
&= \int \frac{d\vec{k}}{(2\pi)^N} \left(\sum_{n\in\mathbb{Z}} K(t, t_n; \vec{k}) \tilde{\phi}(t_n, \vec{k}) \right) e^{i\vec{k}\cdot\vec{x}} \\
&= \int \frac{d\vec{k}}{(2\pi)^N} \sum_{n\in\mathbb{Z}} K(t, t_n; \vec{k}) \left(\int d\vec{x}' \phi(t_n, \vec{x}') e^{-i\vec{k}\cdot\vec{x}'} \right) e^{i\vec{k}\cdot\vec{x}} \\
&= \sum_{n\in\mathbb{Z}} \int d\vec{x}' \mathcal{K}(t, t_n; \vec{x} - \vec{x}') \phi(t_n, \vec{x}'),
\end{aligned} \tag{2.26}$$

where

$$\mathcal{K}(t,t_n;\vec{x}-\vec{x}') := \int \frac{d\vec{k}}{(2\pi)^N} K(t,t_n;\vec{k}) e^{i\vec{k}\cdot(\vec{x}-\vec{x}')}. \tag{2.27}$$

Note that the simple reconstruction formula with the sinc functions no longer holds for the modes $|\vec{k}| < \Lambda$ since we are now oversampling with the lattice $\{t_n = \pi n/\sqrt{2}\Lambda\}_{n\in\mathbb{Z}}$, instead of the lattice $\{t_n = \pi n/r_+(\vec{k})\}_{n\in\mathbb{Z}}$ on which we have $(t_n|P_{r_+(\vec{k})}|t_{n'}) = \delta_{nn'}$. Therefore, we see that any Lorentzian-bandlimited function can be reconstructed from its values on a discrete set of contant-time hypersurfaces, provided that they are spaced sufficiently densely.

What if we flipped the roles of k^0 and $\vec{k}$? Do we get an analogous reconstruction for temporal modes? In $(1+1)$-dimensions, the roles of k^0 and k^1 are symmetric, hence we get the same result. The case is different in higher dimensions (cf. [72,87]). For every fixed k^0, i.e., function of the form $\phi(x) = \psi(\vec{x})e^{ik^0t}$, we still have that the support of ϕ in $\vec{k}$-space is restricted to the region where $|\vec{k}| \in I(k_0)$ (where I is the interval defined above). The volume of this region is

$$\mathrm{Vol}_N(I(k_0)) = \begin{cases} V_N r_+(k^0)^N & \text{if } |k^0| \le \Lambda \\ V_N(r_+(k^0)^N - r_-(k^0)^N) & \text{if } |k^0| > \Lambda \end{cases} \tag{2.28}$$

where V_N is the volume of the unit ball in N dimensions. Since the volume is finite for every fixed k^0, indeed we see that each temporal mode can be reconstructed from a spatial lattice of density proportional to this momentum-space volume. So the situation for fixed temporal modes is analogous to that for fixed spatial modes, but is there a spatial lattice which suffices for a reconstruction of all temporal modes, similar to (2.26)? Recall, this was possible since there was a uniform upper bound, $2\sqrt{2}\Lambda$, for the bandwidths of all the spatial modes. Concretely, we want to know whether $\sup_{k^0} \mathrm{Vol}_N(I(k_0)) < \infty$. For $N = 1$ (i.e., $1+1$ dimensions), by symmetry we have this upper bound to be $2\sqrt{2}\Lambda$. For $N = 2$ we have

$$\mathrm{Vol}_2(I(k_0)) = \begin{cases} \pi[(k^0)^2 + \Lambda^2] & \text{if } |k^0| \le \Lambda \\ 2\pi\Lambda^2 & \text{if } |k^0| > \Lambda \end{cases} \tag{2.29}$$

Hence, the maximal spatial bandwidth is $2\pi\Lambda^2$, and we have an analog of (2.26) with the spatial sample points chosen with this density (note that they are distributed through $(x^1, x^2) \in \mathbb{R}^2$ rather than $t \in \mathbb{R}$). For $N \ge 3$, we have $\lim_{k^0\to\infty} \mathrm{Vol}_N(I(k^0)) = \infty$. Therefore, in dimensions $3+1$ and higher, even though each temporal mode can be reconstructed on a discrete spatial lattice, one requires increasingly higher sampling density for larger frequencies k^0, and therefore there is no sampling lattice that suffices for all temporal modes and hence no analogue of (2.26).

Chapter 3

Bandlimited quantum field theory

Now we will discuss the basics of the application of bandlimitation and sampling theory to quantum field theory. The relevant references we will draw upon for this background material are [68, 70, 71, 74, 100, 102] for the Euclidean-signature case, and [69, 72] for the Lorentzian-signature case.

Recall that the primary interest in introducing sampling theory to quantum field theory is that it allows for discreteness without symmetry breaking. In the previous chapter, we saw explicitly how bandlimited functions on S^1 and $\mathbb{R}$ can be represented by their sample values on a discrete sampling lattice. However, we have not abandoned the underlying continuous space simply by restricting the set of allowed Fourier modes. This is reflected in the fact that there is a family of sampling lattices, none of which is preferred.

The analogous reconstruction property for the case of Lorentzian bandlimitation is qualitatively different than the Euclidean case, as we have seen. Nevertheless, we will examine the Lorentzian bandlimit applied to quantum fields as well.

The main point in carrying out this endeavour is to restrict the space of field configurations that one is considering to consist only of bandlimited functions (either Euclidean- or Lorentzian-signature). In classical field theory, this amounts to a restriction of the set of elements one feeds into the action, $S[\phi]$. The equations of motion, $\delta S[\phi]/\delta\phi = 0$, are formally obtained in the usual way, except that one is taking variations within this new set. In quantum field theory, one could proceed by quantizing the classical solution space, or by restricting the space of fields one is integrating over in the path integral. The new partition function, for example, would be

$$Z[J] = \int_{B(\Lambda)} \mathcal{D}\phi \, e^{iS[\phi]+i(J|\phi)}, \tag{3.1}$$

where $B(\Lambda)$ is the bandlimited space under consideration, and $(\cdot|\cdot)$ is the inner product on this space.

For general constraints, this undertaking can be quite complicated. Fortunately, the task in this case will be rather simple, at least for free theories. On a flat background, fields can be decomposed into Fourier modes, which become decoupled harmonic oscillators in a free theory. Because bandlimitation involves a restriction of the allowed Fourier modes, we will see that this simply amounts to eliminating a subset of these oscillators.

In the first section of this chapter, we will briefly review bandlimited QFT for the (flat) Euclidean case, highlighting certain structural consequences [100, 102] (some further aspects regarding the Fock space structure were clarified in [96], which we will also present here). In the second section, we will review previous work done in the Lorentzian-signature case, involving a calculation of the Feynman propagator using the path integral [27, 69, 72]. We will return to present the contributions of this thesis regarding further aspects of Lorentzian-bandlimited quantum field theory in Chapters 8 and 9, which include a treatment of free and interacting theories, respectively.

3.1 Euclidean case

Euclidean-bandlimited field configurations in $(N+1)$-dimensional flat spacetime take the form:

$$\phi(\vec{x},t) = \int_{\|\vec{k}\|_2<\Lambda} \frac{d\vec{k}}{(2\pi)^N} \tilde{\phi}(\vec{k},t) e^{i\vec{k}\cdot\vec{x}}, \tag{3.2}$$

where $\|\vec{k}\|_2 := \sqrt{\vec{k}^2}$. These fields still live in spacetime, but imposing the Euclidean bandlimit requires us to pick out a preferred frame.

The Hamiltonian for a free real scalar theory restricted to these field configurations takes the form

$$\begin{aligned} H &= \frac{1}{2}\int d\vec{x}\left(\pi(x)^2 + (\nabla\phi(x))^2 + m^2\phi(x)^2\right) \\ &= \frac{1}{2}\int_{\|\vec{k}\|_2<\Lambda} \frac{d\vec{k}}{(2\pi)^N}\left(|\tilde{\pi}(\vec{k},t)|^2 + \omega_k^2|\tilde{\phi}(\vec{k},t)|^2\right) \end{aligned}$$

where $\omega_k := \sqrt{\vec{k}^2 + m^2}$. Each mode of the field evolves independently in time, according to the equation of motion:

$$(\partial_t^2 + \omega_k^2)\tilde{\phi}(\vec{k},t) = 0. \tag{3.3}$$

Therefore, we could think of the procedure as imposing the bandlimit at a fixed initial time, and this will be preserved under time evolution.

Because of the sampling property for this space of fields, we also obtain lattice representations for the Hamiltonian. Given a sampling lattice $\{\vec{x}_n\}_n$ and the corresponding reconstruction formula $\phi(\vec{x}) = \sum_n K(\vec{x}, \vec{x}_n)\phi(\vec{x}_n)$, it is straigtforward to pull the Hamiltonian back to take the form

$$H = \frac{1}{2} \sum_{n,n'} \left(\pi_n M_{nn'} \pi_{n'} + \phi_n W_{nn'} \phi_{n'} \right), \tag{3.4}$$

where $\pi_n \equiv \pi(\vec{x}_n)$, $\phi_n \equiv \phi(\vec{x}_n)$, and

$$\begin{aligned} M_{nn'} &:= \int d\vec{x}\, K(\vec{x}, \vec{x}_n) K(\vec{x}, \vec{x}_{n'}) \\ W_{nn'} &:= \int d\vec{x}\, K(\vec{x}, \vec{x}_n)(-\nabla^2 + m^2) K(\vec{x}, \vec{x}_{n'}). \end{aligned}$$

For example, in dimension $N = 1$ on a Nyquist lattice $\{x_n^{(\alpha)} = \frac{\pi}{\Lambda}(n + \alpha)\}_{n \in \mathbb{Z}}$ (with $\alpha \in [0, 1)$), we have

$$\begin{aligned} M_{nn'} &= \frac{\pi}{\Lambda} \delta_{nn'} \\ W_{nn} &= \frac{\pi\Lambda}{3} + \frac{\pi}{\Lambda} m^2, \quad \text{and} \quad W_{nn'} = \frac{2\Lambda}{\pi} \frac{(-1)^{n-n'}}{(n-n')^2} \quad (n \neq n'). \end{aligned}$$

In this form, the Hamiltonian has lost the manifest translation-invariance of the previous expressions. The original forms can be recovered by using the reproducing kernel (discussed in the previous chapter) to write the field evaluated at a sample point in terms of a continuous operator acting on the entire field configuration $\phi(\vec{x})$.

Although we will not pursue it here, it is possible that these lattice representations admit a rigorous definition of a path integral for the partition function, since it would consist of path integrals for countably many degrees of freedom. Here we will focus on the canonical quantization of bandlimited fields, which is straightforward in momentum space. We have the usual creation and annihilation operators, $a_k^\dagger$ and a_k, defined by

$$a_k := \sqrt{\frac{\omega_k}{2}} \tilde{\phi}(\vec{k}) + \frac{i}{\sqrt{2\omega_k}} \tilde{\pi}(\vec{k}), \tag{3.5}$$

and normalized so that $[a_k, a_{k'}^\dagger] = (2\pi)^N \delta(\vec{k} - \vec{k'})$. Written in terms of these, the Hamiltonian takes the usual form of a collection of harmonic oscillators, but restricted to those

within the bandlimit $\|\vec{k}\|_2 < \Lambda$:

$$H = \int_{\|\vec{k}\|_2<\Lambda} \frac{d\vec{k}}{(2\pi)^N} \omega_k a_k^\dagger a_k + E_0, \tag{3.6}$$

where $E_0 = \frac{1}{2}\int d\vec{x} \int_{\|\vec{k}\|_2<\Lambda} \frac{d\vec{k}}{(2\pi)^N}$ is the zero-point energy. Note that the zero-point energy *density* is now finite.

Viewed as a collection of quantum harmonic oscillators, the Hilbert space of the field theory can formally be written as

$$\bigotimes_{\|\vec{k}\|_2<\Lambda} \mathcal{H}_{\vec{k}}, \tag{3.7}$$

with[1] $\mathcal{H}_{\vec{k}} = L^2(\mathbb{C}, d\tilde{\phi}(\vec{k}))$. There are different ways in which one can make sense of this continuous tensor product. The simplest method is by taking the limit of a net consisting of tensor products of a finite subset of these factors [126]. This construction leads to a non-separable Hilbert space, and typically it is only necessary to consider states in a much smaller separable subspace of this Hilbert space [120, 127]. One can instead use a different construction, called the *exponential Hilbert space* [58, 59, 75, 119], which is applicable if $\mathcal{H}_{\vec{k}}$ is a Fock space. This leads to a separable Hilbert space, and in fact the full Hilbert space will also take the form of a Fock space,

$$\bigotimes_{\|\vec{k}\|_2<\Lambda} \mathcal{H}_{\vec{k}} = \bigotimes_{\|\vec{k}\|_2<\Lambda} L^2(\mathbb{C}, d\tilde{\phi}(\vec{k})) \cong \mathcal{F}[B(\Lambda)], \tag{3.8}$$

where $B(\Lambda)$ is the space of bandlimited fields. By this notation, we mean that for a general single-particle Hilbert space $\mathcal{H}$, the associated Fock space is

$$\mathcal{F}[\mathcal{H}] := \bigoplus_{n=0}^{\infty} \mathcal{H}^{\odot n} = \mathbb{C} \oplus \mathcal{H} \oplus \mathcal{H}^{\odot 2} \oplus \cdots, \tag{3.9}$$

where we use $\odot$ to denote the symmetrized tensor product.

We will not concern ourselves with the details of these constructions. In the end, the Fock space we obtain is consistent with the usual manner in which this is handled in physics, with a basis of particle states constructed from the vacuum $|0\rangle$ as:

$$|k\rangle := a_k^\dagger |0\rangle, \qquad |k_1, k_2\rangle := a_{k_1}^\dagger a_{k_2}^\dagger |0\rangle, \qquad \ldots. \tag{3.10}$$

[1] Note that we are abusing the notation slightly by writing $\mathcal{H}_{\vec{k}} = L^2(\mathbb{C}, d\tilde{\phi}(\vec{k}))$. Since these fields are real-valued, they are also subject to the constraint $\tilde{\phi}(\vec{k})^* = \tilde{\phi}(-\vec{k})$. However, this technical point will not cause any issues, and can be accounted for implicitly by writing $\tilde{\phi}(\vec{k}) = \frac{1}{\sqrt{2\omega_k}}(a_{\vec{k}} + a^\dagger_{-\vec{k}})$.

One important point to make is that since the n-particle states lie in the space $B(\Lambda)^{\odot n}$, the momenta of the individual particles must lie within the bandlimit, but the total momentum of a multiparticle state does not. The total momentum operator is

$$\vec{P} = \int_{\|\vec{k}\|_2 < \Lambda} \frac{d\vec{k}}{(2\pi)^N} \vec{k} a_k^\dagger a_k. \tag{3.11}$$

Its eigenstates are $|k_1, \ldots, k_n\rangle$ with eigenvalue $\sum_{i=1}^n \vec{k}_i$. For bandlimited fields, the magnitude of these eigenvalues is bounded above by $n\Lambda$, rather than Λ. Indeed, if we identify the cutoff with the Planck scale, we do not want to have the total momentum of a multiparticle system to be bounded above by $\hbar\Lambda \sim \hbar/\ell_P \approx 6.52$ kg m s^{-1}.

Clearly the bandlimit will act as an ultraviolet regulator for quantities in the free field theory, such as correlation functions. Hence, we have the benefits of a lattice theory, but without losing translational or rotational symmetry. But how can we think of the quantized field theory in position space? Is it simply a collection of oscillators at the lattice sites with couplings between them? What about the fact that the sample points can be moved around?

In ordinary (non-bandlimited) quantum field theory, one can think of the field in position space as a continuum limit of a collection of oscillators at each point in space that are coupled through the spatial derivative term in the Hamiltonian. Concretely, one can build a Fock space, $\mathcal{H}_{\vec{x}} = L^2(\mathbb{R}, d\phi(\vec{x}))$, at each spatial point using the creation and annihilation operators defined by:

$$b_{\vec{x}} := \sqrt{\frac{m}{2}}\phi(\vec{x}) + \frac{i}{\sqrt{2m}}\pi(\vec{x}). \tag{3.12}$$

These diagonalize the "uncoupled" part of the Hamiltonian, i.e.,

$$\frac{1}{2}\int d\vec{x}\left(\pi(\vec{x})^2 + m^2\phi(\vec{x})^2\right) = \int d\vec{x}\, m b_{\vec{x}}^\dagger b_{\vec{x}} + \text{z.p.e.}. \tag{3.13}$$

The Fock spaces at each spatial point can be combined to form the total Hilbert space

$$\bigotimes_{\vec{x}\in\mathbb{R}^N} \mathcal{H}_{\vec{x}} = \bigotimes_{\vec{x}\in\mathbb{R}^N} L^2(\mathbb{R}, d\phi(\vec{x})) \cong \mathcal{F}[L^2(\mathbb{R}^N, d\vec{x})]. \tag{3.14}$$

Such a decomposition is useful when discussing entanglement between spatial regions of the field. Indeed, one can think of entanglement in the field theory as arising due to the spatial derivative term in the Hamiltonian that couples these local harmonic oscillators.

However, in (non-bandlimited) quantum field theory, this representation of the creation and annihilation operators is unitarily inequivalent from that constructed with the Fourier modes,

$$\bigotimes_{\vec{k}\in\mathbb{R}^N} \mathcal{H}_{\vec{k}} = \bigotimes_{\vec{k}\in\mathbb{R}^N} L^2(\mathbb{C}, d\tilde{\phi}(\vec{k})) \cong \mathcal{F}[L^2(\mathbb{R}^N, d\vec{k})]. \tag{3.15}$$

This unitary inequivalence is possible because the infinite number of oscillators present in quantum field theory preclude the application of the Stone-von Neumann theorem [45,105]. By unitary inequivalence of two Fock spaces, we do not mean that the two Hilbert spaces are not isomorphic (for example, any two separable Hilbert spaces are isomorphic), but rather the representations of the two sets of creation and annihilation operators cannot be intertwined using a unitary operator. Concretely, we can relate the two sets of operators algebraically using a Bogoliubov transformation [96]:

$$\begin{aligned} a_{\vec{k}} &= \sqrt{\frac{\omega_k}{2}}\tilde{\phi}(\vec{k}) + \frac{i}{\sqrt{2\omega_k}}\tilde{\pi}(\vec{k}) \\ &= \sqrt{\frac{\omega_k}{2}}\int d\vec{x}\, e^{-i\vec{k}\cdot\vec{x}}\frac{1}{\sqrt{2m}}(b_{\vec{x}} + b^\dagger_{\vec{x}}) + \frac{i}{\sqrt{2\omega_k}}\int d\vec{x}\, e^{-i\vec{k}\cdot\vec{x}}(-i)\sqrt{\frac{m}{2}}(b_{\vec{x}} - b^\dagger_{\vec{x}}) \\ &= \int d\vec{x}\, e^{-i\vec{k}\cdot\vec{x}}\left[\frac{1}{2}\left(\sqrt{\frac{\omega_k}{m}} + \sqrt{\frac{m}{\omega_k}}\right)b_{\vec{x}} + \frac{1}{2}\left(\sqrt{\frac{\omega_k}{m}} - \sqrt{\frac{m}{\omega_k}}\right)b^\dagger_{\vec{x}}\right]. \end{aligned}$$

A general Bogoliubov transformation takes the form,

$$a_i = \sum_j (\alpha_{ij} b_j + \beta_{ij} b_j^\dagger), \tag{3.16}$$

where the operators α and β must satisfy

$$\alpha\alpha^\dagger - \beta\beta^\dagger = 1, \quad \text{and} \quad \alpha\beta^T = \beta\alpha^T, \tag{3.17}$$

so that both sets of operators obey the canonical commutation relations. The inverse transformation is then

$$b_j = \sum_i (\alpha_{ij}^* a_i - \beta_{ij} a_i^\dagger). \tag{3.18}$$

For our case above, the Bogoliubov coefficients are

$$\alpha_{\vec{k}\vec{x}} := e^{-i\vec{k}\cdot\vec{x}} c_+(\vec{k}), \qquad \beta_{\vec{k}\vec{x}} := e^{-i\vec{k}\cdot\vec{x}} c_-(\vec{k}), \tag{3.19}$$

where $c_\pm(\vec{k}) := \frac{1}{2}[(1 + (\vec{k}/m)^2)^{1/4} \pm (1 + (\vec{k}/m)^2)^{-1/4}]$.

We can represent general creation and annihilation operators $a_i^\dagger$ and a_i on a Fock space, which we will call the a-Fock space and denote $\mathcal{F}_a$. The corresponding vacuum state will be denoted $|0\rangle_a$ and total number operator $N_a := \sum_i a_i^\dagger a_i$. We will also have an analogous b-Fock space. If the two sets of operators are constrained to be related by some general Bogoliubov transformation, then the vacua of these two representations must be related by

$$|0\rangle_a = \mathcal{N} e^{-\frac{1}{2}\sum_{j,k}(\alpha^{-1}\beta)_{jk} b_j^\dagger b_k^\dagger} |0\rangle_b . \tag{3.20}$$

However, the right-hand side is only a valid state in the space $\mathcal{F}_a$ if it is normalizable. Otherwise, this operator mapping $|0\rangle_b$ to $|0\rangle_a$ cannot be extended to a unitary between the two spaces (since then we can not find a finite $\mathcal{N}$ to preserve the norm ${}_b\langle 0|0\rangle_b = 1$). In this case, we say that the two representations are unitarily inequivalent. One can show that the condition of normalizability is equivalent to the condition that the a-vacuum contains finitely many b-particles, and vice-versa. Thus, the two representations are unitarily equivalent if and only if [39, 127]

$${}_a\langle 0| N_b |0\rangle_a = {}_b\langle 0| N_a |0\rangle_b = \sum_{i,j} |\beta_{ij}|^2 < \infty. \tag{3.21}$$

In the case of ordinary quantum field theory, it is simple to see that the Fock spaces generated by $a_{\vec{k}}$, $a_{\vec{k}}^\dagger$ and $b_{\vec{x}}$, $b_{\vec{x}}^\dagger$ are unitarily inequivalent, since

$$\int d\vec{x} \int \frac{d\vec{k}}{(2\pi)^N} |\beta_{\vec{k}\vec{x}}|^2 = \int d\vec{x} \int \frac{d\vec{k}}{(2\pi)^N} |c_-(\vec{k})|^2 = \infty. \tag{3.22}$$

Note that even if two Fock space representations are unitarily inequivalent, one can still make sense of the Bogoliubov transformation as an abstract algebraic relation. It is simply that we cannot represent these creation and annihilation "operators" on the same Fock space.

Unitary equivalence of two representations is a desirable feature in quantum theory because it guarantees that one will obtain the same results for, e.g., expectation values of observables using either representation. However, a theorem from [35] implies that in certain cases, one can find states in unitarily inequivalent representations such that the expectation values of finitely many observables are arbitrarily close [127]. Therefore, it is possible that unitary inequivalence does not cause any issues for realistic physical scenarios[2]. This observation is a motivation for the algebraic approach to quantum field

[2]That being said, the ubiquity of unitary inequivalent representations in quantum field theory can cause theoretical obstacles. For example, the infamous theorem of Haag [45] states that the Hilbert spaces of free and interacting theories are generally unitarily inequivalent, implying that the interaction picture is ill-defined.

theory, emphasizing the importance of the algebraic relations between the operators of the theory rather than trying to single out a preferred Hilbert space representation [45, 46]. Nevertheless, it is still interesting to explore where these inequivalences arise within more concrete approaches to quantum field theory. For instance, in Minkowski spacetime, the Fock spaces one obtains by quantizing a field in inertial coordinates and the coordinates associated with a uniformly accelerating observer (i.e., Rindler coordinates) are unitarily inequivalent. This manifests itself in the well-known Unruh effect, where the (Minkowski) vacuum associated with the inertial coordinates appears as a thermal state when formally written in the Fock space of the uniformly accelerated observer.

Now how does the Hilbert space construction from position space change under bandlimitation? One would anticipate that with sampling theory, the local oscillators in space will now correspond to sample points. However, it was noticed in [100, 102] that one should not simply take a tensor product over the Fock spaces generated at an arbitrary set of lattice points. This is because the field operators at two arbitrary sample points do not necessarily commute. For example, for one-dimensional sampling on $\mathbb{R}$, if we take two sample points x_1 and x_2 that are not an integer number of Nyquist spacings apart, then

$$[\phi(x_1), \pi(x_2)] = i\frac{\Lambda}{\pi}\,\mathrm{sinc}[\Lambda(x_1 - x_2)] \neq 0. \tag{3.23}$$

Therefore, it is not consistent to represent these operators on a Hilbert space of the form $\mathcal{H}_{x_1} \otimes \mathcal{H}_{x_2}$ as $\phi(x_1) \otimes 1$ and $1 \otimes \pi(x_2)$.

In general, we have

$$[\phi(\vec{x}), \pi(\vec{x}')] = i(\vec{x}|P_\Lambda|\vec{x}'), \tag{3.24}$$

along with the usual $[\phi(\vec{x}), \phi(\vec{x}')] = [\pi(\vec{x}), \pi(\vec{x}')] = 0$. If one can find an orthogonal frame $\{P_\Lambda|\vec{x}_n)\}_n$ (for example, corresponding to a Nyquist lattice on $\mathbb{R}$), then $[\phi(\vec{x}_n), \pi(\vec{x}_{n'})] \sim i\delta_{nn'}$ and it is possible to formulate a simple Hilbert space construction. Explicitly, one can define

$$b_n := C_n^{-1/2} b_{\vec{x}_n} = C_n^{-1/2}\left(\sqrt{\frac{m}{2}}\phi(\vec{x}_n) + \frac{i}{\sqrt{2m}}\pi(\vec{x}_n)\right), \tag{3.25}$$

where $C_n := (\vec{x}_n|P_\Lambda|\vec{x}_n)$, so that $[b_n, b_{n'}^\dagger] = \delta_{nn'}$. This gives us a Fock space $\mathcal{H}_n = L^2(\mathbb{R}, d\phi(\vec{x}_n))$ at the sample point $\vec{x}_n$. The total Hilbert space can then be defined as a countable tensor product over factors at each sample point:

$$\bigotimes_n \mathcal{H}_n = \bigotimes_n L^2(\mathbb{R}, d\phi(\vec{x}_n)) \cong \mathcal{F}[\ell^2(\mathbb{R})]. \tag{3.26}$$

When this construction is possible, is this Hilbert space unitarily equivalent to the space constructed using Fourier modes within the bandlimit, $\bigotimes_{\|\vec{k}\|_2<\Lambda} \mathcal{H}_{\vec{k}} \cong \mathcal{F}[B(\Lambda)]$?

In [96] we showed that, at least in the case where C_n is the same for all n (which occurs for Nyquist lattices on $\mathbb{R}$, with $C_n = \Lambda/\pi$), these two spaces remain unitarily inequivalent after bandlimitation. Indeed, the relevant Bogoliubov coefficients are similar to those obtained before,

$$\alpha_{n\vec{x}} := C_n^{-1/2} e^{-i\vec{k}\cdot\vec{x}} c_+(\vec{k}), \qquad \beta_{n\vec{x}} := C_n^{-1/2} e^{-i\vec{k}\cdot\vec{x}} c_-(\vec{k}). \tag{3.27}$$

Therefore, we want to know if the following expression is finite:

$$\sum_n \int_{\|\vec{k}\|_2<\Lambda} \frac{d\vec{k}}{(2\pi)^N} |\beta_{n\vec{x}}|^2 = \left(\sum_n C_n^{-1}\right) \left(\int_{\|\vec{k}\|_2<\Lambda} \frac{d\vec{k}}{(2\pi)^N} |c_-(\vec{k})|^2\right). \tag{3.28}$$

If C_n is independent of n, then we see that one obtains a divergence due to the infinite volume of space (specifically, because of infinitely many sample points). Hence, these representations are not unitarily equivalent in this case. Note that if one also introduces an infrared cutoff, as in the case of bandlimited fields on S^1, then the analogous representations will be unitarily equivalent by the Stone-von Neumann theorem, since one only has finitely many degrees of freedom.

If one finds two different orthogonal frames, such as two shifted Nyquist lattices for $\mathbb{R}$, does one end up with two different Hilbert spaces? Suppose we are given two such lattices, say $\{\vec{x}_n\}_n$ and $\{\vec{y}_m\}_m$. Because of the sampling property, one has a reconstruction formula for samples on each of these lattices, e.g., $\phi(\vec{x}) = \sum_n K(\vec{x}, \vec{x}_n)\phi(\vec{x}_n)$. It is easy to see that this implies the corresponding Bogoliubov transformation between the creation and annihilation operators at the two sets of sample points is:

$$b_{\vec{y}_m} = \sum_n K(\vec{y}_m, \vec{x}_n) b_{\vec{x}_n}. \tag{3.29}$$

We see that the beta coefficients are all zero. Therefore, not only are the two corresponding Fock space representations unitarily equivalent, but they are actually the same [96]. In fact, this change of orthogonal sampling frame can be viewed as simply a change of basis in the single-particle Hilbert space. If we denote K as the operator implementing this change of basis (which will have matrix elements $K(\vec{y}_m, \vec{x}_n)$ and will be unitary for lattices giving rise to orthonormal frames), then we can write this as: $K\mathcal{F}[\mathcal{H}] = \mathcal{F}[K\mathcal{H}]$.

We have seen that, although the implementation of Euclidean bandlimitation in quantum field theory is straightforward in momentum space, sampling theory shows us that the structure in position space can be nontrivial. This is especially true when considering sampling lattices that do not produce orthogonal frames, which is the generic case (for example, in $\mathbb{R}^n$ with $n > 1$). This gives rise to both conceptual and technical subtleties in identifying local subsystems for the purposes of studying entanglement between local degrees of freedom. However, we will postpone this discussion to the next chapter.

3.2 Lorentzian case

Previous work on the Lorentzian case [27,72] has focused on a path integral approach, which is manifestly covariant and well-adapted to the modification with a Lorentzian bandlimit. We will review some of this previous work here, and in Chapter 8 return to the analysis of the field theory more akin to our review of the Euclidean case, in order to investigate other features of this model.

For the case of flat spacetime, in [72] the modification of the Feynman propagator due to the bandlimit $|k^2| = |(k^0)^2 - \vec{k}^2| < \Lambda^2$ was found. One can begin with the partition function,

$$Z[J] = \int_{B(\Lambda)} \mathcal{D}\phi \, e^{-\frac{i}{2}(\phi|(\Box+m^2)|\phi)+i(J|\phi)}, \tag{3.30}$$

where the functional integration is restricted to the space of Lorentzian-bandlimited functions. Although in the Euclidean-bandlimited case, the lattice representations may help in making this path integral well-defined, for the Lorentzian bandlimit this will likely not be the case due to the continuum of degrees of freedom. Note that in the above expression $(\cdot|\cdot)$ is the L^2 inner product on $B(\Lambda)$, and in position space, $\Box = \partial_t^2 - \nabla^2$.

Formally completing the square in the exponent is elementary,

$$\begin{aligned}&\tfrac{-i}{2}(\phi|(\Box+m^2)|\phi) + i(J|\phi)\\ &\quad = \tfrac{-i}{2}(\phi - (\Box+m^2)^{-1}J|(\Box+m^2)|\phi - (\Box+m^2)^{-1}J) + \tfrac{i}{2}(J|(\Box+m^2)^{-1}|J),\end{aligned}$$

but we should be careful as to what we mean by $(\Box+m^2)^{-1}$. Of course, there is the usual issue that $(\Box+m^2)$ is not invertible for on-shell field configurations, but we can use the Feynman contour in the Fourier-space representation of this operator to circumvent these poles. The point is that now the operators $(\Box+m^2)$ and $(\Box+m^2)^{-1}$ are acting on the bandlimited Hilbert space $B(\Lambda)$, so we should apply the bandlimited projector P_Λ on either side of these operators in order to obtain the correct expressions. Therefore, the spacetime representation is

$$(x|(\Box+m^2)^{-1}|x') = \int_{|k^2|<\Lambda^2} \frac{dk}{(2\pi)^n} \frac{-1}{k^2 - m^2 + i\epsilon} e^{ik\cdot(x-x')}. \tag{3.31}$$

Therefore, we get

$$Z[J] = Z[0] e^{\frac{i}{2}(J|(\Box+m^2)^{-1}|J)}, \tag{3.32}$$

from which we can extract the following two-point function:

$$\begin{aligned} G_F(x_1, x_2) &:= \frac{\int_{B(\Lambda)} \mathcal{D}\phi\, \phi(x_1)\phi(x_2) e^{iS[\phi]}}{\int_{B(\Lambda)} \mathcal{D}\phi\, e^{iS[\phi]}} \\ &= \frac{1}{i}\frac{\delta}{\delta J(x_1)}\frac{1}{i}\frac{\delta}{\delta J(x_2)}\bigg|_{J=0} \frac{Z[J]}{Z[0]} \\ &= (-i)(x_1|(\Box + m^2)^{-1}|x_2). \end{aligned}$$

Note that because G_F is the inverse of $(\Box + m^2)$ on the bandlimited subspace, from (3.31) we can see that this function obeys

$$(\Box_x + m^2)G_F(x, x') = -i(x|P_\Lambda|x'), \tag{3.33}$$

where the bandlimited projector, P_Λ, which is the identity operator on $B(\Lambda)$, is given by

$$(x|P_\Lambda|x') = \int_{|k^2|<\Lambda^2} \frac{dk}{(2\pi)^n} e^{ik\cdot(x-x')}. \tag{3.34}$$

By focusing on the representation of the Feynman propagator, G_F, in Fourier space at equal times, one can obtain a more useful indication of the modification due to the bandlimit. This was used in [72] as a preliminary example before their treatment of a cosmological background, in which case $\tilde{G}_F(t = 0, \vec{k})$ was used to determine the impact that the bandlimit would have on the cosmic microwave background.

Let us evaluate $\tilde{G}_F(t = 0, \vec{k})$ for the flat case. First, recall that we can split the region $|k^0 - \vec{k}^2| < \Lambda^2$ into intervals of k^0 values for each fixed $\vec{k}$:

$$k_0 \in I(\vec{k}) := \begin{cases} [-r_+(\vec{k}), r_+(\vec{k})], & \text{if } |\vec{k}| \leq \Lambda \\ [-r_+(\vec{k}), -r_-(\vec{k})] \cup [r_-(\vec{k}), r_+(\vec{k})], & \text{if } |\vec{k}| > \Lambda, \end{cases} \tag{3.35}$$

where $r_\pm(\vec{k}) := \sqrt{\vec{k}^2 \pm \Lambda^2}$. Then the task is to evaluate

$$\tilde{G}_F(t = 0, \vec{k}) = \int_{I(\vec{k})} \frac{dk^0}{2\pi} \frac{i}{(k^0)^2 - \omega_k^2 + i\epsilon}. \tag{3.36}$$

For a fixed $\vec{k}$, this is can be carried out by taking the usual k^0 contour and subtracting the complement of $I(\vec{k})$, which is simple to evaluate in closed form. One finds

$$\tilde{G}_F(t = 0, \vec{k}) = \begin{cases} \frac{1}{2\omega_k} + \frac{1}{2\pi i}\frac{1}{\omega_k} \ln\left|\frac{r_+(\vec{k})+\omega_k}{r_+(\vec{k})-\omega_k}\right|, & \text{if } |\vec{k}| \leq \Lambda \\ \frac{1}{2\omega_k} + \frac{1}{2\pi i}\frac{1}{\omega_k}\left(\ln\left|\frac{r_+(\vec{k})+\omega_k}{r_+(\vec{k})-\omega_k}\right| - \ln\left|\frac{\omega_k+r_-(\vec{k})}{\omega_k-r_-(\vec{k})}\right|\right), & \text{if } |\vec{k}| > \Lambda \end{cases} \tag{3.37}$$

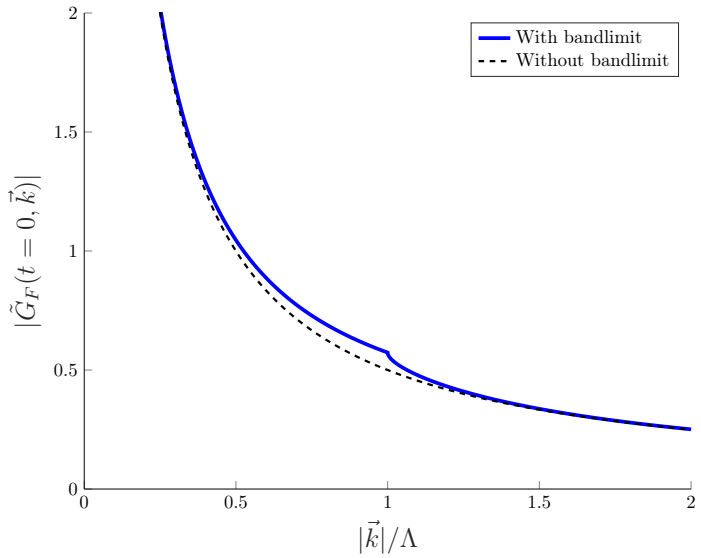

Figure 3.1: Magnitude of the equal-time Feynman propagator in Fourier space, $|\tilde{G}_F(t=0,\vec{k})|$, as a function of the mode amplitude $|\vec{k}|$. The propagator modified by the bandlimit is compared to the ordinary case without the bandlimit. The mass here is $m = 10^{-5}\Lambda$.

Note in the ordinary (non-bandlimited) theory, this quantity is simply $\tilde{G}_F(t=0,\vec{k}) = 1/2\omega_k$. A plot of this as a function of $|\vec{k}|$ is provided in Figure 3.1.

In [27, 72], this was further developed for cosmological spacetimes. We will not be examining these cases in this thesis, so we will refer the reader to these references for details. The basic idea is to find the eigenvectors of the d'Alembertian operator on these spacetimes, use these to construct a projector onto a bandlimited subspace, and then apply this projector to a choice of propagator.

Chapter 4

Statistical moments on manifolds

The present chapter along with the next two will be devoted to contructing and exploring a notion of local density of the degrees of freedom in bandlimited field theory. The premise for introducing such a concept will be discussed in the next chapter. There, we will see that quantifying this idea for nontrivial examples will require the ability to calculate the mean and variance of probability distributions on manifolds that are not simply Euclidean. In preparation for Chapters 5 and 6, in this chapter we will examine methods for computing such quantities. This warrants some discussion since we will see that one encounters some pitfalls if these quantities are naively calculated in analogy with their Euclidean counterparts, and an appropriate extension to non-Euclidean spaces is not necessarily obvious. Not only would this require a significant detour if included in the following chapters, but the problem turns out to be interesting in its own right and so we would like to present a relatively self-contained account here.

That there are issues in calculating statistical moments for probability distributions on non-Euclidean manifolds becomes clear after wrestling with the following deceptively simple problem [63]. Suppose a collection of sample points[1] are drawn from a probability distribution on a circle. For example, these could correspond to directions of some objects moving in a plane. Suppose we have two samples for points on the circle, given by angles $\pi/4$ and $7\pi/4$. What is their sample mean? Clearly in a physical scenario where these points on the circle correspond to directions in a plane, there is a preferred direction of 0. However, the arithmetic mean of these two numbers is π—the opposite of our expectation. (This situation is illustrated in Figure 4.1.) Now consider changing coordinates by

[1]Note that although we have been extensively discussing "sampling theory" in this thesis, our use of the term "sample" in this chapter will be exclusively in the statistical sense, as opposed to the appearance of the term elsewhere in the text.

translating $\theta \mapsto \theta + \pi/2 \,(\bmod 2\pi)$. The two samples are now labelled by $3\pi/4$ and $\pi/4$ (respectively), which have an arithmetic mean of $\pi/2$, corresponding to the point labelled by 0 in the old coordinates. So in these coordinates we obtain the correct result. However, the issue arises again in these new coordinates if we had been given the two samples $5\pi/4$ and $7\pi/4$ (with the "correct" arithmetic mean $3\pi/2$) in the old coordinates, which would correspond to $7\pi/4$ and $\pi/4$ (with the "incorrect" arithmetic mean π) in the new coordinates. Hence, we see that the point corresponding to the arithmetic mean of the angular samples depends on the choice of origin. In other words, the arithmetic mean is not covariant with respect to a change of coordinates.

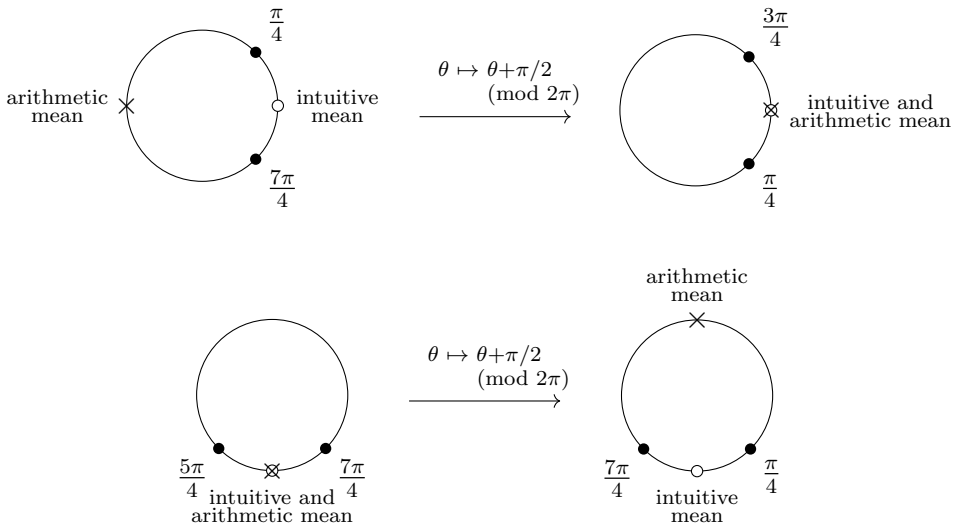

Figure 4.1: Arithmetric versus intuitive means for sample points on a circle. The arithmetic mean does not always agree with the intuitive mean, and further is not covariant with respect to changes of coordinates.

Superficially, this problem is reminiscent of the issue of branch cuts in complex analysis. One could think of the above procedure as attempting to take the arithmetic mean of the arguments of a set of complex numbers with modulus one (which could be phrased as taking the geometric mean of the complex numbers themselves). Although one could attempt to deal with the issue in a similar manner as for the complex plane, it is not clear how this could be generalized for arbitrary manifolds.

Here we will explore methods for quantifying appropriate measures of location and dispersion for a probability distribution on a general smooth manifold, which ordinarily

are taken to be the mean and variance for a random variable in $\mathbb{R}^n$. In particular, we want to find measures that transform appropriately under coordinate transformations.

We will begin in Section 4.1 by reviewing relevant background on so-called "directional statistics," developed to tackle the cases of S^1 and S^2 (as well as some extensions) [63, 84, 85]. Then, Section 4.2 will present definitions for the case of a general manifold, starting by abstracting certain features of the methods of directional statistics. We will see that there will be different means and variances depending on the choice of geometry for the manifold. The generalization of the methods of directional statistics yield extrinsic definitions for these quantities [50, 51], but one can also formulate intrinsic definitions [38, 76, 130]. Generally, these will not be the same, and we will see there is a kind of trade-off to be made when choosing between them [16, 17, 57]. Section 4.3 consists of an application of these ideas to the case of an n-torus with a Riemannian metric comprised of the flat metric plus a perturbation. This example will serve to illustrate the general discussion of Section 4.3, but the results will also be required in Chapter 6.

4.1 Background on directional statistics

Here we will examine a method for calculating a notion of mean and variance for a random variable that takes values on a circle, which will provide sufficient insight to suggest an approach for the general case. The review in this section is based on the treatments in [63, 84, 85].

First we will consider sets of sample points, which can then be straightforwardly applied to a distribution. The key trick is to think of a point on the circle as corresponding to the angle of a unit vector in $\mathbb{R}^2$. Suppose we are given a set of samples $\{\theta_i\}_{i=1}^N$. The coordinates in $\mathbb{R}^2$ corresponding to the sample θ_i will be given by $(x_i, y_i) = (\cos\theta_i, \sin\theta_i)$. Then define the *resultant vector*,

$$(\bar{x}, \bar{y}) := \left(\frac{1}{N} \sum_{i=1}^{N} \cos\theta_i, \frac{1}{N} \sum_{i=1}^{N} \sin\theta_i \right). \tag{4.1}$$

Note that although the vector corresponding to each sample lies on the unit circle, generally the resultant vector will not. Nevertheless, the *circular mean*, $\bar{\theta}$, will be taken to be the direction of the resultant vector, i.e., the solution to

$$\cos\bar{\theta} = \frac{\bar{x}}{\bar{\rho}}, \quad \sin\bar{\theta} = \frac{\bar{y}}{\bar{\rho}}, \quad \text{where } \bar{\rho} := \sqrt{\bar{x}^2 + \bar{y}^2}. \tag{4.2}$$

The circular mean will be our "measure of location" for sample points on a circle. To illustrate its validity, let us revisit the example presented in the introductory paragraphs of this chapter. Consider two samples: $\theta_1 = \pi/4$ and $\theta_2 = 7\pi/4$. The components of the resultant vector are: $(\bar{x}, \bar{y}) = (1/\sqrt{2}, 0)$, yielding a circular mean of $\bar{\theta} = 0$ on $[0, 2\pi)$, which is the intuitively correct result.

We noted earlier that an issue with the naive arithmetic mean of the angles is that it is not covariant. Let us demonstrate that the circular mean is covariant with respect to translations (we will postpone a discussion of general coordinate transformations to the next section). Consider a global translation of the samples by α, i.e., $\theta_i \mapsto \theta_i' = \theta_i + \alpha$. The new components of the resultant vector are

$$\begin{aligned}
\bar{x}' &= \frac{1}{N}\sum_i \cos\theta_i' \\
&= \frac{1}{N}\sum_i (\cos\theta_i \cos\alpha - \sin\theta_i \sin\alpha) \\
&= \bar{x}\cos\alpha - \bar{y}\sin\alpha \\
&= \bar{\rho}\cos\bar{\theta}\cos\alpha - \bar{\rho}\sin\bar{\theta}\sin\alpha \\
&= \bar{\rho}\cos(\bar{\theta} + \alpha),
\end{aligned}$$

and similarly,

$$\bar{y}' = \bar{\rho}\sin(\bar{\theta} + \alpha),$$

where we have used the relations $\bar{x} = \bar{\rho}\cos\bar{\theta} = \frac{1}{N}\sum_i \cos\theta_i$ and $\bar{y} = \bar{\rho}\sin\bar{\theta} = \frac{1}{N}\sum_i \sin\theta_i$. We see that the circular mean in these new coordinates is $\bar{\theta}' = \bar{\theta} + \alpha$, thus indeed covariant under translations. Note also that the length of the resultant vector, $\bar{\rho}$, is invariant under this transformation.

One may notice that the circular mean will be ill-defined if $\bar{\rho} = 0$. For example, this will occur in the case of samples $\{0, \pi/2, \pi, 3\pi/2\}$ which are equidistantly distributed around the circle. However, in this situation it is reasonable that one should leave the circular mean undefined because there is no appropriate sense in which one could choose a preferred point on the circle (or direction in $\mathbb{R}^2$) as the mean of these samples.

The magnitude of the resultant vector, $\bar{\rho}$, will always vanish whenever the sample points are maximally separated from one another in this way. On the other hand, if all of the samples are the same, $\theta_i = \theta\ \forall i$, then the resultant vector is $(\bar{x}, \bar{y}) = (\cos\theta, \sin\theta)$ with $\bar{\rho} = 1$. This suggests that some function of $\bar{\rho}$, such as $1 - \bar{\rho}$, could be used as a measure for the dispersion of the sample points.

We will show that this is indeed a good notion. First, let us write the distance between the circular mean, $\bar{\theta}$, and a sample point, $\theta_i \in [0, 2\pi)$, as

$$d_i \equiv d(\theta_i, \bar{\theta}) := \min(|\theta_i - \bar{\theta}|, 2\pi - |\theta_i - \bar{\theta}|) \in [0, \pi]. \tag{4.3}$$

Then the *dispersion* of this sample point with respect to $\bar{\theta}$ will be taken to be the following monotone increasing function of d_i:

$$D_i := 1 - \cos d_i = 1 - \cos(\theta_i - \bar{\theta}). \tag{4.4}$$

Our measure of dispersion for the entire set of sample data will then be

$$D := \tfrac{1}{N} \sum_{i=1}^{N} D_i = 1 - \tfrac{1}{N} \sum_{i=1}^{N} \cos(\theta_i - \bar{\theta}), \tag{4.5}$$

which we will call the *circular variance*. Notice that this can be rewritten,

$$\begin{aligned} \tfrac{1}{N} \sum_{i=1}^{N} \cos(\theta_i - \bar{\theta}) &= \tfrac{1}{N} \sum_{i} (\cos\theta_i \cos\bar{\theta} + \sin\theta_i \sin\bar{\theta}) \\ &= \bar{x} \cos\bar{\theta} + \bar{y} \sin\bar{\theta} \\ &= \bar{\rho} \cos^2\bar{\theta} + \bar{\rho} \sin^2\bar{\theta} \\ &= \bar{\rho}. \end{aligned}$$

Hence,

$$D = 1 - \bar{\rho}. \tag{4.6}$$

Notice also that this shows $\bar{\rho} = \frac{1}{N} \sum_{i=1}^{N} \cos(\theta_i - \bar{\theta}) \leq 1$, and since by definition $\bar{\rho} \geq 0$, we have $\bar{\rho} \in [0, 1]$. Therefore the circular variance lies in the interval $D \in [0, 1]$, achieving a maximum when the sample data is maximally dispersed around the circle ($\bar{\rho} = 0$) and minimised when the sample data is clustered at the same point ($\bar{\rho} = 1$). Earlier we also showed that $\bar{\rho}$ is invariant under translations, hence the circular variance is as well.

Discussing a finite set of sample data is useful for visualising the content of these definitions, but ultimately we are interested in the mean and variance as summary statistics for a probability distribution on a circle. It is simple to apply the above constructs to this setting. Consider a probability distribution $p(\theta)$ satisfying

$$p(\theta) \geq 0, \quad p(\theta + 2\pi) = p(\theta), \quad \int_0^{2\pi} d\theta \, p(\theta) = 1. \tag{4.7}$$

Throughout we will denote expectation values by

$$\langle f(\theta)\rangle_\theta := \int_0^{2\pi} d\theta\, p(\theta) f(\theta), \tag{4.8}$$

where the subscript θ included in $\langle\cdot\rangle_\theta$ denotes the random variable to be integrated over, to avoid confusion when there are multiple variables within the brackets.

Analogous to the above definitions for samples, we define the resultant vector,

$$(x, y) := (\langle\cos\theta\rangle_\theta, \langle\sin\theta\rangle_\theta) \equiv \left(\int_0^{2\pi} d\theta\, p(\theta)\cos(\theta), \int_0^{2\pi} d\theta\, p(\theta)\sin(\theta)\right), \tag{4.9}$$

the circular mean, μ, by

$$\cos\mu := \frac{x}{\rho}, \quad \sin\mu := \frac{y}{\rho}, \quad \rho := \sqrt{x^2 + y^2}, \tag{4.10}$$

and the circular variance,

$$\sigma^2 := 1 - \langle\cos(\theta - \mu)\rangle_\theta = 1 - \rho. \tag{4.11}$$

It is simple to see that these quantities will have the same properties as the sample quantities defined above. Note also that when $p(\theta)$ is highly localized around the mean μ, we have $\langle\cos(\theta-\mu)\rangle_\theta \approx 1 - \frac{1}{2}\langle(\theta-\mu)^2\rangle_\theta$ and so $\sigma^2 \approx \frac{1}{2}\langle(\theta-\mu)^2\rangle_\theta$, therefore recovering the definition for $\mathbb{R}$.

It is possible to quantify the sense in which the circular variance is a measure of the "spread" of a probability distribution through a so-called Chebyshev inequality. In the case of a probability distribution, $p(x)$, on $\mathbb{R}^n$, the Chebyshev inequality [36] is

$$\Pr[\|x - \mu\| \geq L] \leq \frac{\sigma^2}{L^2}, \tag{4.12}$$

where $\|\cdot\|$ denotes the Euclidean norm on $\mathbb{R}^n$, and $\mu := \langle x\rangle_x$ and $\sigma^2 := \langle(x-\mu)^2\rangle_x$ are the usual statistical moments. The Chebyshev inequality is simple to prove:

$$\begin{aligned}
\sigma^2 &= \int_{\mathbb{R}^n} dx\, p(x)\|x-\mu\|^2 \\
&\geq \int_{\|x-\mu\|\geq L} dx\, p(x)\|x-\mu\|^2 \\
&\geq L^2 \int_{\|x-\mu\|\geq L} dx\, p(x) \\
&= L^2 \Pr[\|x-\mu\| \geq L].
\end{aligned}$$

Intuitively, a probability distribution is "mostly contained" in a certain region if there is a large probability of finding a drawn sample in that region. Suppose we want to find a scale L characterizing the size of a region (centered at the mean) which contains at least $1-\varepsilon$ of the measure of the distribution (where $\varepsilon \in [0,1]$). That is, we want to find an L such that

$$\Pr[\|x-\mu\| \leq L] \geq 1-\varepsilon. \tag{4.13}$$

This is equivalent to finding an L such that

$$\Pr[\|x-\mu\| \geq L] \leq \varepsilon. \tag{4.14}$$

Now, using the Chebyshev inequality, we can argue that it is sufficient for

$$\frac{\sigma^2}{L^2} \leq \varepsilon \iff L \geq \frac{\sigma}{\sqrt{\varepsilon}}. \tag{4.15}$$

Naturally we see that to include a large proportion of the probability (small ε), we must choose L to be large. However, typically one does not want to commit to a specific arbitrary ε in order to characterize the size of the "spread" of the probability distribution. Hence, it is useful to summarize the size in terms of the proportionality factor σ. At the very least, it gives a means to compare the sizes of different probability distributions. That is, if a probability distribution has a larger variance than another, then it will typically require a larger region for a fixed ε. Although it is possible to obtain tighter bounds when considering certain classes of distributions, the Chebyshev inequality will suffice for our purposes in the subsequent chapters.

Now we will show that the circular variance we have defined exhibits a Chebyshev-type inequality [84,85], and hence is a useful measure of the spread of a probability distribution in the sense just described. First, let us recall that $1-\cos d(\theta,\mu)$ is a monotonic increasing function of the distance between θ and μ, i.e.,

$$d(\theta,\mu) := \min(|\theta-\mu|, 2\pi-|\theta-\mu|) \in [-\pi,\pi], \tag{4.16}$$

and hence $|\sin[\frac{1}{2}d(\theta,\mu)]| = \frac{1}{2}\sqrt{1-\cos d(\theta,\mu)}$ is as well. (We will have more to say about these different notions of distance in the next section.) Using this, the derivation is similar

to the $\mathbb{R}^n$ case:

$$\begin{aligned}
\sigma^2 &= 1 - \langle \cos(\theta - \mu) \rangle_\theta \\
&= \langle 2 \sin^2[\tfrac{1}{2}(\theta - \mu)] \rangle_\theta \\
&= 2 \int_0^{2\pi} d\theta \, p(\theta) \sin^2[\tfrac{1}{2}(\theta - \mu)] \\
&\geq 2 \int_{d(\theta,\mu) \geq L} d\theta \, p(\theta) \sin^2[\tfrac{1}{2}(\theta - \mu)] \\
&= 2 \int_{|\sin[\frac{1}{2}d(\theta,\mu)]| \geq |\sin(\frac{1}{2}L)|} d\theta \, p(\theta) \sin^2[\tfrac{1}{2}(\theta - \mu)] \\
&\geq 2 \sin^2(\tfrac{1}{2}L) \int_{|\sin[\frac{1}{2}(\theta-\mu)]| \geq |\sin(\frac{1}{2}L)|} d\theta \, p(\theta) \\
&= 2 \sin^2(\tfrac{1}{2}L) \Pr\left[|\sin[\tfrac{1}{2}(\theta - \mu)]| \geq |\sin(\tfrac{1}{2}L)| \right].
\end{aligned}$$

Therefore, the corresponding Chebyshev inequality for the circular variance is:

$$\Pr[d(\theta, \mu) \geq L] \leq \frac{\sigma^2}{2 \sin^2(\frac{1}{2}L)}. \tag{4.17}$$

As an example for the circular mean and variance, consider a probability distribution given by the square of a Dirichlet kernel centered at $\theta_0 \in [0, 2\pi)$:

$$p(\theta) = \frac{\sin^2[(2M+1)(\theta - \theta_0)/2]}{2\pi(2M+1)\sin^2[(\theta - \theta_0)/2]} = \frac{1}{2\pi(2M+1)} \left(\sum_{m=-M}^{M} e^{im(\theta - \theta_0)} \right)^2, \tag{4.18}$$

where M is a fixed positive integer. It is easy to check that this is normalized. We can calculate the components of the resultant vector as the real and imaginary parts of the following integral:

$$\phi := \int_0^{2\pi} d\theta \, p(\theta) e^{i\theta}. \tag{4.19}$$

Notice that the phase and magnitude of ϕ correspond to μ and ρ (respectively), i.e.,

$\phi = \rho e^{i\theta}$. We obtain

$$\begin{aligned}
\phi &= \frac{1}{2\pi(2M+1)} \sum_{m,m'=-M}^{M} e^{-i(m+m')\theta_0} \int_0^{2\pi} d\theta \, e^{i(m+m'+1)\theta} \\
&= \frac{1}{2\pi(2M+1)} \sum_{m,m'=-M}^{M} e^{-i(m+m')\theta_0} \, 2\pi\delta_{m',-m-1} \\
&= \frac{1}{2M+1} \sum_{m=-M}^{M-1} e^{i\theta_0} \\
&= \frac{2M}{2M+1} e^{i\theta_0}.
\end{aligned}$$

Note that upon evaluating the Kronecker delta function at $m' = -m-1$, we had to take into account that both m' and m are restricted to the range $[-M, M]$, which results in the upper bound of the sum over m to be truncated in the next step because $\delta_{m',-M-1} = 0$. Now we can read off

$$\mu = \theta_0, \quad \rho = \frac{2M}{2M+1}, \tag{4.20}$$

and hence

$$\sigma^2 = 1 - \rho = \frac{1}{2M+1}. \tag{4.21}$$

Similar techniques can be used to define notions of mean and variance on a sphere. The idea is to think of S^2 as a subset of $\mathbb{R}^3$. One then proceeds to calculate a resultant vector in $\mathbb{R}^3$, whose direction defines the mean direction on S^2 and whose length can be used to define the variance [84, 85]. In equations, given a probability distribution $p(\theta, \phi)$ on S^2,

$$\begin{aligned}
(\bar{x}, \bar{y}, \bar{z}) &:= (\langle \sin\theta\cos\phi \rangle_{\theta,\phi}, \langle \sin\theta\sin\phi \rangle_{\theta,\phi}, \langle \cos\theta \rangle_{\theta,\phi}) \\
\mu &:= (\bar{\theta}, \bar{\phi}) \quad \text{such that} \quad \tan\bar{\theta} = \frac{\sqrt{\bar{x}^2 + \bar{y}^2}}{\bar{z}}, \quad \tan\bar{\phi} = \frac{\bar{y}}{\bar{x}} \\
\sigma^2 &:= 1 - \rho := 1 - \sqrt{\bar{x}^2 + \bar{y}^2 + \bar{z}^2}.
\end{aligned}$$

There are other spaces whose elements correspond to "directional data" in some sense, which fall under the heading of directional statistics (see [85] and references therein). For example, this includes cases where random variables take values in a space of orthonormal frames (Stiefel manifolds) or subspaces of $\mathbb{R}^n$ (Grassmann manifolds). There has also been substantial work on shape spaces, which are quotients of Riemannian manifolds by the action of a Lie group. However, we would like a method which will apply to manifolds without any particular symmetry assumptions. We will now turn to this general case.

4.2 General manifolds

4.2.1 Basic definitions

We will now use these methods from directional statistics as inspiration for developing a notion for the mean and variance of a probability distribution, p, on an arbitrary smooth manifold, $\mathcal{M}$. In particular, we will capitalize on the idea of embedding the manifold $\mathcal{M}$ into a Euclidean space $\mathbb{R}^N$ (with $N \geq \dim \mathcal{M}$). This will lead to the concepts of *extrinsic* mean and variance [50, 51].

The Whitney embedding theorem guarantees that any smooth n-dimensional manifold can be smoothly embedded into $\mathbb{R}^{2n}$ (see, e.g., [80]). The theorem provides $2n$ as the smallest dimension required for the ambient Euclidean space, and it is an interesting topological problem to determine the minimum dimension needed for different classes of manifolds. Here, our interest is rather in providing a method of calculation, and so we will keep N arbitrary as it may occasionally be useful to choose a value larger than $2n$ (although practical computations may be more tedious if it is too large).

To this end, let $\mathcal{M}$ be a smooth n-dimensional manifold with coordinates[2] $(y^a)_{a=1}^n$. Let $p(y)$ be a probability distribution on $\mathcal{M}$, such that $p(y) \geq 0$ and $\int dy\, p(y) = 1$. Note that in order for the normalization of the probability distribution to remain invariant under a change of coordinates, we require $p(y)$ to be a scalar density, i.e., under $y^a \mapsto \tilde{y}^a$ we require $p(y) \mapsto \left|\partial y^a / \partial \tilde{y}^{\tilde{a}}\right| p(y)$.

Now suppose we have a smooth embedding $\psi : \mathcal{M} \to \mathbb{R}^N$. With coordinates $(x^i)_{i=1}^N$ on $\mathbb{R}^N$, we can write the embedding as $x^i = \psi^i(y)$. Define the *resultant vector* by

$$\bar{x}^i := \int dy\, p(y)\psi^i(y). \tag{4.22}$$

Note that since $\psi^i(y)$ is a scalar function on $\mathcal{M}$, the resultant vector will be invariant under general coordinate transformations on $\mathcal{M}$. We also see that this vector will be covariant with respect to (global) affine coordinate transformations on $\mathbb{R}^N$.

Generally $\bar{x}^i$ will not lie in the image of the embedding, $\psi(\mathcal{M})$. For example, we saw in the previous section that the resultant vector in $\mathbb{R}^2$ for a probability distribution on the unit circle typically resides inside the circle (and recall we used the magnitude of this

[2] Of course, generally one will require multiple coordinate charts to cover the manifold $\mathcal{M}$. For notational simplicity we will proceed formally using only one chart, but it should be clear how to apply these ideas more generally.

vector to construct a notion of variance). Therefore, it does not generally make sense to invert the embedding to arrive at a point on $\mathcal{M}$ corresponding to the mean value of $p(y)$. Instead, we will define the mean, μ^a, of $p(y)$ to be the closest point in the image of $\mathcal{M}$ under ψ to the resultant vector $\bar{x}^i$, i.e.,

$$\mu = \underset{y \in \mathcal{M}}{\operatorname{argmin}} \, \|\bar{x} - \psi(y)\|^2, \tag{4.23}$$

where $\|\cdot\|$ denotes the Euclidean norm on $\mathbb{R}^N$. We will not delve into the issue, but we should remark that there may be situations where μ is either not unique or not well-defined (as in the case of the circle when $\rho = 0$).

If there is a unique value for the mean, we then define the variance as:

$$\sigma^2 = \int dy \, p(y) \|\psi(y) - \psi(\mu)\|^2. \tag{4.24}$$

This definition is intuitive, and analogous to the typical definition in Euclidean space, but most importantly obeys a Chebyshev-type inequality:

$$\begin{aligned}
\sigma^2 &= \int dy \, p(y) \|\psi(y) - \psi(\mu)\|^2 \\
&\geq \int_{\|\psi(y) - \psi(\mu)\| \geq L} dy \, p(y) \|\psi(y) - \psi(\mu)\|^2 \\
&\geq L^2 \int_{\|\psi(y) - \psi(\mu)\| \geq L} dy \, p(y)
\end{aligned}$$

so that

$$\Pr[\|\psi(y) - \psi(\mu)\|^2 \geq L] \leq \frac{\sigma^2}{L^2}. \tag{4.25}$$

That is, the probability of $y \in \mathcal{M}$ being greater than a distance L from the mean μ decays quadratically with L with a proportionality factor of σ^2.

Note that although we are embedding $\mathcal{M}$ in $\mathbb{R}^N$, one should not think of the procedure as considering $p(y)$ to be a probability distribution in $\mathbb{R}^N$ with support only on some subset of the ambient Euclidean space. For example, a probability distribution nonzero only on the unit circle in $\mathbb{R}^2$ has measure zero. Rather, the use of the embedding is in pulling back structures from $\mathbb{R}^N$ to $\mathcal{M}$.

Let us show that these definitions reproduce the formulas of directional statistics in the special case of $\mathcal{M} = S^1$. We can choose the same embedding as before, $\psi : S^1 \to \mathbb{R}^2$

defined by $\theta \mapsto (x, y) := (\cos\theta, \sin\theta)$. The resultant vector is $(\bar{x}, \bar{y}) = (\langle\cos\theta\rangle_\theta, \langle\sin\theta\rangle_\theta)$. The mean is

$$\mu = \underset{\theta\in[0,2\pi)}{\operatorname{argmin}} \|(\bar{x}, \bar{y}) - (\cos\theta, \sin\theta)\|^2. \tag{4.26}$$

An explicit solution to this minimization is:

$$\begin{aligned} 0 &\stackrel{!}{=} \frac{\partial}{\partial\theta}\|(\bar{x}, \bar{y}) - (\cos\theta, \sin\theta)\|^2 \\ &= \frac{\partial}{\partial\theta}\left(\rho^2 - 2(\bar{x}\cos\theta + \bar{y}\sin\theta) + 1\right) \\ &= 2\bar{x}\sin\theta - 2\bar{y}\cos\theta \iff \tan\theta = \frac{\bar{y}}{\bar{x}}. \end{aligned}$$

So $\mu = \operatorname{atan}(\bar{y}/\bar{x})$, which coincides with the definition of the previous section. Note that in the above calculation we defined $\rho := \sqrt{\bar{x}^2 + \bar{y}^2}$ as in the previous section. The variance is

$$\begin{aligned} \sigma^2 &= \int_0^{2\pi} d\theta\, p(\theta)\|(\cos\theta, \sin\theta) - (\cos\mu, \sin\mu)\|^2 \\ &= \int_0^{2\pi} d\theta\, p(\theta)[2 - 2(\cos\theta\cos\mu + \sin\theta\sin\mu)] \\ &= 2 - 2(\bar{x}\cos\mu + \bar{y}\sin\mu) \\ &= 2(1 - \rho), \end{aligned}$$

which is the same as in the previous section (up to a factor of 2). One can similarly verify that these definitions also reproduce those of directional statistics for S^2.

These are simple extensions of the work that has been done in directional statistics, and reproduce the previous formulas for special cases of $\mathcal{M}$. However, there is an issue that we will now turn to discuss, which was perhaps not obvious from examining particular cases, but arises more naturally from this abstract formulation: do the values for the mean and variance with this approach depend on the choice of embedding $\psi : \mathcal{M} \to \mathbb{R}^N$?

4.2.2 Embedding dependence and distance functions

First, we notice that in the case of S^1 there is a rather trivial kind of embedding dependence, but it will help sharpen our understanding of the issue. Suppose instead of embedding points of S^1 into the unit circle in $\mathbb{R}^2$, we instead mapped them to points on a circle of radius R. Although this will not change the value of the mean μ, the variance will change

by $\sigma^2 \mapsto R^2\sigma^2$. This scaling affects every probability distribution in the same way, and so would not change how one would compare the spread of different distributions.

The reason that there is a difference is of course because we have changed the notion of distance on the circle induced by the embedding, i.e., for general $\psi : \mathcal{M} \to \mathbb{R}^N$, the induced distance function is

$$d_\psi(y, y') := \|\psi(y) - \psi(y')\|. \tag{4.27}$$

Although this is often called a *metric*, to avoid confusion we will call this a *distance function* because we will be discussing Riemannian metrics shortly, and the distance functions induced by those Riemannian metrics will typically not be the same as the distance functions we will discuss now.

With this notation, we can write the variance succinctly as $\sigma^2 = \langle d(y, \mu)^2 \rangle_y$. Recall our mean is defined as $\mu = \text{argmin}_{y \in \mathcal{M}} \|\bar{x} - \psi(y)\|^2$, but it will be useful for this discussion to rewrite this entirely in terms of distances between points on the manifold $\mathcal{M}$ (recall that the resultant vector $\bar{x}$ typically does not lie within $\psi(\mathcal{M})$). First, let us define the dispersion with respect to y as

$$D(y) := \langle d_\psi(y', y)^2 \rangle_{y'} = \int dy'\, p(y') \|\psi(y') - \psi(y)\|^2. \tag{4.28}$$

Then the mean can equivalently be defined as the point on the manifold which minimizes the dispersion,

$$\mu = \operatorname*{argmin}_{y \in \mathcal{M}} D(y). \tag{4.29}$$

Demonstrating this equivalence is straightforward. On one hand we have,

$$\begin{aligned}
\mu &= \operatorname*{argmin}_{y \in \mathcal{M}} \|\bar{x} - \psi(y)\|^2 \\
&= \operatorname*{argmin}_{y \in \mathcal{M}} \left(\|\bar{x}\|^2 - 2\bar{x} \cdot \psi(y) + \|\psi(y)\|^2 \right) \\
&= \operatorname*{argmin}_{y \in \mathcal{M}} \left(-2\bar{x} \cdot \psi(y) + \|\psi(y)\|^2 \right),
\end{aligned}$$

where we dropped the $\|\bar{x}\|^2$ term since it does not depend on y. On the other hand we

have,

$$\begin{aligned}\mu &= \operatorname*{argmin}_{y\in\mathcal{M}} \int dy'\, p(y')\|\psi(y') - \psi(y)\|^2 \\ &= \operatorname*{argmin}_{y\in\mathcal{M}} \int dy'\, p(y') \left(\|\psi(y')\|^2 - 2\psi(y')\cdot\psi(y) + \|\psi(y)\|^2\right) \\ &= \operatorname*{argmin}_{y\in\mathcal{M}} \left(-2\bar{x}\cdot\psi(y) + \|\psi(y)\|^2\right).\end{aligned}$$

Hence they are equivalent because the two functions being minimised in the definitions differ only by a quantity which does not depend on y.

We see that the mean and variance are determined by the distances between points on $\psi(\mathcal{M})$ induced by the geometry of the ambient Euclidean space. Of course, one would expect the mean and variance to depend on the geometry since they involve measures of distance and size. Any two embeddings giving the same induced distance will give the same result. However, it is clear that without any further assumptions, there are many different embeddings which may give different notions of distance, since the geometry is not dictated simply by requiring the embedding to be smooth. For example, it is easy to visualize many ways of smoothly embedding a circle into a plane which give very different geometries.

Let us now consider situations where the manifold is already equipped with some intrinsic geometry. This could just be some general distance function $d_{\mathcal{M}} : \mathcal{M}\times\mathcal{M}\to\mathbb{R}$ (which is positive definite, symmetric, and obeys the triangle inequality), or it could be the distance function induced by a Riemannian metric g,

$$d_g(y,y') := \inf_{\gamma} \int_{\gamma} d\tau \sqrt{g_{ab}\dot{x}^a\dot{x}^b}, \tag{4.30}$$

where γ is a curve with endpoints y and y'.

We have now arrived at definitions for the mean and variance solely in terms of distances between points on $\mathcal{M}$. We could also define these quantities purely intrinsically using only a distance function $d_{\mathcal{M}}$ on $\mathcal{M}$ (without the need for an embedding),

$$\begin{aligned}\mu &= \operatorname*{argmin}_{\tilde{\mu}\in\mathcal{M}} \langle d_{\mathcal{M}}(y,\tilde{\mu})^2\rangle_y \\ \sigma^2 &= \langle d_{\mathcal{M}}(y,\mu)^2\rangle_y.\end{aligned}$$

The formula for the variance is one which could have been guessed at the very beginning, after assuming some geometry on the manifold. However, the definition for the mean is perhaps less obvious.

These are the *intrinsic* definitions of mean and variance [16, 17, 38, 57, 76, 130]. Of course, these coincide with the earlier definitions when $d_{\mathcal{M}}$ is the same as the distance function induced by a particular embedding into a Euclidean space. However, given a $d_{\mathcal{M}}$ on $\mathcal{M}$, it is not always possible to find an isometric (in the sense of metric spaces, i.e., preserving the distance function) embedding into $\mathbb{R}^N$ with the usual Euclidean distance function. For example, it is well-known that the sphere S^2 with the metric $d\theta^2 + \sin^2\theta d\phi^2$ and corresponding induced (geodesic) distance function cannot be embedded into any Euclidean space while preserving distances between points.[3] In fact, we encountered this in the previous section, where we had the geodesic distance on the circle (metric $g = d\theta^2$),

$$d_g(\theta, \theta') = \min\{|\theta - \theta'|, 2\pi - |\theta - \theta'|\} = \pi - |\pi - |\theta - \theta'||, \tag{4.31}$$

which, after embedding into $\mathbb{R}^2$, corresponds to the circumferential distance between the points around the circle. Note that there are two different geodesics between any two points on the circle (one going around each way), which is why we need the min. In contrast, the geodesic distance in $\mathbb{R}^2$, induced by the embedding $\psi : \theta \mapsto (\cos\theta, \sin\theta)$, is

$$d_\psi(\theta, \theta') = \|(\cos\theta, \sin\theta) - (\cos\theta', \sin\theta')\| = 2|\sin[\tfrac{1}{2}(\theta - \theta')]|. \tag{4.32}$$

The reason the geodesic distances are different, even though the embedding is a Riemannian isometry (i.e., preserves the Riemannian metric, and hence lengths of curves), is because the geodesic in $\mathbb{R}^2$ does not lie within the image of the embedding. Rather, the distance function is the length of the chord between the two points on the circle. Hence, even though the Riemannian metric and curve lengths are preserved, the distance function is not.

What is the virtue of using the embedding of $\mathcal{M}$ into a Euclidean space to calculate statistical moments, if there is a (possibly different) intrinsic definition that reflects the original geometry of the manifold? Although the intrinsic definitions are in a sense more natural, using the embeddings can be practically much more convenient. For example, let us revisit our original example of determining the mean of two sample data points $\pi/4$ and $7\pi/4$ on S^1. For the purposes of the calculation, we can think of this as a distribution $p(\theta) = \frac{1}{2}\delta(\theta - \pi/4) + \frac{1}{2}\delta(\theta - 7\pi/4)$. Then using the intrinsic distance, $d_g(\theta, \theta') =$

[3] For a very simple demonstration using only the metric space structure, see [103].

$\min\{|\theta - \theta'|, 2\pi - |\theta - \theta'|\}$,

$$\begin{aligned}\mu &= \underset{\theta\in[0,2\pi)}{\operatorname{argmin}} \left[\tfrac{1}{2}d_g(\tfrac{\pi}{4},\theta)^2 + \tfrac{1}{2}d_g(\tfrac{7\pi}{4},\theta)^2\right] \\ &= \underset{\theta\in[0,2\pi)}{\operatorname{argmin}} \begin{cases} \frac{1}{2}(\theta - \frac{\pi}{4})^2 + \frac{1}{2}(\theta + \frac{\pi}{4})^2 & \text{if } \theta \in [0, \frac{3\pi}{4}] \\ \frac{1}{2}(\theta - \frac{\pi}{4})^2 + \frac{1}{2}(\theta - \frac{7\pi}{4})^2 & \text{if } \theta \in [\frac{3\pi}{4}, \frac{5\pi}{4}] \\ \frac{1}{2}(\theta - \frac{9\pi}{4})^2 + \frac{1}{2}(\theta - \frac{7\pi}{4})^2 & \text{if } \theta \in [\frac{5\pi}{4}, 2\pi] \end{cases}\end{aligned}$$

The local minima on these intervals are at 0, π, and 2π. Checking these and the endpoints of the intervals, we find that the minimum of the dispersion is $\pi^2/16$ when $\theta = 0$, hence $\mu = 0$. Whereas for the embedded distance, we worked out an analytic formula for the mean, $\mu = \operatorname{atan}(\langle \sin\theta \rangle_\theta / \langle \cos\theta \rangle_\theta)$, which we can calculate as

$$\mu = \operatorname{Arg}\left(\tfrac{1}{2}e^{i\frac{\pi}{4}} + \tfrac{1}{2}e^{i\frac{7\pi}{4}}\right) = \operatorname{Arg}(\cos\tfrac{\pi}{4}) = 0.$$

Although calculation of the mean is less tedious in the second case, calculation of the variance in both cases is straightforward. Using the intrinsic definition we get $\sigma^2 = \frac{\pi^2}{16} \approx 0.617$, whereas with the embedded distance, $\sigma^2 = 2(1-\rho) = 2 - \sqrt{2} \approx 0.586$.

This was only the case of two sample data points. Clearly the first method becomes even more tedious with more sample data points (since it will involve splitting into a multitude of subintervals). For a distribution it is possible to formulate the first method in a less tedious manner. However it turns out that finding explicit expressions for μ and σ^2 is difficult. Furthermore, this is also a case where the geodesics are rather trivial. Generally one would have to first solve the geodesic equation to obtain an expression for the geodesic distance between any two points before calculating the dispersion. The distance function in $\mathbb{R}^N$ is typically much simpler (although the task in this case is to find an appropriate embedding, which may be challenging, but we will discuss this more in the next section).

We see that using an embedding of $\mathcal{M}$ into a Euclidean space can (in certain circumstances) give a more practical method of calculating a mean and variance, even though it will generally yield different values than the use of intrinsic methods. Indeed, in the following chapters we will be using such an embedding.

Let us now return to the issue of choosing an appropriate embedding. Generally different embeddings will induce different distance functions on $\mathcal{M}$. If we restrict our attention to cases where there is a Riemannian metric g on $\mathcal{M}$, we can at least eliminate some of the ambiguity by trying to reflect the intrinsic geometry as much as possible by demanding that the embedding preserves the metric. Then, although geodesic distances between points will be different in the two spaces, lengths of curves within $\mathcal{M}$ will remain the same.

Let us then fix a particular Riemannian metric g on $\mathcal{M}$ and insist that the embedding $\psi : \mathcal{M} \to \mathbb{R}^N$ preserves the metric (i.e., $\psi^*\delta = g$, where δ_{ij} is the Euclidean metric). The existence of such a map is no longer guaranteed by the Whitney embedding theorem, but we have the Nash embedding theorem which states that any smooth n-dimensional Riemannian manifold admits a (global) smooth isometric embedding into $\mathbb{R}^N$ (see, e.g., [47, 116]). The theorem also gives bounds for how large a dimension N is required, but again, here we will not be overly concerned with minimizing N.

If we assume the embeddings are isometric, are the mean and variance uniquely determined? In other words, do all isometric embeddings yield the same induced distance function on $\mathcal{M}$? More explicitly, given two isometric embeddings $\psi : \mathcal{M} \to \mathbb{R}^N$ and $\tilde{\psi} : \mathcal{M} \to \mathbb{R}^{\tilde{N}}$ (where we allow $\tilde{N} \neq N$), we would like to know if $\|\psi(y) - \psi(y')\| = \|\tilde{\psi}(y) - \tilde{\psi}(y')\|$ for all $y, y' \in \mathcal{M}$. Since embeddings are injective, this is equivalent to the condition that $\tilde{\psi} \circ \psi^{-1}$ is an isometry (of the Riemannian metric and the distance function) of the subsets $\psi(\mathcal{M})$, $\tilde{\psi}(\mathcal{M})$ of these Euclidean spaces. This occurs if and only if, when restricted to $\psi(\mathcal{M})$, $\tilde{\psi} \circ \psi^{-1}$ is a composition of a linear orthogonal transformation plus a translation. In geometry, this property is a concept known as *rigidity* [47, 116]. There are known examples and counterexamples for certain classes of manifolds, although most of the work has been focused on the case of embedding 2-dimensional surfaces into $\mathbb{R}^3$. For example, it is known that any metric on S^2 with positive Gauss curvature has a smooth isometric embedding into $\mathbb{R}^3$, which is unique up to an isometry of $\mathbb{R}^3$ [47]. It is an interesting question to consider which classes of manifolds are rigid in this sense, as this would guarantee unique values for the mean and variance we have defined. However, it will become clear that imposing any such assumptions or restrictions on the class of manifolds we consider will be too strong in order to proceed with the particular cases that will be examined in this thesis. Indeed, in the next section we will furnish an example of two different isometric embeddings of an n-torus in two different dimensional Euclidean spaces and explicitly show that the mean obtained by these two embeddings are different.

However, this does not imply that the approach of calculating statistical moments through embeddings into $\mathbb{R}^N$ is invalid. Although there remains an ambiguity in the choice of embedding, we at least have a set of measures for the location and dispersion of probability distributions on an arbitrary manifold. If we fix a particular embedding, we can still use this method to compare different distributions. By at least requiring that the embedding is isometric (in the Riemannian sense), the hope is that this is enough of a restriction on the geometry so that the dependence on the choice of embedding is not too large. It is clear that further work needs to be done to determine how different the results can be with different embeddings (perhaps focused on how different they will be from a use of the intrinsic distance, which is in a sense the most natural one, even if difficult

to use). Also, it would be important to know if one is able to get contradictory results, e.g., whether the variance of a distribution is larger than another under one embedding, but smaller under another. It could be that some palatable assumption can be made to guarantee that the values are sufficiently close for certain applications. There have been some analyses carried out for the purposes of statistics [16, 17, 57], but one would have to study this more for the purposes considered in this thesis. We will not go into these issues much further, but will simply be employing this method in the following chapters.

Before proceeding, let us summarize the definitions and our discussion of them. Given a probability distribution p and a distance function $d_{\mathcal{M}}$ on a smooth manifold $\mathcal{M}$, we define the mean and variance of p as (respectively):

$$\mu := \operatorname*{argmin}_{\tilde{\mu} \in \mathcal{M}} \langle d_{\mathcal{M}}(y, \tilde{\mu})^2 \rangle_y \tag{4.33}$$

$$\sigma^2 := \langle d_{\mathcal{M}}(y, \mu)^2 \rangle_y, \tag{4.34}$$

where $\langle f(y) \rangle_y := \int_{\mathcal{M}} dy\, p(y) f(y)$. This definition of the mean μ is covariant, and σ^2 invariant, with respect to coordinate transformations on the manifold. The distribution obeys a Chebyshev-type inequality,

$$\Pr[d_{\mathcal{M}}(y, \mu) \geq L] \leq \frac{\sigma^2}{L^2}. \tag{4.35}$$

Given a smooth embedding $\psi : \mathcal{M} \to \mathbb{R}^N$, we obtain a distance function on $\mathcal{M}$ induced by the Euclidean distance in $\mathbb{R}^N$, namely $d_\psi(y, y') := \|\psi(y) - \psi(y')\|$, which we can use in the above definitions. If there is a Riemannian metric g on $\mathcal{M}$, we can further require this embedding to preserve the metric (i.e., an isometry of Riemannian manifolds). Alternatively, one could use the geodesic distance induced by the metric as an intrinsic distance function on $\mathcal{M}$.

When there is a Riemannian metric on $\mathcal{M}$, there is a trade-off in choosing between the intrinsic and induced/extrinsic distance functions. The intrinsic distance function faithfully reflects the (intrinsic) geometry of the manifold, and is in a sense more natural, however practical calculations can be quite tedious. Using induced distance functions is much simpler in certain situations, but there is seemingly no preferred choice of embedding, leading to some ambiguity in what should constitute appropriate values for the mean and variance. Despite this, the embedding dependence may not be a fatal flaw with the approach, as it will still allow us to compare sizes of different distributions after fixing an embedding.

4.3 Application: geometric perturbation on T^n

Beyond supplying theoretical background that we will need in Chapters 5 and 6, the tools developed in this chapter will be applied to a particular example in Chapter 6 of a probability distribution on an n-torus, T^n, with both a flat metric and a perturbation of the flat metric. For later use, as well as to provide further illustration of the above theoretical discussion, in this section we will construct an appropriate isometric embedding of T^n into a Euclidean space and the corresponding mean and variance.

Let $T^n = S^1 \times S^1 \times \cdots \times S^1$ (n times) be given coordinates $\theta \equiv (\theta_i)_{i=1}^n \in [0, 2\pi)^n$. Consider first the case of equipping T^n with the flat metric $g = \sum_{i=1}^n d\theta_i^2$. Since it is just a product of circles, there is a very simple isometric embedding of T^n into $\mathbb{R}^{2n}$, given by

$$(\theta_1, \theta_2, \ldots, \theta_n) \mapsto (\cos\theta_1, \sin\theta_1, \cos\theta_2, \sin\theta_2, \ldots, \cos\theta_n, \sin\theta_n). \tag{4.36}$$

Suppose we are given a probability distribution p on T^n, which is nonnegative, integrates to 1, and is 2π-periodic in each θ_i. The expressions for the mean and variance generalize straightforwardly from the S^1 case. Indeed, we find for the mean

$$\begin{aligned}\mu &= \operatorname*{argmin}_{\tilde{\mu}\in\mathcal{M}} \sum_{i=1}^n \|(\langle\cos\theta_i\rangle_\theta, \langle\sin\theta_i\rangle_\theta) - (\cos\tilde{\mu}_i, \sin\tilde{\mu}_i)\|^2 \\ &= \operatorname*{argmin}_{\tilde{\mu}\in\mathcal{M}} \sum_{i=1}^n \left(\langle\cos\theta_i\rangle_\theta \cos\tilde{\mu}_i + \langle\sin\theta_i\rangle_\theta \sin\tilde{\mu}_i\right),\end{aligned}$$

which is similar to the S^1 case, and we can see is minimized by

$$\mu_i = \operatorname{atan}(\langle\sin\theta_i\rangle_\theta / \langle\cos\theta_i\rangle_\theta). \tag{4.37}$$

The variance is

$$\begin{aligned}\sigma^2 &= \langle \sum_{i=1}^n \|(\cos\theta_i, \sin\theta_i) - (\cos\mu_i, \sin\mu_i)\|^2 \rangle_\theta \\ &= 2\sum_{i=1}^n (1 - \rho_i),\end{aligned} \tag{4.38}$$

where $\rho_i := \sqrt{\langle\cos\theta_i\rangle_\theta^2 + \langle\sin\theta_i\rangle_\theta^2}$.

Now let us proceed to consider perturbing the metric $\delta_{ij} \mapsto \delta_{ij} + h_{ij}$, with $|h_{ij}| \ll 1$. Throughout we will be working to first order in the perturbation h_{ij}. First, we must find

an embedding into $\mathbb{R}^N$ such that the induced metric on the image of T^n is $\delta_{ij} + h_{ij}$, at least to first order.

Generally this problem can be phrased in terms of a set of partial differential equations [47]. Let us first consider a general smooth manifold $\mathcal{M}$, and let $\psi : \mathcal{M} \to \mathbb{R}^N$ be an isometric embedding of $\mathcal{M}$ with a *background* metric g. Upon a perturbation of the metric, $g \mapsto g + h$, we aim to find a perturbation of the embedding, $\psi + \tilde{\psi} : \mathcal{M} \to \mathbb{R}^N$, such that $(\psi + \tilde{\psi})^* \delta = g + h$, or

$$\partial_i(\psi + \tilde{\psi}) \cdot \partial_j(\psi + \tilde{\psi}) = g_{ij} + h_{ij},$$

where $\cdot$ denotes the Euclidean inner product (i.e., $\partial_i \psi \cdot \partial_j \psi = \delta_{ab} \partial_i \psi^a \partial_j \psi^b$). Since $\psi^* \delta = g$, we have $\partial_i \psi \cdot \partial_j \psi = g_{ij}$. Then we can rewrite the above as

$$\partial_i \psi \cdot \partial_j \tilde{\psi} + \partial_i \tilde{\psi} \cdot \partial_j \psi + \partial_i \tilde{\psi} \cdot \partial_j \tilde{\psi} = h_{ij}.$$

Since ψ is the known and fixed solution to the unperturbed problem, this is a nonlinear PDE for $\tilde{\psi}$. If we assume that $\tilde{\psi}$ is first order in the perturbation, then to first order we can neglect the non-linear term $\partial_i \tilde{\psi} \cdot \partial_j \tilde{\psi}$. After rewriting the derivatives, to first order we have

$$-2(\partial_i \partial_j \psi) \cdot \tilde{\psi} + \partial_i(\tilde{\psi} \cdot \partial_j \psi) + \partial_j(\tilde{\psi} \cdot \partial_i \psi) = h_{ij}. \tag{4.39}$$

Now, observe that if we can find a $\tilde{\psi}$ satisfying

$$\begin{aligned} (\partial_i \psi) \cdot \tilde{\psi} &= 0 \\ (\partial_i \partial_j \psi) \cdot \tilde{\psi} &= -\tfrac{1}{2} h_{ij} \end{aligned} \tag{4.40}$$

it will be sufficient to solve the above equation. Note that this is no longer a differential equation, but simply a linear system that we wish to solve for the vector $\tilde{\psi} \in \mathbb{R}^N$. This linear system is generally useful in studying isometric embeddings of Riemannian manifolds, even beyond perturbations to first order by reintroducing the nonlinear term and carefully setting up an iteration process [47]. We will simply look for a solution (to first order) for our particular problem on T^n.

Let us begin by analysing the case $n = 2$. We will then use our findings for this case to guess the solution for general n. First, let us write out the linear system for $\tilde{\psi}$, using the background embedding $\psi : T^2 \to \mathbb{R}^4$ given by $(\theta_1, \theta_2) \mapsto (\cos\theta_1, \sin\theta_1, \cos\theta_2, \sin\theta_2)$. We have

$$\begin{bmatrix} -\sin\theta_1 & \cos\theta_1 & 0 & 0 \\ 0 & 0 & -\sin\theta_2 & \cos\theta_2 \\ -\cos\theta_1 & -\sin\theta_1 & 0 & 0 \\ 0 & 0 & -\cos\theta_2 & -\sin\theta_2 \\ 0 & 0 & 0 & 0 \end{bmatrix} \tilde{\psi} = \begin{bmatrix} 0 \\ 0 \\ -\frac{1}{2}h_{11} \\ -\frac{1}{2}h_{22} \\ -\frac{1}{2}h_{12} \end{bmatrix} \tag{4.41}$$

Clearly, we see that there is no solution to the system since the last equation cannot be satisfied.

We will fix this by finding a different isometric embedding of the flat 2-torus, i.e., a different solution ψ to the unperturbed problem, so that it yields a different linear system which admits a solution. Note that the linear system (4.40) has $n+n(n+1)/2 = n(n+3)/2$ equations (independently of N). Generally, we do not need the linear operator on the left-hand side to be full rank, even for arbitrary h_{ij}, since some of the components of the vector on the right-hand side are always fixed to 0. However, it is clear that embedding into a higher dimensional space gives us more degrees of freedom to work with, and so may make it easier to find a system which admits at least one solution.

We will show that the following embedding, $\psi : T^2 \to \mathbb{R}^8$, works for the zeroth order problem,

$$(\theta_1, \theta_2) \mapsto \tfrac{1}{\sqrt{3}}(\cos\theta_1, \sin\theta_1, \cos\theta_2, \sin\theta_2, \\ \cos(\theta_1-\theta_2), \sin(\theta_1-\theta_2), \cos(\theta_1+\theta_2), \sin(\theta_1+\theta_2)). \tag{4.42}$$

We want to show that this is an isometric embedding of the flat metric on the torus, i.e., that $\partial_i\psi \cdot \partial_j\psi = \delta_{ij}$. We have

$$\frac{\partial\psi}{\partial\theta_1} = \tfrac{1}{\sqrt{3}}(-\sin\theta_1, \cos\theta_1, 0, 0, -\sin(\theta_1-\theta_2), \cos(\theta_1-\theta_2), -\sin(\theta_1+\theta_2), \cos(\theta_1+\theta_2))$$
$$\frac{\partial\psi}{\partial\theta_2} = \tfrac{1}{\sqrt{3}}(0, 0, -\sin\theta_2, \cos\theta_2, \sin(\theta_1-\theta_2), -\cos(\theta_1-\theta_2), -\sin(\theta_1+\theta_2), \cos(\theta_1+\theta_2)),$$

from which it is easy to verify

$$\|\frac{\partial\psi}{\partial\theta_1}\|^2 = \|\frac{\partial\psi}{\partial\theta_2}\|^2 = 1$$
$$\frac{\partial\psi}{\partial\theta_1} \cdot \frac{\partial\psi}{\partial\theta_2} = 0.$$

Now let us return to the embedding of a metric perturbation $\delta_{ij} \mapsto \delta_{ij} + h_{ij}$ on T^2 and the linear system (4.40). Using our new zeroth order embedding $\psi : T^2 \mapsto \mathbb{R}^8$, the linear system becomes

$$\tfrac{1}{\sqrt{3}}\begin{bmatrix} -\sin\theta_1 & \cos\theta_1 & 0 & 0 & -\sin(\theta_1-\theta_2) & \cos(\theta_1-\theta_2) & -\sin(\theta_1+\theta_2) & \cos(\theta_1+\theta_2) \\ 0 & 0 & -\sin\theta_2 & \cos\theta_2 & \sin(\theta_1-\theta_2) & -\cos(\theta_1-\theta_2) & -\sin(\theta_1+\theta_2) & \cos(\theta_1+\theta_2) \\ -\cos\theta_1 & -\sin\theta_1 & 0 & 0 & -\cos(\theta_1-\theta_2) & -\sin(\theta_1-\theta_2) & -\cos(\theta_1+\theta_2) & -\sin(\theta_1+\theta_2) \\ 0 & 0 & -\cos\theta_2 & -\sin\theta_2 & -\cos(\theta_1-\theta_2) & -\sin(\theta_1-\theta_2) & -\cos(\theta_1+\theta_2) & -\sin(\theta_1+\theta_2) \\ 0 & 0 & 0 & 0 & \cos(\theta_1-\theta_2) & \sin(\theta_1-\theta_2) & -\cos(\theta_1+\theta_2) & -\sin(\theta_1+\theta_2) \end{bmatrix} \tilde{\psi} = \begin{bmatrix} 0 \\ 0 \\ -\frac{1}{2}h_{11} \\ -\frac{1}{2}h_{22} \\ -\frac{1}{2}h_{12} \end{bmatrix}$$

We will now solve this system. It will be useful to note that some of the 2×2 blocks of the above operator can be identified as compositions of rotations and reflections, so it will be convenient to define:

$$R(\theta) := \begin{bmatrix} \cos\theta & \sin\theta \\ -\sin\theta & \cos\theta \end{bmatrix}, \quad Z := \begin{bmatrix} 1 & 0 \\ 0 & -1 \end{bmatrix}. \tag{4.43}$$

Some useful identities are $R(\theta)R(\theta') = R(\theta + \theta')$ and $R(\theta)ZR(\theta') = ZR(\theta' - \theta)$. After rearranging some rows, the system can be easily solved:

$$\left[\begin{array}{cccccccc|c} -\cos\theta_1 & -\sin\theta_1 & 0 & 0 & -\cos(\theta_1-\theta_2) & -\sin(\theta_1-\theta_2) & -\cos(\theta_1+\theta_2) & -\sin(\theta_1+\theta_2) & -\frac{\sqrt{3}}{2}h_{11} \\ -\sin\theta_1 & \cos\theta_1 & 0 & 0 & -\sin(\theta_1-\theta_2) & \cos(\theta_1-\theta_2) & -\sin(\theta_1+\theta_2) & \cos(\theta_1+\theta_2) & 0 \\ 0 & 0 & -\cos\theta_2 & -\sin\theta_2 & -\cos(\theta_1-\theta_2) & -\sin(\theta_1-\theta_2) & -\cos(\theta_1+\theta_2) & -\sin(\theta_1+\theta_2) & -\frac{\sqrt{3}}{2}h_{22} \\ 0 & 0 & -\sin\theta_2 & \cos\theta_2 & \sin(\theta_1-\theta_2) & -\cos(\theta_1-\theta_2) & -\sin(\theta_1+\theta_2) & \cos(\theta_1+\theta_2) & 0 \\ 0 & 0 & 0 & 0 & \cos(\theta_1-\theta_2) & \sin(\theta_1-\theta_2) & -\cos(\theta_1+\theta_2) & -\sin(\theta_1+\theta_2) & -\frac{\sqrt{3}}{2}h_{12} \end{array}\right]$$

$$= \left[\begin{array}{cccc|c} -ZR(\theta_1) & 0 & -ZR(\theta_1-\theta_2) & -ZR(\theta_1+\theta_2) & \begin{pmatrix} -\frac{\sqrt{3}}{2}h_{11} \\ 0 \end{pmatrix} \\ 0 & -ZR(\theta_2) & -R(\theta_1-\theta_2) & -ZR(\theta_1+\theta_2) & \begin{pmatrix} -\frac{\sqrt{3}}{2}h_{11} \\ 0 \end{pmatrix} \\ 0\ \ 0 & 0\ \ 0 & \cos(\theta_1-\theta_2)\ \ \sin(\theta_1-\theta_2) & -\cos(\theta_1+\theta_2)\ \ -\sin(\theta_1+\theta_2) & -\frac{\sqrt{3}}{2}h_{12} \end{array}\right]$$

$$\sim \left[\begin{array}{cccc|c} I & 0 & R(-\theta_2) & R(\theta_2) & R(-\theta_1)\begin{pmatrix} \frac{\sqrt{3}}{2}h_{11} \\ 0 \end{pmatrix} \\ 0 & I & ZR(\theta_1) & R(\theta_1) & R(-\theta_2)\begin{pmatrix} \frac{\sqrt{3}}{2}h_{11} \\ 0 \end{pmatrix} \\ 0\ \ 0\ \ 0\ \ 0 & \cos(\theta_1-\theta_2)\ \ \sin(\theta_1-\theta_2) & -\cos(\theta_1+\theta_2)\ \ -\sin(\theta_1+\theta_2) & & -\frac{\sqrt{3}}{2}h_{12} \end{array}\right]$$

We see that there is a 3-dimensional solution space, each point of which corresponds to a different isometric embedding. We will just require a single solution, so let us choose the last four components of $\tilde{\psi}$ to be

$$-\tfrac{\sqrt{3}}{4}h_{12}\left(\cos(\theta_1-\theta_2), \sin(\theta_1-\theta_2), -\cos(\theta_1+\theta_2), -\sin(\theta_1+\theta_2)\right),$$

which solves the bottom line. Then the full solution is

$$\tilde{\psi}(\theta_1,\theta_2) = \begin{bmatrix} R(-\theta_1)\begin{pmatrix}\frac{\sqrt{3}}{2}h_{11}\\0\end{pmatrix} + \frac{\sqrt{3}}{4}h_{12}R(-\theta_2)\begin{pmatrix}\cos(\theta_1-\theta_2)\\\sin(\theta_1-\theta_2)\end{pmatrix} - \frac{\sqrt{3}}{4}h_{12}R(\theta_2)\begin{pmatrix}\cos(\theta_1+\theta_2)\\\sin(\theta_1+\theta_2)\end{pmatrix} \\ R(-\theta_2)\begin{pmatrix}\frac{\sqrt{3}}{2}h_{22}\\0\end{pmatrix} + \frac{\sqrt{3}}{4}h_{12}ZR(\theta_1)\begin{pmatrix}\cos(\theta_1-\theta_2)\\\sin(\theta_1-\theta_2)\end{pmatrix} - \frac{\sqrt{3}}{4}h_{12}R(\theta_1)\begin{pmatrix}\cos(\theta_1+\theta_2)\\\sin(\theta_1+\theta_2)\end{pmatrix} \\ -\frac{\sqrt{3}}{4}h_{12}\begin{pmatrix}\cos(\theta_1-\theta_2)\\\sin(\theta_1-\theta_2)\end{pmatrix} \\ \frac{\sqrt{3}}{4}h_{12}\begin{pmatrix}\cos(\theta_1+\theta_2)\\\sin(\theta_1+\theta_2)\end{pmatrix} \end{bmatrix}$$

$$= \begin{bmatrix} \frac{\sqrt{3}}{2}h_{11}\begin{pmatrix}\cos\theta_1\\\sin\theta_1\end{pmatrix} \\ \frac{\sqrt{3}}{2}h_{22}\begin{pmatrix}\cos\theta_2\\\sin\theta_2\end{pmatrix} \\ -\frac{\sqrt{3}}{4}h_{12}\begin{pmatrix}\cos(\theta_1-\theta_2)\\\sin(\theta_1-\theta_2)\end{pmatrix} \\ \frac{\sqrt{3}}{4}h_{12}\begin{pmatrix}\cos(\theta_1+\theta_2)\\\sin(\theta_1+\theta_2)\end{pmatrix} \end{bmatrix}, \tag{4.44}$$

where we used the following to simplify:

$$R(\theta)\begin{bmatrix}\cos\alpha\\\sin\alpha\end{bmatrix} = \begin{bmatrix}\cos\theta & \sin\theta\\-\sin\theta & \cos\theta\end{bmatrix}\begin{bmatrix}\cos\alpha\\\sin\alpha\end{bmatrix} = \begin{bmatrix}\cos(\alpha-\theta)\\\sin(\alpha-\theta)\end{bmatrix}.$$

Therefore, to first order in h_{ij}, we have an isometric embedding of T^2 with the metric $\delta_{ij}+h_{ij}$ into $\mathbb{R}^8$, given by

$$(\psi+\tilde{\psi}):(\theta_1,\theta_2)\mapsto \begin{bmatrix} \left(\frac{1}{\sqrt{3}}+\frac{\sqrt{3}}{2}h_{11}\right)\begin{pmatrix}\cos\theta_1\\\sin\theta_1\end{pmatrix} \\ \left(\frac{1}{\sqrt{3}}+\frac{\sqrt{3}}{2}h_{22}\right)\begin{pmatrix}\cos\theta_2\\\sin\theta_2\end{pmatrix} \\ \left(\frac{1}{\sqrt{3}}-\frac{\sqrt{3}}{4}h_{12}\right)\begin{pmatrix}\cos(\theta_1-\theta_2)\\\sin(\theta_1-\theta_2)\end{pmatrix} \\ \left(\frac{1}{\sqrt{3}}+\frac{\sqrt{3}}{4}h_{12}\right)\begin{pmatrix}\cos(\theta_1+\theta_2)\\\sin(\theta_1+\theta_2)\end{pmatrix} \end{bmatrix}. \tag{4.45}$$

Now let us use this solution to guess a solution for general n, and then show that it works. For the zeroth order problem (flat metric), we will choose the embedding $\psi: T^n \to$

$\mathbb{R}^{2n^2}$ to be

$$\begin{aligned}\psi : (\theta_i)_{i=1}^n \mapsto & \frac{1}{\sqrt{2n-1}}\left[\bigoplus_{i=1}^n \begin{pmatrix}\cos\theta_i\\ \sin\theta_i\end{pmatrix}, \bigoplus_{j>i}\begin{pmatrix}\cos(\theta_i-\theta_j)\\ \sin(\theta_i-\theta_j)\end{pmatrix}, \bigoplus_{j>i}\begin{pmatrix}\cos(\theta_i+\theta_j)\\ \sin(\theta_i+\theta_j)\end{pmatrix}\right] \\ = & \frac{1}{\sqrt{2n-1}}\left[\cos\theta_1, \sin\theta_1, \ldots, \cos\theta_n, \sin\theta_n,\right. \\ & \cos(\theta_1-\theta_2), \sin(\theta_1-\theta_2), \ldots, \cos(\theta_1-\theta_n), \sin(\theta_1-\theta_n), \\ & \cos(\theta_2-\theta_3), \sin(\theta_2-\theta_3), \ldots, \cos(\theta_{n-1}-\theta_n), \sin(\theta_{n-1}-\theta_n), \\ & \cos(\theta_1+\theta_2), \sin(\theta_1+\theta_2), \ldots, \cos(\theta_1+\theta_n), \sin(\theta_1+\theta_n), \\ & \left.\cos(\theta_2+\theta_3), \sin(\theta_2+\theta_3), \ldots, \cos(\theta_{n-1}+\theta_n), \sin(\theta_{n-1}+\theta_n)\right],\end{aligned}$$

where $\bigoplus_{j>i} \equiv \bigoplus_{i=1}^n \bigoplus_{j=i+1}^n$. One can infer what is meant by this notation by comparing with the $n = 2$ case. We want to show the embedding is isometric, i.e., that $\partial_i\psi \cdot \partial_j\psi = \delta_{ij}$. To that end, writing $\theta \equiv (\theta_i)_{i=1}^n$,

$$\begin{aligned}\partial_k\psi(\theta) = & \frac{1}{\sqrt{2n-1}}\left[\bigoplus_{i=1}^n \delta_{ki}\begin{pmatrix}-\sin\theta_i\\ \cos\theta_i\end{pmatrix},\right. \\ & \bigoplus_{j>i}\left(\delta_{ki}\begin{pmatrix}-\sin(\theta_i-\theta_j)\\ \cos(\theta_i-\theta_j)\end{pmatrix} - \delta_{kj}\begin{pmatrix}-\sin(\theta_i-\theta_j)\\ \cos(\theta_i-\theta_j)\end{pmatrix}\right), \\ & \left.\bigoplus_{j>i}\left(\delta_{ki}\begin{pmatrix}-\sin(\theta_i+\theta_j)\\ \cos(\theta_i+\theta_j)\end{pmatrix} + \delta_{kj}\begin{pmatrix}-\sin(\theta_i+\theta_j)\\ \cos(\theta_i+\theta_j)\end{pmatrix}\right)\right] \\ = & \frac{1}{\sqrt{2n-1}}\left[\bigoplus_{i=1}^n \delta_{ki}\begin{pmatrix}-\sin\theta_i\\ \cos\theta_i\end{pmatrix}, \bigoplus_{j>i}(\delta_{ki}-\delta_{kj})\begin{pmatrix}-\sin(\theta_i-\theta_j)\\ \cos(\theta_i-\theta_j)\end{pmatrix}, \bigoplus_{j>i}(\delta_{ki}+\delta_{kj})\begin{pmatrix}-\sin(\theta_i+\theta_j)\\ \cos(\theta_i+\theta_j)\end{pmatrix}\right]\end{aligned}$$

Then, using

$$\left[\bigoplus_{i=1}^n \delta_{ki}\begin{pmatrix}-\sin\theta_i\\ \cos\theta_i\end{pmatrix}\right] \cdot \left[\bigoplus_{i=1}^n \delta_{ki}\begin{pmatrix}-\sin\theta_i\\ \cos\theta_i\end{pmatrix}\right] = \sum_{i=1}^n \delta_{ki}\delta_{ki} = 1,$$

and

$$\begin{aligned}
&\left[\bigoplus_{j>i}(\delta_{ki}\pm\delta_{kj})\begin{pmatrix}-\sin(\theta_i\pm\theta_j)\\ \cos(\theta_i\pm\theta_j)\end{pmatrix}\right]\cdot\left[\bigoplus_{j>i}(\delta_{ki}\pm\delta_{kj})\begin{pmatrix}-\sin(\theta_i\pm\theta_j)\\ \cos(\theta_i\pm\theta_j)\end{pmatrix}\right]\\
&\quad=\sum_{i=1}^{n}\sum_{j=i+1}^{n}(\delta_{ki}\delta_{ki}\pm\delta_{ki}\delta_{kj}\pm\delta_{kj}\delta_{ki}+\delta_{kj}\delta_{kj})\\
&\quad=\sum_{j=k+1}^{n}1+0+0+\sum_{i=1}^{k-1}1\\
&\quad=n-1,
\end{aligned}$$

we get

$$\|\partial_k\psi(\theta)\|^2=\frac{1}{2n-1}(1+2(n-1))=1.$$

For $k'\neq k$, note that

$$\left[\bigoplus_{i=1}^{n}\delta_{ki}\begin{pmatrix}-\sin\theta_i\\ \cos\theta_i\end{pmatrix}\right]\cdot\left[\bigoplus_{i=1}^{n}\delta_{k'i}\begin{pmatrix}-\sin\theta_i\\ \cos\theta_i\end{pmatrix}\right]=\sum_{i=1}^{n}\delta_{ki}\delta_{k'i}=0,$$

and

$$\begin{aligned}
&\left[\bigoplus_{j>i}(\delta_{ki}\pm\delta_{kj})\begin{pmatrix}-\sin(\theta_i\pm\theta_j)\\ \cos(\theta_i\pm\theta_j)\end{pmatrix}\right]\cdot\left[\bigoplus_{j>i}(\delta_{k'i}\pm\delta_{k'j})\begin{pmatrix}-\sin(\theta_i\pm\theta_j)\\ \cos(\theta_i\pm\theta_j)\end{pmatrix}\right]\\
&\quad=\sum_{i=1}^{n}\sum_{j=i+1}^{n}(\delta_{ki}\delta_{k'i}\pm\delta_{ki}\delta_{k'j}\pm\delta_{kj}\delta_{k'i}+\delta_{kj}\delta_{k'j})\\
&\quad=\pm1,
\end{aligned}$$

so,

$$\partial_k\psi(\theta)\cdot\partial_{k'}\psi=\frac{1}{2n-1}(0-1+1)=0.$$

Therefore, indeed we have

$$\partial_i\psi\cdot\partial_j\psi=\delta_{ij},$$

thus ψ is an isometric embedding of T^n with the flat metric into $\mathbb{R}^{2n^2}$.

Now, for a metric perturbation $\delta_{ij}\mapsto\delta_{ij}+h_{ij}$ on T^n, we want to find a perturbation of the embedding map, $\psi+\tilde{\psi}:T^n\mapsto\mathbb{R}^{2n^2}$ which is isometric. With the zeroth order

embedding ψ just defined, recall this amounts to solving the linear system (4.40) for $\tilde{\psi}$. We will simply guess a form for $\tilde{\psi}$, in analogy with the solution we found for the $n = 2$ case, and then show that it solves the linear system. Let

$$\tilde{\psi} : (\theta_i)_{i=1}^n \mapsto \frac{\sqrt{2n-1}}{2} \left[\bigoplus_{i=1}^n h_{ii} \begin{pmatrix} \cos\theta_i \\ \sin\theta_i \end{pmatrix}, \bigoplus_{j>i} (-\tfrac{1}{2} h_{ij}) \begin{pmatrix} \cos(\theta_i - \theta_j) \\ \sin(\theta_i - \theta_j) \end{pmatrix}, \bigoplus_{j>i} (\tfrac{1}{2} h_{ij}) \begin{pmatrix} \cos(\theta_i + \theta_j) \\ \sin(\theta_i + \theta_j) \end{pmatrix} \right]. \tag{4.46}$$

First, let us show $(\partial_k \psi) \cdot \tilde{\psi} = 0$. Using the formula we worked out for $\partial_k \psi$ above, we find

$$\begin{aligned} (\partial_k \psi) \cdot \tilde{\psi} = \frac{1}{2} \Bigg(& \sum_{i=1}^n \delta_{ki} h_{ii} [-\sin\theta_i \cos\theta_i + \cos\theta_i \sin\theta_i] \\ & + \sum_{j>i} (\delta_{ki} - \delta_{kj})(-\tfrac{1}{2} h_{ij}) [-\sin(\theta_i - \theta_j)\cos(\theta_i - \theta_j) + \cos(\theta_i - \theta_j)\sin(\theta_i - \theta_j)] \\ & + \sum_{j>i} (\delta_{ki} + \delta_{kj})(\tfrac{1}{2} h_{ij}) [-\sin(\theta_i + \theta_j)\cos(\theta_i + \theta_j) + \cos(\theta_i + \theta_j)\sin(\theta_i + \theta_j)] \Bigg) \\ = 0, & \end{aligned}$$

since all of the terms in the square brackets vanish. Now we need an expression for $\partial_k \partial_l \psi$. We find

$$\begin{aligned} \partial_k \partial_l \psi(\theta) = \frac{1}{\sqrt{2n-1}} \Bigg[& \bigoplus_{i=1}^n \delta_{ki}\delta_{li} \begin{pmatrix} -\cos\theta_i \\ -\sin\theta_i \end{pmatrix}, \\ & \bigoplus_{j>i} (\delta_{ki} - \delta_{kj})(\delta_{li} - \delta_{lj}) \begin{pmatrix} -\cos(\theta_i - \theta_j) \\ -\sin(\theta_i - \theta_j) \end{pmatrix} \\ & \bigoplus_{j>i} (\delta_{ki} + \delta_{kj})(\delta_{li} + \delta_{lj}) \begin{pmatrix} -\cos(\theta_i + \theta_j) \\ -\sin(\theta_i + \theta_j) \end{pmatrix} \Bigg]. \end{aligned}$$

Now recall we want to show $(\partial_k \partial_l \psi) \cdot \tilde{\psi} = -\frac{1}{2} h_{kl}$:

$$(\partial_k \partial_l \psi) \cdot \tilde{\psi} = \frac{1}{2} \left(\sum_{i=1}^n (-\delta_{ki}\delta_{li}) h_{ii} + \sum_{j>i} (\delta_{ki} - \delta_{kj})(\delta_{li} - \delta_{lj})(\tfrac{1}{2} h_{ij}) + \sum_{j>i} (\delta_{ki} + \delta_{kj})(\delta_{li} + \delta_{lj})(-\tfrac{1}{2} h_{ij}) \right).$$

For $l = k$,

$$(\partial_k^2 \psi) \cdot \tilde{\psi} = -\tfrac{1}{2} h_{kk} + \tfrac{1}{4} \sum_{j>i} (\delta_{ki} + \delta_{kj}) h_{ij} - \tfrac{1}{4} \sum_{j>i} (\delta_{ki} + \delta_{kj}) h_{ij} = -\tfrac{1}{2} h_{kk},$$

and for $l \neq k$,

$$(\partial_k \partial_l \psi) \cdot \tilde{\psi} = 0 - \tfrac{1}{4} \sum_{j>i} (\delta_{ki}\delta_{lj} + \delta_{li}\delta_{kj}) h_{ij} - \tfrac{1}{4} \sum_{j>i} (\delta_{ki}\delta_{lj} + \delta_{li}\delta kj) h_{ij} = -\tfrac{1}{2} h_{kl},$$

where we used the fact that $h_{kl} = h_{lk}$. Therefore, we have established that $\psi + \tilde{\psi} : T^n \to \mathbb{R}^{2n^2}$, with

$$\begin{aligned} \psi + \tilde{\psi} : (\theta_i)_{i=1}^n \mapsto \Bigg[& \bigoplus_{i=1}^n \left(\tfrac{1}{\sqrt{2n-1}} + \tfrac{\sqrt{2n-1}}{2} h_{ii} \right) \begin{pmatrix} \cos\theta_i \\ \sin\theta_i \end{pmatrix}, \\ & \bigoplus_{j>i} \left(\tfrac{1}{\sqrt{2n-1}} - \tfrac{\sqrt{2n-1}}{4} h_{ij} \right) \begin{pmatrix} \cos(\theta_i - \theta_j) \\ \sin(\theta_i - \theta_j) \end{pmatrix}, \\ & \bigoplus_{j>i} \left(\tfrac{1}{\sqrt{2n-1}} + \tfrac{\sqrt{2n-1}}{4} h_{ij} \right) \begin{pmatrix} \cos(\theta_i + \theta_j) \\ \sin(\theta_i + \theta_j) \end{pmatrix} \Bigg] \end{aligned} \tag{4.47}$$

is, to first order in h_{ij}, isometric in the sense $(\psi + \tilde{\psi})^* \delta = \delta + h$, or equivalently, $\partial_i(\psi + \tilde{\psi}) \cdot \partial_j(\psi + \tilde{\psi}) = \delta_{ij} + h_{ij}$.

Now we have an isometric embedding, what are the expressions for the mean and variance? First, let us work out the distance function induced by this embedding.

$$d_{\psi+\tilde{\psi}}(\theta, \theta')^2 = \|(\psi + \tilde{\psi})(\theta)\|^2 + \|(\psi + \tilde{\psi})(\theta')\|^2 - 2(\psi + \tilde{\psi})(\theta) \cdot (\psi + \tilde{\psi})(\theta') \tag{4.48}$$

To first order, we have

$$\|(\psi + \tilde{\psi})(\theta)\|^2 = \frac{n^2}{2n-1} + h(\theta), \quad \text{where} \quad h(\theta) \equiv \sum_i h_{ii}(\theta), \tag{4.49}$$

and

$$\begin{aligned} (\psi + \tilde{\psi})(\theta) \cdot (\psi + \tilde{\psi})(\theta') = & \sum_{i=1}^n \left(\frac{1}{2n-1} + \frac{1}{2} h_{ii}(\theta) + \frac{1}{2} h_{ii}(\theta') \right) \cos(\theta - \theta') \\ & + \frac{1}{2n-1} \sum_{j>i} \left(\cos[(\theta_i - \theta_j) - (\theta'_i - \theta'_j)] + \cos[(\theta_i + \theta_j) - (\theta'_i + \theta'_j)] \right) \\ & - \frac{1}{4} \sum_{j>i} (h_{ij}(\theta) + h_{ij}(\theta')) \left(\cos[(\theta_i - \theta_j) - (\theta'_i - \theta'_j)] - \cos[(\theta_i + \theta_j) - (\theta'_i + \theta'_j)] \right). \end{aligned}$$

Therefore, we can write

$$\begin{aligned} d_{\psi+\tilde{\psi}}(\theta,\theta')^2 = \frac{2n^2}{2n-1} &+ h(\theta) + h(\theta') \\ &- \sum_{i=1}^{n} \left(\frac{2}{2n-1} + h_{ii}(\theta) + h_{ii}(\theta') \right) \cos(\theta - \theta') \\ &- \frac{2}{2n-1} \sum_{j>i} \left(\cos[(\theta_i - \theta_j) - (\theta'_i - \theta'_j)] + \cos[(\theta_i + \theta_j) - (\theta'_i + \theta'_j)] \right) \\ &+ \frac{1}{2} \sum_{j>i} (h_{ij}(\theta) + h_{ij}(\theta')) \left(\cos[(\theta_i - \theta_j) - (\theta'_i - \theta'_j)] - \cos[(\theta_i + \theta_j) - (\theta'_i + \theta'_j)] \right). \end{aligned}$$

We will not be able to work out expressions for μ or σ^2 in closed form, but let us see how the calculation would proceed. Using the trick $\langle \cos(\theta - \mu) \rangle_\theta = \Re\{ \langle e^{i\theta} \rangle_\theta e^{-i\mu} \}$, we can write

$$\begin{aligned} \langle d_{\psi+\tilde{\psi}}(\theta,\mu)^2 \rangle_\theta = \frac{2n^2}{2n-1} &- \frac{2}{2n-1} \sum_{i=1}^{n} \Re\{ \langle e^{i\theta_i} \rangle_\theta e^{-i\mu_i} \} \\ &- \frac{2}{2n-1} \sum_{j>i} \Re\{ \langle e^{i(\theta_i - \theta_j)} \rangle_\theta e^{-i(\mu_i - \mu_j)} + \langle e^{i(\theta_i + \theta_j)} \rangle_\theta e^{-i(\mu_i + \mu_j)} \} \\ &+ \langle h(\theta) \rangle_\theta + h(\mu) - \sum_{i=1}^{n} \Re\{ \langle h_{ii}(\theta) e^{i\theta_i} \rangle_\theta e^{-i\mu_i} + h_{ii}(\mu) \langle e^{i\theta_i} \rangle_\theta e^{-i\mu_i} \} \\ &+ \frac{1}{2} \sum_{j>i} \Re\{ \langle h_{ij}(\theta) e^{i(\theta_i - \theta_j)} \rangle_\theta e^{-i(\mu_i - \mu_j)} + h_{ij}(\mu) \langle e^{i(\theta_i - \theta_j)} \rangle_\theta e^{-i(\mu_i - \mu_j)} \\ &- \langle h_{ij}(\theta) e^{i(\theta_i + \theta_j)} \rangle_\theta e^{-i(\mu_i + \mu_j)} - h_{ij}(\mu) \langle e^{i(\theta_i + \theta_j)} \rangle_\theta e^{-i(\mu_i + \mu_j)} \} \end{aligned}$$

Of course this formula is rather unusable in its general form, but it is simple in principle. In specific cases, given a probability distribution one would first calculate $\langle e^{i\theta_i} \rangle_\theta$, $\langle e^{i(\theta_i \pm \theta_j)} \rangle_\theta$, $\langle h(\theta) \rangle_\theta$, $\langle h_{ii}(\theta) e^{i\theta_i} \rangle_\theta$, and $\langle h_{ij}(\theta) e^{i(\theta_i \pm \theta_j)} \rangle_\theta$. These would then be plugged into the above expression. The mean is the value of $\mu = (\mu_i)_{i=1}^n$ which minimises this expression. The value of the expression at the minimum will equal the variance σ^2.

Note that in the process of solving the perturbative problem, we concocted an embedding of the flat n-torus which is different than the simple one presented at the beginning of this section. It turns out that the induced distances for these two embeddings are not the same, thus giving an example relevant to the discussion at the end of the last section. Explicitly, for $n = 2$, let $\psi_1 : T^2 \to \mathbb{R}^4$ be the embedding $(\theta_1, \theta_2) \mapsto (\cos\theta_1, \sin\theta_1, \cos\theta_2, \sin\theta_2)$

and let $\psi_2 : T^2 \to \mathbb{R}^8$ be the embedding associated with the zeroth order solution to the perturbation problem we have been considering, given by (4.42). Then,

$$\|\psi_1(\theta) - \psi_1(\theta')\|^2 = 4 - 2\cos(\theta_1 - \theta_1') - 2\cos(\theta_2 - \theta_2'),$$

whereas,

$$\begin{aligned}\|\psi_2(\theta) - \psi_2(\theta')\|^2 &= \frac{8}{3} - \frac{2}{3}\cos(\theta_1 - \theta_1') - \frac{2}{3}\cos(\theta_2 - \theta_2') - \frac{4}{3}\cos(\theta_1 - \theta_1')\cos(\theta_2 - \theta_2') \\ &= \frac{2}{3}\|\psi_1(\theta) - \psi_1(\theta')\|^2 - \frac{4}{3}\cos(\theta_1 - \theta_1')\cos(\theta_2 - \theta_2').\end{aligned}$$

One can also easily show that these two induced distance functions can lead to different values for the mean. For example, consider three sample data points $(\theta_1, \theta_2) = (0, 0), (\frac{\pi}{4}, \frac{\pi}{4}), (\frac{\pi}{4}, \frac{7\pi}{4})$. One can calculate numerically that the point μ that minimises the average dispersion of these points is $\mu \approx (0.530, 0)$ using the induced distance from the first embedding, and $\mu \approx (0.489, 0)$ using the second. Therefore, although before we discussed how the intrinsic and induced distance functions will generally lead to different values for the mean and variance of a distribution, here we have demonstrated that two different induced distance functions can as well.

Chapter 5

Subsystem localization in bandlimited field theory

In this chapter, we will be revisiting some observations made in [100, 102] regarding the localization and density of degrees of freedom in Euclidean-bandlimited quantum field theory. In this previous work, we elucidated how one should think about information density in the context of sampling theory for fields, as it turns out to be subtle because the sample points are not fixed. Nevertheless, it was shown that there is a fundamental incompressibility of the degrees of freedom of the fields. We will review this work in the first section of this chapter.

In the following section, we will build on these observations to develop a more explicit notion of a local density of degrees of freedom in a bandlimited field theory, which quantifies the ideas of [100, 102] more precisely. This notion of local density will be in contrast to the global notions of sample density discussed in Chapter 2. In the case of a flat background, we will find that these two notions coincide because the theory is translation-invariant. In this chapter, we will focus on the case of a flat background in order to first establish these ideas where everything is rather simple. However, the interest is primarily in applying them to non-symmetric cases, which we will begin to investigate in Chapter 6, where we examine perturbing the background geometry away from flat.

5.1 Previous work on subsystem localization

In [100, 102], we showed that the Euclidean bandlimit regulates the ground state correlations of a free scalar field theory (in 1+1 dimensional flat spacetime), as well as the

ground state entanglement entropy between localized spatial degrees of freedom. In ordinary quantum field theory, often one is interested in entanglement between continuous spatial regions, such as left and right Rindler wedges, for example. In bandlimited quantum field theory, the natural notion of a localized subsystem is of a collection of sample points (see [100, 102]). The simplest choice of subsystem is a set of Nyquist-spaced points. In [100, 102], it was shown that the ground state entanglement entropy of such a set of spatially-separated points for a free, scalar, massless field in 1+1 dimensional flat spacetime varies with the number of points, N, as

$$S(N) \sim \tfrac{1}{3} \log N, \tag{5.1}$$

which is a fit to the curve in Figure 5.1. This theory has an infrared divergence, so for these results an infrared cutoff $\omega \ll \Lambda$ was also introduced. Including the dependence of $S(N)$ on ω, in [100, 102] it was found that, as $\omega/\Lambda \to 0$, we have $S \sim \frac{1}{3} \log N + \frac{1}{2} \log(\log(\Lambda/\omega))$.

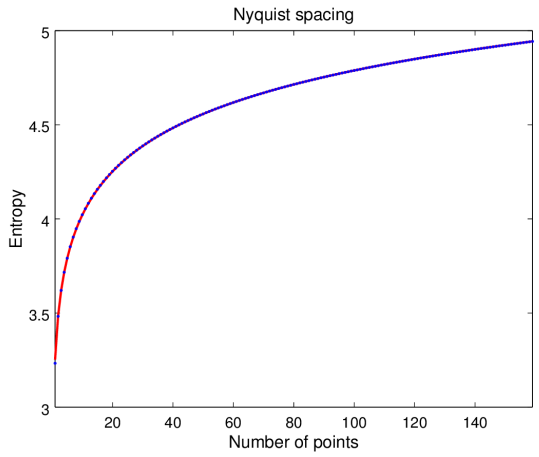

Figure 5.1: Entanglement entropy of a free, scalar, massless bandlimited quantum field theory in 1+1 dimensional flat spacetime in the ground state for a set of Nyquist-spaced sample points, as a function of the number of samples. The blue dots are the values of the numerically-calculated entropy, and the red line passing through them is the fit to $c_0 \log N + c_1$.

Intuitively, N Nyquist-spaced sample points occupy a region of size $L = \frac{\pi}{\Lambda} N$, in which case the above result can be written $S(N) \sim \frac{1}{3} \log(\Lambda L)$. This is consistent with other results for a conformal field theory obtained using other methods [53].

The difference between bandlimited QFT and QFT on a spatial lattice is that one is not committed to a particular lattice, and any finite number of sample points can be moved

anywhere (the only requirement is that the average density is sufficiently large). Choosing samples at points different from a Nyquist lattice will not correspond to an orthonormal frame, but they still span a closed subspace of the space of field configurations, and can be identified as a subsystem of the full field theory. That is, we can factorize the full Hilbert space of the field theory with one tensor factor associated with this subset of degrees of freedom.

In [100, 102], we then investigated how the entropy of a subset of points depends on their relative spacing. Specifically, we were interested in how the entropy changes as the points are moved closer together, below the Nyquist spacing, which is something that could not occur in a lattice theory.

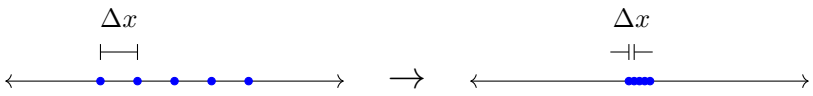

The coincidence limit of these points corresponds to a degenerate case where there is only one degree of freedom. Hence, one might expect that the entanglement entropy of these points decreases continuously down to match that of a single point in the coincidence limit. Indeed, physically one would expect the bandlimit to be a regulator for the information density of the field theory. By moving the degrees of freedom closer together, they intuitively occupy a smaller region of space. Hence one might expect the entropy to decrease and retain a roughly constant information density.

Rather, we found Figure 5.2, which shows the entanglement entropy of a fixed number of points ($N = 5$) as a function of their spacing. The entanglement entropy remains roughly constant as the degrees of freedom are pushed together. Recall that we showed $S(N) \sim \frac{1}{3} \log N$ for Nyquist-spaced points, and so even when pushed together, the entropy of these points is larger than that of a single sample point.

For completeness, let us note that as the points are moved far apart, the correlations between them decay, and hence the entropy increases. In [100, 102] we observed that this corresponds to a transition to a volume law, $S(N) \sim N$. One could approximate this situation in a simple lattice theory, and this result corresponds to what one would expect on intuitive grounds.

Because the entanglement entropy is roughly constant when the spacing is below Nyquist, the information density would appear to be increasing, if one were to take the subsystem size to be roughly N times the spacing between the points. This seems contradictory to the idea that these fields exhibit a finite information density. But are these

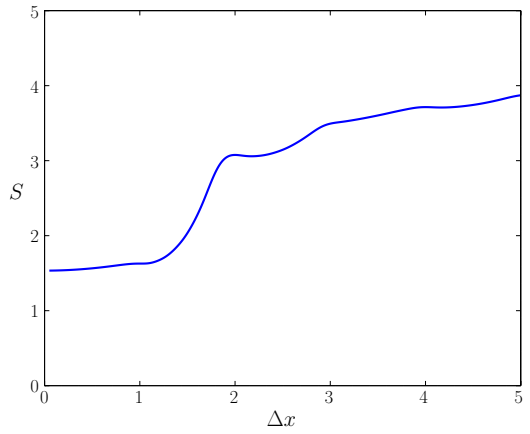

Figure 5.2: Ground state entanglement entropy of $N = 5$ sample points as a function of their spacing. The Δx-axis is in units of the Nyquist spacing, so that $\Delta x = 1$ corresponds to a spacing of Λ/π. [100, 102]

points really occupying a smaller region of space as they are pushed together? Let us examine this more closely.

To get a sense of where the information of this subsystem is localized, we extracted a spatial profile from calculating the mutual information between the subsystem and different points in space. Suppose we fix an arrangement of N sample points, which will correspond to the subsystem of interest. Now consider the mutual information between these points and another sample point at some arbitrary x,

$$I(N : x) = S(N) + S(x) - S(N, x). \tag{5.2}$$

When x is far away from the subsystem, we expect the mutual information to be small. If x is brought closer to the subsystem, the mutual information should increase and peak when x lies "within" the subsystem defined by the N sample points. Since we can vary x continuously over $\mathbb{R}$, $I(N : x)$ as a function of x should give an indication of the spatial profile of the subsystem N.

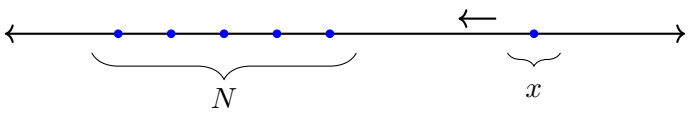

For example, if we choose N adjacent Nyquist lattice points, we find Figure 5.3, which confirms this intuition.

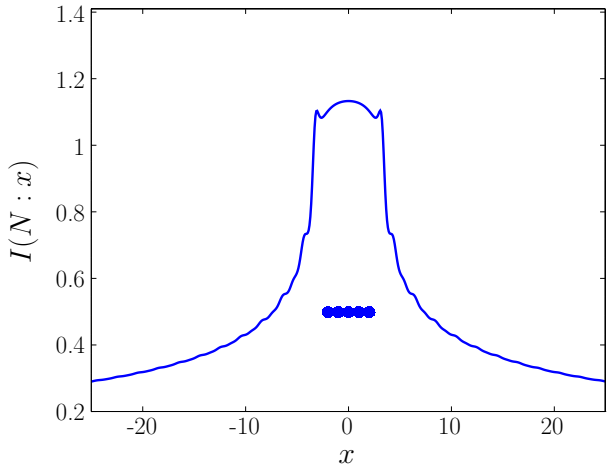

Figure 5.3: Mutual information between a subsystem of $N = 5$ Nyquist-spaced sample points and an additional sample point at x, as a function of the position x (in units of the Nyquist spacing). [100, 102]

Now let us examine how this profile changes with the spacing between the points. Recall that our intuition would suggest that as the spacing decreases below the Nyquist spacing, the profile of the subsystem should become more narrow as the points occupy a smaller region of space. Instead, we found Figure 5.4.

As the points get far apart, naturally they appear as isolated profiles associated with single points. However, notice that below the Nyquist spacing, the profile remains roughly the same. (See Figure 5.5 showing the same result as Figure 5.4 but focused on this region.) Therefore, although the sample points are taken close together, it seems that they occupy roughly the same region of space as if they were placed at a Nyquist density. Hence, in this sense, the degrees of freedom are "incompressible" in space. Further, this indicates that the information density remains roughly constant as the points are pushed together, since their entanglement entropy remains roughly constant as well as the size of the region they occupy. Thus, this resolves the apparent contradiction, and the field theory consistently exhibits a finite information density, despite the fact that we have a continuous underlying space and can move the sample points around as we please.

The idea behind this mutual information profile was that it indicates the localization

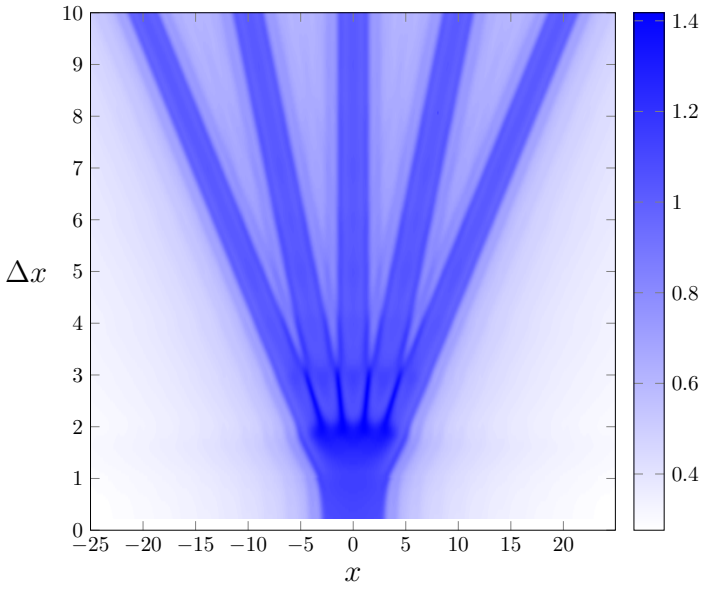

Figure 5.4: Mutual information profile for a subsystem of $N = 5$ sample points in the global ground state. The x-axis corresponds to the position (in units of Nyquist spacing) of the additional sample point included in the calculation of $I(N : x)$, and the Δx-axis corresponds to the spacing between the $N = 5$ sample points, also in units of the Nyquist spacing (so that $\Delta x = 1$ corresponds to a spacing of Λ/π). [100, 102]

of the information in the subsystem. We also noted in [100, 102] that one could get a preliminary glimpse of the incompressibility by examining the subsystem projector in the space of classical field configurations. Consider our Hilbert space of bandlimited functions $B(\Lambda)$. We can find a discrete set of $P_\Lambda|x_n)$'s which form a frame for $B(\Lambda)$, but let us choose some finite subset $\{P_\Lambda|x_n)\}_{n=1}^N$ corresponding to (distinct) sample points of a subsystem. These span a closed subspace of $B(\Lambda)$, so let us construct the projector onto this subspace in the (non-orthogonal) basis $\{P_\Lambda|x_n)\}_{n=1}^N$. First, let $\{|e_\ell)\}_{\ell=1}^N$ be an orthonormal basis for this subspace, expanded in terms of the basis $\{P_\Lambda|x_n)\}_{n=1}^N$ as

$$|e_\ell) = \sum_{n=1}^{N} B_{\ell n} P_\Lambda |x_n), \tag{5.3}$$

where $B_{\ell n}$ is some appropriate set of coefficients. Now the projector onto this subspace of

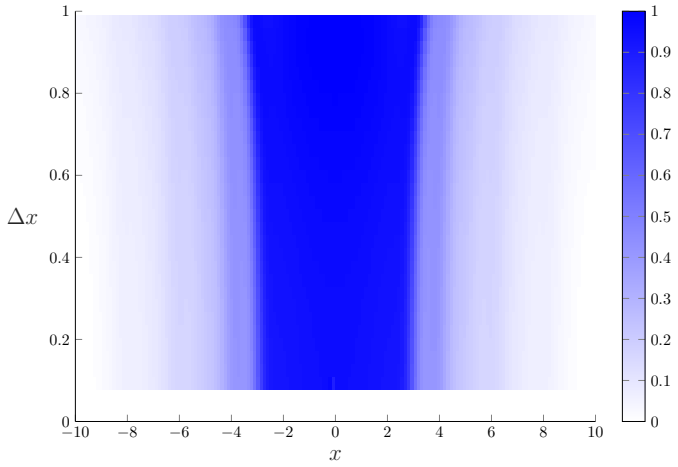

Figure 5.5: Mutual information profile for a subsystem of $N = 5$ sample points in the global ground state, focused on a range of spacings below the Nyquist spacing. The x-axis corresponds to the position (in units of Nyquist spacing) of the additional sample point included in the calculation of $I(N : x)$, and the Δx-axis corresponds to the spacing between the $N = 5$ sample points, also in units of the Nyquist spacing (so that $\Delta x = 1$ corresponds to a spacing of Λ/π).

N sample points can be written

$$\begin{aligned} P_N &= \sum_{\ell} |e_\ell)(e_\ell| \\ &= \sum_{\ell,n,n'} B_{\ell n} B^*_{\ell n'} P_\Lambda |x_n)(x_{n'}| P_\Lambda \\ &= \sum_{n,n'} (B^\dagger B)_{n'n} P_\Lambda |x_n)(x_{n'}| P_\Lambda. \end{aligned}$$

We want a more useful expression for the matrix $B^\dagger B$. Consider the matrix $Q_{nn'} := (x_n|P_\Lambda|x_{n'})$. This matrix is the inverse of $B^\dagger B$,

$$\begin{aligned} Q_{nn'} &= (x_n|P_\Lambda|x_{n'}) \\ &= \sum_{\ell,\ell'} [(e_\ell|(B^{-1})^*_{n\ell}][(B^{-1})_{n'\ell'}|e_{\ell'})] \\ &= (B^{-1}(B^{-1})^\dagger)_{n'n}. \end{aligned}$$

So $Q^T = (B^\dagger B)^{-1}$, then we can write

$$P_N = \sum_{n,n'=1}^{N} (Q^{-1})_{nn'} P_\Lambda|x_n)(x_{n'}|P_\Lambda. \tag{5.4}$$

If we examine the diagonal elements of P_N in the continuous overcomplete basis (whose elements are $P_\Lambda|x)$ for each $x \in \mathbb{R}$), we obtain a function

$$P_N(x) := (x|P_N|x) = \sum_{n,n'=1}^{N} (Q^{-1})_{nn'} (x|P_\Lambda|x_n)(x_{n'}|P_\Lambda|x). \tag{5.5}$$

Recall from Chapter 2 that $(x|P_\Lambda|x') = \frac{\Lambda}{\pi}\mathrm{sinc}[\Lambda(x-x')]$ in the case of sampling in $\mathbb{R}$. Figure 5.6 is a plot of this function for a similar setup as the mutual information profile we examined above. Namely, the sample points are taken to be equally spaced, and we look at how it changes as the spacing between the points is varied. We see that it is qualitatively similar to the mutual information profile for the same arrangement of points. In particular, we notice how the width remains roughly constant as we decrease below the Nyquist spacing.

This ends the review of the work in [100, 102]. In this thesis, we will build on some of these observations. First, can we obtain a more precise characterization of the localization of these subsystems, beyond merely a visual assessment of plots? Is it possible to give a more careful demonstration of the incompressibility of the degrees of freedom? This is especially important because of the apparent numerical instability of the calculation at very small spacings (note the truncation of the plot in the Δx direction in Figures 5.4 and 5.5), which is the region in which we are interested. (Note, some measures were taken in [100, 102] to ensure that the incompressibility feature was not simply due to this instability, but here we would like to establish it analytically.)

5.2 Quantifying subsystem size and local sample density

Intuitively, we expect that the incompressibility of the information in the field theory, as expressed by the mutual information profile, should be a kinematical feature and not depend on the state of the field. Indeed, the expectation that the bandlimit imposes a finite information density is not specific to the ground state. The fact that the subsystem

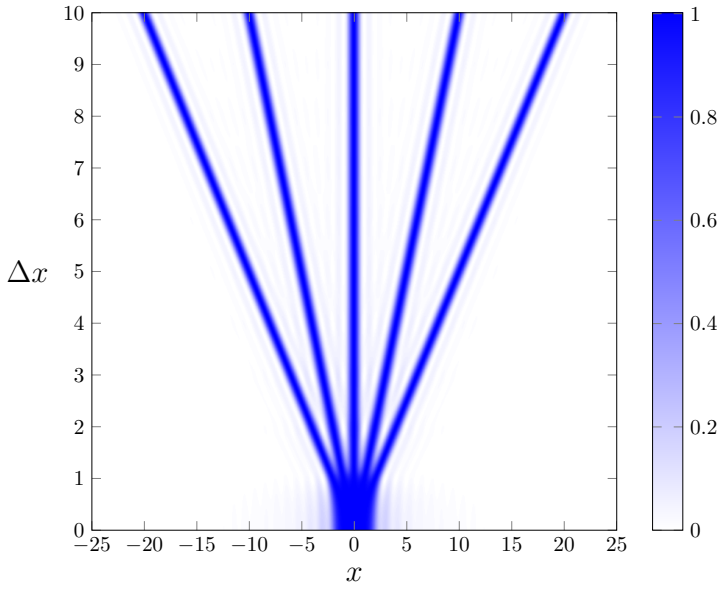

Figure 5.6: Plot of the spatial profile, $(x|P_n|x)$, of a subset of $N = 5$ equally-spaced sample points. The x-axis corresponds to the argument of the spatial profile $(x|P_n|x)$, and the Δx-axis corresponds to the spacing between the sample points. Both axes are in units of the Nyquist spacing. [100, 102]

projector in the space of field configurations exhibits this incompressibility is an indication of this.

For example, this can be shown for the quantum field in a thermal state, $\rho = \frac{1}{Z}e^{-\beta H}$. Indeed, in [100, 102], we showed that these states exhibit the same behaviour that the entanglement entropy does not significantly decrease below the Nyquist spacing (Figure 5.7). We can also show that they exhibit a similar incompressibility below the Nyquist spacing, as demonstrated by the mutual information profile of Figure 5.8. This feature can also be reproduced for a thermal state of the classical bandlimited field theory, where the entropy of a subsystem is taken to be the entropy of the probability distribution $p(\{\phi_n, \pi_n\}_n) = \frac{1}{Z}e^{-\beta H(\{\phi_n,\pi_n\}_n)}$ after marginalizing out all but the sample points in the subsystem. (For details, see [100, 102], particularly with regards to the phase space measure for the samples.) The result is shown in Figure 5.9, which looks identical to the quantum case. Therefore, this indicates that the incompressibility is simply a kinematical feature, sourced in the fact that the field configurations are drawn from the space of bandlimited functions $B(\Lambda)$.

With some appropriate measure of size, σ, one could define a notion of information

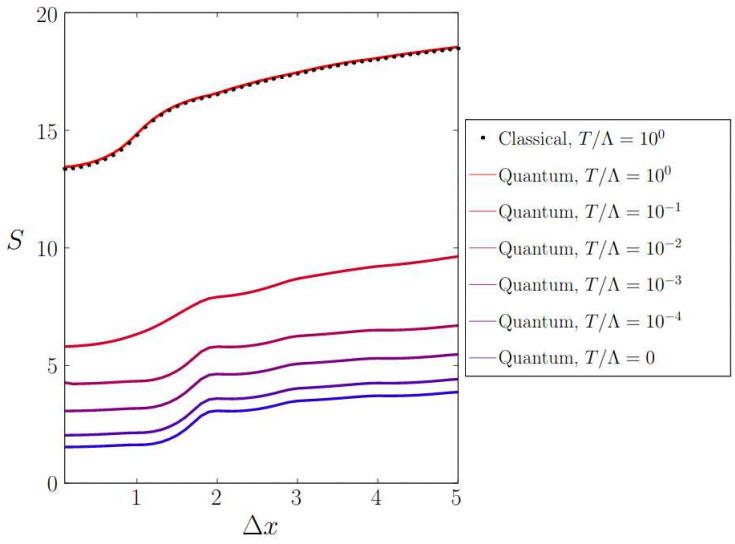

Figure 5.7: Entanglement entropy of $N = 5$ sample points as a function of their spacing, for a global thermal state at an assortment of temperatures (in units of the cutoff Λ). Also included is the entropy of the same collection of sample points for a classical field theory in a thermal state of temperature $T/\Lambda = 1$. The Δx-axis is in units of the Nyquist spacing. [100, 102]

density in the field as something of the form $S(N)/\sigma$. Despite the fact that the bandlimit acts as a regulator for the field theory, there will not be an upper bound to the information density, since we can artificially increase the entropy of the oscillators. For example, one could put the system in a thermal state with a very large temperature, hence making $S(N)$ arbitrarily large. Therefore, this demonstration of the incompressibility would appear to be showing an incompressibility of the degrees of freedom of the field, rather than an upper bound on the information density. Although questions about the information density should be investigated further, we will proceed to focus on quantifying the incompressibility of the degrees of freedom of the field theory. Specifically, we will quantify the size of a subsystem of sample points and investigate how this quantity changes as the sample points are brought close together. Because this is a kinematical feature of the field configurations, instead of focusing on the mutual information profile, we want express the subsystem sizes solely in terms of objects in $B(\Lambda)$.

We will begin by revisiting our observation that the diagonal elements of the subsystem projector in the frame $\{P_\Lambda|x)\}_{x\in\mathbb{R}}$, given by (5.5), shows the incompressibility of the degrees of freedom below the Nyquist spacing, as illustrated in Figure 5.6. Let us posit that this function derived from the projector onto the subsystem defined by the samples $\{P_\Lambda|x_n)\}_{n=1}^N$

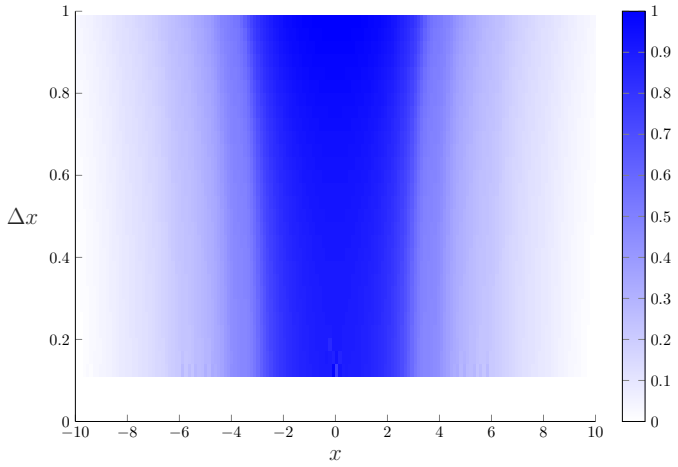

Figure 5.8: Mutual information profile for a subsystem of $N = 5$ sample points in a global thermal state of temperature $T/\Lambda = 10^{-1}$. Here we focus on a range of spacings below the Nyquist spacing. The x-axis corresponds to the position of the additional sample point included in the calculation of $I(N : x)$, and the Δx-axis corresponds to the spacing between the $N = 5$ sample points. Both axes are in units of the Nyquist spacing.

characterizes the manner in which these degrees of freedom are distributed through space. Note that our development of the function $(x|P_N|x)$ in terms of $Q_{nn'} := (x_n|P_\Lambda|x_{n'})$ and $(x|P_\Lambda|x_n)$ did not depend in any way on the fact that the underlying manifold was $\mathbb{R}$. Indeed, this general form will apply to any function space with the sampling property. The function $(x|P_N|x)$ only involves combinations of $(x|P_\Lambda|x')$ evaluated at certain points, hence the particular function space under consideration simply provides the form of $(x|P_\Lambda|x')$. Therefore the spatial profile is in principle simple to calculate, since all we need to know are components of the bandlimited projector in the position representation.

Given $(x|P_N|x)$ as a definition of the spatial distribution of the subsystem, we would like to extract some quantities which summarize its location and size. Athough it appears from Figure 5.6 that the distribution is sharply localized to a particular region, we know in the case of $\mathbb{R}$ that it decays only as $1/x^2$. One could begin to introduce thresholds, deciding that the subsystem is located in a region where $(x|P_N|x)$ is larger than a certain value, but then the size will depend on this arbitrary threshold. We would like to find something better. Notice that $(x|P_N|x) \geq 0$ and $\operatorname{tr} P_N = \int dx\, (x|P_N|x) = N$, so if we

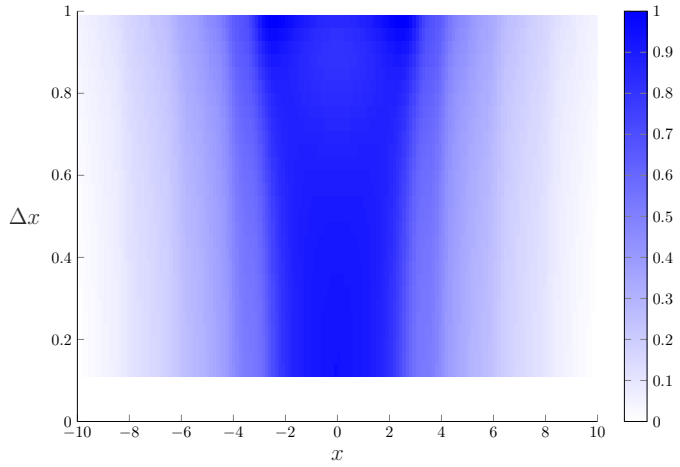

Figure 5.9: Mutual information profile for a subsystem of $N = 5$ sample points in a global thermal state of a classical bandlimited field theory, with temperature $T/\Lambda = 1$. Here we focus on a range of spacings below the Nyquist spacing. The x-axis corresponds to the position of the additional sample point included in the calculation of $I(N : x)$, and the Δx-axis corresponds to the spacing between the $N = 5$ sample points. Both axes are in units of the Nyquist spacing.

divide by N, then

$$p(x) := \frac{1}{N}(x|P_N|x) = \frac{1}{N}\sum_{n,n'=1}^{N}(Q^{-1})_{nn'}(x|P_\Lambda|x_n)(x_{n'}|P_\Lambda|x), \tag{5.6}$$

is a normalized probability distribution. Therefore, we can use the mean and variance as summary measures of the location and size of the subsystem. Recall from Chapter 4 that the variance is a proportionality factor indicating how far one has to go away from the mean to enclose a certain proportion of the measure of the distribution (quantified by the Chebyshev inequality). This is why the variance will be a good measure of size, as it captures the same idea as introducing a threshold, but without the arbitrariness of choosing a particular value. Note that in dimensions larger than 1 the variance corresponds to a characteristic linear size (squared) of the subsystem and not a volume.

Although we will be using this probability distribution extracted from the subsystem projector, as well as calculating the associated mean and variance, we will not be assigning any kind of probabilistic or statistical interpretation to the distribution. This would be applicable, for example, if one were considering $B(\Lambda)$ as a space of bandlimited wavefunctions in quantum mechanics. However, here this space represents the space of classical field configurations, which are not considered to be wavefunctions in any sense. Hence, the

"variance" does not correspond to any kind of uncertainty. We are merely using the fact that the object $p(x)$ satisfies the mathematical definition of a probability distribution, and so we can employ the techniques of probability theory to characterize its location and size.

This course seems appealing, however there is a problem with applying it to the sampling theory on $\mathbb{R}$ since the distribution is heavy-tailed, and the mean and variance do not exist. To see this, let us choose the sample points to be Nyquist-spaced, and so $Q_{nn'} = (x_n|P_\Lambda|x_{n'}) = \frac{\Lambda}{\pi}\delta_{nn'}$ and

$$p(x) = \frac{1}{N}\frac{\Lambda}{\pi}\sum_{n=1}^{N}\frac{\sin^2[\Lambda(x-x_n)]}{\Lambda^2(x-x_n)^2}. \tag{5.7}$$

Hence $p(x)$ decays only as $1/x^2$ and so $\int dx\, p(x)x$ and $\int dx\, p(x)x^2$ both diverge.

Therefore, in the case of sampling on $\mathbb{R}$, this method does not seem to work. However, we would not have an issue with divergences of this kind for sampling on S^1, for example, so let us proceed to study this case. One could then approximate the case of $\mathbb{R}$ by taking the size of the circle S^1 to be very large. Note that in order to calculate the mean and variance of $p(x)$ on S^1 (or generally manifolds other than $\mathbb{R}^N$), we will need to employ techniques discussed in Chapter 4.

Let us calculate the size of the subsystem consisting of a single sample point $x_1 \in S^1$, to illustrate the method. Recall, on S^1 the position representation of the bandlimited projector is

$$\begin{aligned}(x|P_\Lambda|x') &= \sum_{m=-M}^{M}(x|k_m)(k_m|x') \\ &= \frac{1}{L}\sum_{m=-M}^{M}e^{ik_m(x-x')} \\ &= \frac{1}{L}\frac{\sin[(2M+1)(x-x')\frac{\pi}{L}]}{\sin[(x-x')\frac{\pi}{L}]},\end{aligned}$$

where L is the length of the circle, and $M := \lceil\frac{L\Lambda}{2\pi}\rceil$. Then $Q_{11} = (x_1|P_\Lambda|x_1) = (2M+1)/L$, and

$$p(x) = \frac{1}{L(2M+1)}\frac{\sin^2[(2M+1)(x-x')\frac{\pi}{L}]}{\sin^2[(x-x')\frac{\pi}{L}]}. \tag{5.8}$$

Now we can use the methods of the previous chapter to calculate a mean and variance for this distribution. In fact, this distribution was used as an example in Section 4.1. Using

an isometric embedding $\psi : x \mapsto \left(L\cos\left(\frac{2\pi x}{L}\right), L\sin\left(\frac{2\pi x}{L}\right)\right)$, we calculate

$$\phi := \int_0^L dx\, p(x) L e^{\frac{2\pi i}{L}x} = L\frac{2M}{2M+1} e^{\frac{2\pi i}{L}x_1}. \tag{5.9}$$

Then the mean is $\mu = \frac{L}{2\pi}\arg\phi = x_1$ and the variance is

$$\sigma^2 = 2L(L - |\phi|) = \frac{2L^2}{2M+1}. \tag{5.10}$$

Recall that $L/(2M+1)$ is the Nyquist spacing for S^1, with bandlimit $|k_m| \leq \Lambda$ (and $M = \lceil \frac{L\Lambda}{2\pi} \rceil$). Note that as $L \to \infty$, we find $\sigma^2 \sim 2L\frac{\pi}{\Lambda}$, where $\frac{\pi}{\Lambda}$ is the Nyquist density for $\mathbb{R}$.

In order to verify the incompressibility of degrees of freedom, we will only demonstrate using two points. We will calculate the size of a subsystem of two points as a function of their separation. Let $x_1 = x_0 - \frac{L}{2M+1}\frac{\delta}{2}$ and $x_2 = x_0 + \frac{L}{2M+1}\frac{\delta}{2}$, so that their separation is δ times the Nyquist spacing. We have

$$Q = \frac{2M+1}{L}\begin{pmatrix} 1 & D\left(\frac{\pi\delta}{2M+1}\right) \\ D\left(\frac{\pi\delta}{2M+1}\right) & 1 \end{pmatrix}, \quad \text{with } D(z) := \frac{\sin[(2M+1)z]}{(2M+1)\sin(z)}. \tag{5.11}$$

Then

$$p(x) = \frac{1}{2}\frac{L}{2M+1}\frac{1}{1 - D\left(\frac{\pi\delta}{2M+1}\right)^2}\left[(x|P_\Lambda|x_1)^2 + (x|P_\Lambda|x_2)^2 - 2D\left(\frac{\pi\delta}{2M+1}\right)(x|P_\Lambda|x_1)(x|P_\Lambda|x_2)\right], \tag{5.12}$$

and we find

$$\begin{aligned}\phi &:= \int_0^L dx\, p(x) L e^{\frac{2\pi i}{L}x} \\ &= e^{\frac{2\pi i}{L}x_0}\frac{L}{2M+1}\frac{1}{1 - D\left(\frac{\pi\delta}{2M+1}\right)^2}\left[2M\cos\left(\frac{\pi\delta}{2M+1}\right) - D\left(\frac{\pi\delta}{2M+1}\right)\frac{\sin[2M\pi\delta/(2M+1)]}{\sin[\pi\delta/(2M+1)]}\right].\end{aligned}$$

Then the mean is the intuitive result, $\mu = \frac{L}{2\pi}\arg\phi = x_0 = (x_1+x_2)/2$, and the variance is given by $\sigma^2 = 2L(L - |\phi|)$.

Figure 5.10 shows a plot of σ^2 as a function of δ for a particular choice of $M = 50$. Notice that the size of the subsystem does not decrease, but in fact increases below the Nyquist spacing, $\delta \leq 1$. If we increase M further to 10^3 (Figure 5.11), we notice the variance behaves even more peculiarly, as it takes its largest value in the coincidence limit, and

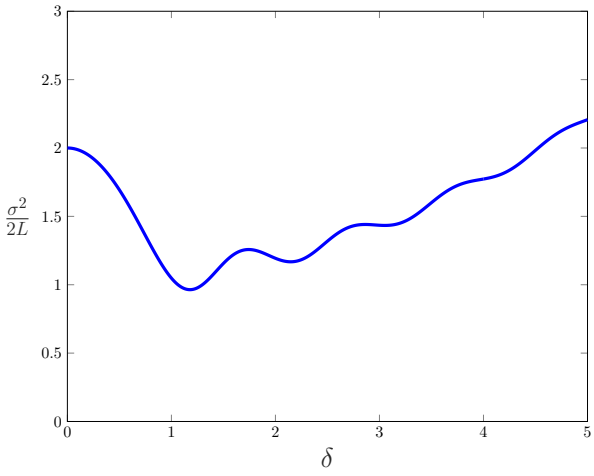

Figure 5.10: Size of a subsystem of $N = 2$ sample points as quantified by $\sigma^2/2L$ (in Nyquist units, hence divided by another $L/(2M+1)$), as a function of the separation of the two points δ (in Nyquist units). The cutoff is $M = 50$.

oscillates around the single sample point value of $\sigma^2 = 2L^2/(2M+1)$ for $\delta \geq 1$ (note that the vertical axis is in Nyquist units, so 1 on the axis corresponds to $\sigma^2 = 2L^2/(2M+1)$). Intuitively it is not clear why this happens. The probability distributions for the cases of $\delta = 0.01$ (close to the coincidence limit) and $\delta = 1$ (Nyquist-spacing) are plotted in Figure 5.12 (with the distribution for a single point for comparison). Visually these cases for two samples appear to be localized to the same region, which is larger than the region occupied by a single sample point. However, clearly this is not reflected in the variance, which perhaps is simply sensitive to the "fringes" that appear outside of the main interval (between -1.5 and 1.5 Nyquist spacings away from the mean). This behaviour seems to persist for larger N, although the inversion of Q becomes numerically unstable for small δ.

Regardless, we can calculate σ^2 for the coincidence limit $\delta \to 0$, and show that it does not reduce to the value of a single sample point, hence demonstrating the incompressibility. From the plots, it appears to be twice the value of a single point. Note that in this limit, the matrix Q is not invertible, yet it turns out that σ^2 is continuous there, so taking this limit yields the resulting size of the subsystem when the two points are taken arbitrarily

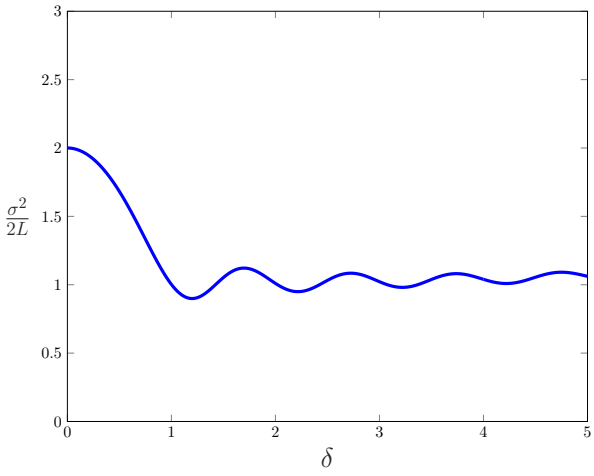

Figure 5.11: Size of a subsystem of $N = 2$ sample points as quantified by $\sigma^2/2L$ (in Nyquist units, hence divided by another $L/(2M+1)$), as a function of the separation of the two points δ (in Nyquist units). The cutoff is $M = 1000$.

close together. Using,

$$D\left(\frac{\pi\delta}{2M+1}\right) = 1 - \tfrac{2}{3}\tfrac{M(M+1)}{(2M+1)^2}\pi^2\delta^2 + \mathcal{O}(\delta^4),$$
$$\frac{\sin[2M\pi\delta/(2M+1)]}{\sin[\pi\delta/(2M+1)]} = 2M + \tfrac{1}{3}\tfrac{M(1-2M)}{2M+1}\pi^2\delta^2 + \mathcal{O}(\delta^4),$$

we find,

$$\sigma^2 = \frac{4L^2}{2M+1} + \mathcal{O}(\delta^2). \tag{5.13}$$

So, we see in the limit $\delta \to 0$, σ^2 is twice the value of the subsystem consisting of a single sample point.

If we were to take $\sigma^2/2L$ as the size of a subsystem, then the subsytem consisting of a single point has size $L/(2M+1)$ (the Nyquist spacing) and that of two points in the coincidence limit is $2L/(2M+1)$. Note that this division by $2L$ to identify the subsystem size as $\sigma^2/2L$ seems appropriate since it gives the intuitive results in these cases, as well as the case of a uniform distribution $p(x) = 1/L$ associated with a complete set of samples, which gives $\phi = 0$ and $\sigma^2 = 2L^2$, and so the subsystem size would be L.

Hence we have established a quantity that characterizes the size of a subsystem of sample points for bandlimited functions on S^1. We verified more carefully the incompressibility of degrees of freedom for bandlimited functions, which corresponds in a way to the

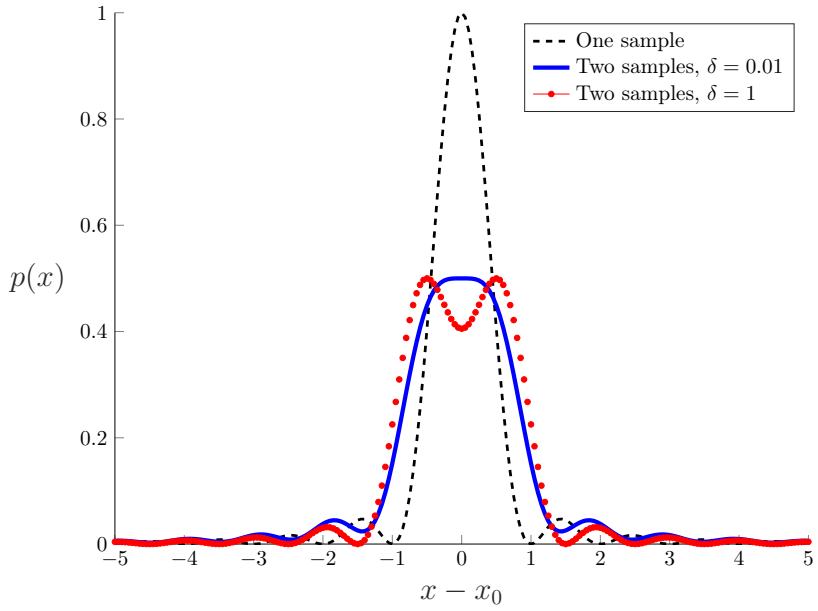

Figure 5.12: Probability distributions characterizing the spatial profile of $N = 2$ sample points at separation $\delta = 0.01$ (near the coincidence limit) and $\delta = 1$ (Nyquist spacing). The distribution for a single sample point is shown for comparison. The vertical axis is the probability (multiplied by the Nyquist spacing $L/(2M + 1)$) and the horizontal axis is Nyquist spacings away from the mean x_0.

incompressibility of information in bandlimited classical and quantum field theory. Now let us see how the density of degrees of freedom in bandlimited field theory is modulated by geometric perturbations of the underlying manifold.

We will conclude this chapter by introducing a notion of local density of degrees of freedom for bandlimited fields, which we will call the *local sample density*. The local sample density at a point x will be identified with the inverse size of a single sample point located at x. For the case of S^1, this would be $2L/\sigma^2 = (2M + 1)/L$ for all $x \in S^1$. Because the space of bandlimited fields on S^1 is translation-invariant, it is natural that the local sample density should be constant in space, and equal to the global sample density $(2M + 1)/L$. However, in cases where one does not have translation invariance, one would expect the subsystem size of a single sample point to depend on its position. This will be the subject of the investigation in Chapter 6.

The local sample density is different than the notions of sample density discussed in Chapter 2, which indicate requirements for global reconstruction of bandlimited functions.

In contrast, because the subsystem profiles are fairly localized, this local sample density gives a sense of how many samples are required in a particular region to capture the majority of the content of a function contained in that region. The incompressibility of the degrees of freedom supports the consistency of this idea, since N samples placed at the Nyquist density or higher seem to occupy a region of size N times the size of a single sample. There appear to be issues with using σ^2 to quantify the size of a region occupied by $N > 1$ samples, and this should be investigated further to determine whether this measure is generally appropriate.

Chapter 6

Subsystem localization with geometric perturbations

Here we are going to conduct an investigation into bandlimitation on a curved manifold. Specifically, we will explore how the local sample density, introduced at the end of the previous chapter, depends on the geometry of the manifold.

In [71], it was recognized that the number of samples required to reconstruct a bandlimited function on a (compact) curved space can be written, using an asymptotic expansion for the heat kernel, as:

$$N = \frac{1}{(4\pi)^{n/2}} \int d^n x \sqrt{|g|} \left[\frac{\Lambda^n}{\Gamma(n/2+1)} + \frac{\Lambda^{n-2}}{\Gamma(n/2)} \frac{R}{6} + \mathcal{O}(\Lambda^{n-4}, R^2) \right], \tag{6.1}$$

where $\mathcal{O}(R^2)$ stands for terms quadratic in the curvature, such as $R_{\rho\sigma\mu\nu}R^{\rho\sigma\mu\nu}$, $R_{\mu\nu}R^{\mu\nu}$, R^2, etc. (see also [42, 43, 49] as well as [40] Section 5.4). This expression is derived as the number of eigenvalues of the Laplacian below a cutoff Λ^2. For a compact manifold, this gives the (finite) dimension of the bandlimited Hilbert space in terms of the volume of the manifold plus curvature corrections. Note that the leading-order term is simply the Weyl law.

As discussed in Chapter 2, since the Hilbert space is finite-dimensional, we expect to be able to generally reconstruct a function in the bandlimited subspace by a finite number of sample values. Dividing by the volume, we get the sample density,

$$\frac{N}{V} = \frac{1}{(4\pi)^{n/2}} \left[\frac{\Lambda^n}{\Gamma(n/2+1)} + \frac{\Lambda^{n-2}}{\Gamma(n/2)} \frac{\langle R \rangle}{6} + \mathcal{O}(\Lambda^{n-4}, \langle R^2 \rangle) \right], \tag{6.2}$$

where $\langle R \rangle \equiv (\int d^n x \sqrt{|g|} R)/(\int d^n x \sqrt{|g|})$. The leading order term gives the sample density for a flat geometry, but here we will pursue an investigation of the nature of the corrections due to the curvature. In particular, rather than focusing on the global sample density, we would like to know to what extent the local curvature affects the local sample density, as defined in the previous chapter. In Chapter 5, we discussed how this is related to the information density and incompressibility of the degrees of freedom of bandlimited fields.

Of course, since bandlimitation is fundamentally nonlocal, we expect that the local sample density will also be affected by the curvature throughout the manifold. We would like to also investigate the importance of local versus nonlocal contributions (for example, how the dependence decays with distance), particularly when the cutoff is large (for example, near the Planck scale). For example, from the above formula, we see that the sample density increases with increasing average Ricci curvature. Is this also true locally? I.e., does the local sample density at a point increase with the curvature in the neighbourhood of that point? We would like to verify this, and ultimately would be interested in how quickly the nonlocal influences decay.

In this chapter we will only be considering Riemannian manifolds and bandlimitation of the associated Laplace-Beltrami operator. As we have described in Chapter 2, the pseudo-Riemannian case is qualitatively different, as it requires an infinite sample density and hence the present investigation would not make sense. (If we were to consider finding the spatial profile of a finite number of samples, (5.6) is ill-defined since the projected position vectors, $\{P_\Lambda|x)\}_x$, are not normalizable.)

In this chapter, we will only look at perturbations of the geometry away from the flat geometry, in order to simplify the analysis. We will not obtain a result in closed form, but hopefully the tools we develop here will help to push this work further in the future.

6.1 General perturbations

Let $(\mathcal{M}, g)$ be a Riemannian manifold, and Δ_g the associated Laplacian. We will take $\mathcal{M}$ to be the n-torus T^n, with coordinates $(x^1, \ldots, x^n) \in [0, L)^n$. The choice of a compact manifold is so that we can employ the methods of Chapter 4 and 5. We can then consider L to be large in order to approximate the case of a manifold with the topology of $\mathbb{R}^n$, if desired.

The Laplacian will act on the space of square-integrable functions $L^2(T^n, g)$, which are L-periodic in each coordinate x^i. We then impose a bandlimit Λ^2 on the eigenvalues of

Δ_g, and get the bandlimited subspace $B(\Lambda) := P_\Lambda L^2(T^n, g)$. The projector onto this bandlimited subspace, P_Λ, can be used to construct the probability distribution corresponding to the spatial profile of a subsystem of sample points using (5.6) from Chapter 5. We can then calculate the mean and variance of this distribution as measures of the location and size of a particular subsystem. The variance of a subsystem of a single sample point is inversely proportional to the notion of local sample density introduced at the end of the last chapter. Recall that in order to calculate a diffeomorphism-invariant variance for a probability distribution on T^n, we will need to employ the methods of Chapter 4. In particular, we will require the isometric embeddings developed in Section 4.3.

Note that our definition of local sample density does not require us to find a sampling lattice for $B(\Lambda) := P_\Lambda L^2(T^n, g)$, only position-space components of the bandlimited projector, $(x|P_\Lambda|x')$. Although it is clear in principle what needs to be done for an arbitrary metric g, it is not generally possible to find a concrete representation of $(x|P_\Lambda|x')$ that can be used to proceed with the calculation. Therefore, here we will be considering perturbations away from the flat Euclidean metric on T^n, $g_{ij} = \delta_{ij} + h_{ij}$, and perform all calculations only to first order in h_{ij}. It may be interesting in the future to consider a similar, non-perturbative, calculation for certain cases of Riemannian manifolds.

We will break the calculation into steps contained in the following subsections. The main task is to calculate $(x|P_\Lambda|x')$. This begins by calculating the perturbed spectrum and eigenvectors. The perturbed eigenvectors within the bandlimited subspace are combined to find the perturbed bandlimited projector.

6.2 Unperturbed problem

We begin with the unperturbed problem, i.e., with metric $g_{ij} = \delta_{ij}$, in order to review the basic setup and to establish notation and normalization conventions. Sampling theory with a flat metric on T^n is a straightforward generalization of sampling on S^1, except that we will not obtain an explicit expression for $(x|P_\Lambda|x')$ nor an explicit reconstruction formula.

Using coordinates $x \equiv (x^1, \ldots, x^n) \in [0, L)^n$ on T^n, the functions in $L^2(T^n, \delta)$ have position space representation $\phi(x) \equiv (x|\phi)$, with $(x|x') = \delta^{(n)}(x - x')$ and $\int_{T^n} dx\, |x)(x| = 1$. The Laplacian in position space is $\Delta_\delta = \partial^2 = \partial_i \partial^i$, with domain consisting of elements of $L^2(T^n, \delta)$ which are L-periodic in each x^i. With this domain, the eigenvalues of Δ_δ are $\lambda_m = -(k_m)^2 = -\left(\frac{2\pi m}{L}\right)^2$ with $m \in \mathbb{Z}^n$. Note that the spectrum of Δ_δ is degenerate. For example, changing the sign of a component of $m \in \mathbb{Z}^n$ or permuting the components typically yields an $m' \neq m$ such that $\lambda_m = \lambda_{m'}$. The dimension of each degenerate

eigenspace is finite-dimensional (see, e.g., [28]). The eigenvectors are

$$(x|k_m) = \frac{1}{L^{n/2}} e^{ik_m \cdot x}, \quad \text{where } k_m \cdot x = (k_m)^i x_i, \tag{6.3}$$

with normalization $(k_m|k_{m'}) = \delta_{mm'}$ and resolution of identity $\sum_{m\in\mathbb{Z}^n} |k_m)(k_m| = 1$.

Now impose a bandlimit $|\lambda_m| \leq \Lambda^2$ (or $|k_m| \leq \Lambda$). Let the set of m's satisfying the bandlimit be denoted

$$M_\Lambda := \{m \in \mathbb{Z}^n : m^2 = \delta_{ij} m^i m^j \leq \left(\tfrac{L\Lambda}{2\pi}\right)^2\}. \tag{6.4}$$

An arbitrary bandlimited function can be written,

$$\phi(x) = \frac{1}{L^{n/2}} \sum_{m\in M_\Lambda} \phi_m e^{ik_m \cdot x}, \quad \text{with } \phi_m := (k_m|\phi). \tag{6.5}$$

The projector onto bandlimited subspace is $P_\Lambda := \sum_{m\in M_\Lambda} |k_m)(k_m|$. The projected position vectors will be written $\{P_\Lambda|x)\}_{x\in T^n}$. These are no longer orthonormal, and the overlaps given by

$$(x|P_\Lambda|x') = \frac{1}{L^n} \sum_{m\in M_\Lambda} e^{ik_m \cdot (x-x')}. \tag{6.6}$$

In dimension $n = 1$, this evaluates to a Dirichlet kernel. Note that $(x|P_\Lambda|x) = \frac{|M_\Lambda|}{L^n}$, where L^n is the position space volume. We also have a continuous resolution of identity using these position vectors $\int_{T^n} dx\, P_\Lambda|x)(x|P_\Lambda = P_\Lambda$.

6.3 Scalar densities and Laplacian perturbation

The typical setting for a perturbation problem is to consider two operators, A and $A+\delta A$, acting on some Hilbert space $\mathcal{H}$. If the perturbation δA is small, then the spectra and eigenvectors of the two operators should be close, and those of $A + \delta A$ can be solved for order-by-order in the size of the perturbation.

In our problem, the Laplacian, Δ_g, for an arbitrary metric, g, acts on (a dense domain of) the Hilbert space $\mathcal{H}_S(g) := L^2(\mathcal{M}, g)$, which is a space of scalar functions on the manifold such that $(\phi|\phi)_g = \int_\mathcal{M} \sqrt{|g|} dx\, |\phi(x)|^2 < \infty$. Notice that the definition of the inner product, which determines the functions admitted to the Hilbert space, depends on the choice of metric. Therefore, our perturbation problem does not adhere to the typical

setup, because the operator Δ_δ acts on the Hilbert space $\mathcal{H}_S(\delta)$, whereas the perturbed operator $\Delta_{\delta+h}$ acts on a different Hilbert space $\mathcal{H}_S(\delta+h)$. Therefore, for example, it is not necessarily clear what it means to say that an eigenvector of $\Delta_{\delta+h} = \Delta_\delta + \delta\Delta_h$ is close to one of Δ_δ because they lie in different Hilbert spaces. Therefore, it is not clear what something like

$$|\phi_\lambda) = |\phi_\lambda^{(0)}) + |\phi_\lambda^{(1)}) + \cdots \tag{6.7}$$

should mean, since $|\phi_\lambda^{(0)}) \in \mathcal{H}_S(\delta)$ but $|\phi_\lambda) \in \mathcal{H}_S(\delta+h)$.

There are a couple of different ways to approach this problem. One is to consider a family of inner products on some fixed linear space, as in [95]. Here we will use an approach inspired by [91] (Subsection 12.3.1), where we represent both Δ_δ and $\Delta_{\delta+h}$ on a common Hilbert space of scalar *densities* rather than scalars, which does not depend on any choice of geometry, and then we solve the perturbation problem there.

Let $\mathcal{H}_D$ denote the Hilbert space of scalar densities, which are functions $\psi(x)$ such that $\int_\mathcal{M} dx\, |\psi(x)|^2 < \infty$. The difference between these and scalar functions is that they are defined to transform under coordinate changes $x^i \to \bar{x}^i$ by

$$\psi(x) \mapsto \bar{\psi}(\bar{x}) = \left|\frac{\partial x^i}{\partial \bar{x}^j}\right|^{1/2} \psi(x). \tag{6.8}$$

In this way, the inner product on $\mathcal{H}_D$,

$$\langle\psi|\psi'\rangle := \int_\mathcal{M} dx\, \psi^*(x)\psi'(x), \tag{6.9}$$

is diffeomorphism-invariant. Thus, the definition of $\mathcal{H}_D$ is independent of any choice of metric. Note that for the next few sections, we will be using angled brackets $|\psi\rangle$ to denote elements of $\mathcal{H}_D$ in order to distinguish from elements $|\phi)$ of $\mathcal{H}_S(g)$. We will not be dealing with quantum states at any point in this chapter, so hopefully this temporary notation will not cause any confusion.

Now for a particular choice of metric, g, there is a Hilbert space isomorphism between the space of scalars and scalar densities, which we shall denote $V_g : \mathcal{H}_S(g) \to \mathcal{H}_D$, and which is given by $V_g : \phi(x) \mapsto |g(x)|^{1/4}\phi(x)$. Clearly, this preserves the inner product,

$$\langle V_g\phi|V_g\phi'\rangle_{\mathcal{H}_D} = \int_\mathcal{M} dx\sqrt{|g|}\, \phi^*(x)\phi'(x) = (\phi|\phi')_{\mathcal{H}_S(g)}. \tag{6.10}$$

This can be represented somewhat more abstractly by introducing

$$(x|x') = \frac{1}{\sqrt{|g|}}\delta^{(n)}(x-x') \quad \text{and } 1 = \int dx\sqrt{|g|}\, |x)(x| \quad \text{on } \mathcal{H}_S(g) \tag{6.11}$$

and

$$\langle x|x'\rangle = \delta^{(n)}(x-x'), \quad 1 = \int dx\, |x\rangle\langle x| \quad \text{on } \mathcal{H}_D. \tag{6.12}$$

We see that these position-type vectors are consistent with the identification of functions in $\mathcal{H}_S(g)$ as $\phi(x) = (x|\phi)$ and functions in $\mathcal{H}_D$ as $\psi(x) = \langle x|\psi\rangle$. Then,

$$V_g = \int_{\mathcal{M}} dx |g(x)|^{1/4} |x\rangle(x| : \mathcal{H}_S(g) \to \mathcal{H}_D. \tag{6.13}$$

The inverse of V_g is simply $V_g^{-1} = V_g^\dagger = \int_{\mathcal{M}} dx|g(x)|^{1/4}|x\rangle\langle x| : \mathcal{H}_D \to \mathcal{H}_S(g)$.

Now any operator, such as Δ_g, on $\mathcal{H}_S(g)$ can be represented by another operator, $\tilde{\Delta}_g := V_g \Delta_g V_g^\dagger$, on $\mathcal{H}_D$. To any eigenvector $|\lambda) \in \mathcal{H}_S(g)$ of Δ_g, there is a corresponding eigenvector $V_g|\lambda) \in \mathcal{H}_D$ of $\tilde{\Delta}_g$ with the same eigenvalue:

$$\tilde{\Delta}_g V_g|\lambda) = V_g \Delta_g \cancel{V_g^\dagger V_g}|\lambda) = \lambda V_g|\lambda). \tag{6.14}$$

Conversely, if $|\lambda\rangle$ is an eigenvector of $\tilde{\Delta}_g$, then $V_g^\dagger|\lambda\rangle$ is an eigenvector of Δ_g with the same eigenvalue.

Returning to the perturbation problem, we see now that the benefit of introducing this space of scalar densities is that we can represent both Δ_δ and $\Delta_{\delta+h}$ by new operators $\tilde{\Delta}_\delta := V_\delta \Delta_\delta V_\delta^\dagger$ and $\tilde{\Delta}_{\delta+h} := V_{\delta+h}\Delta_{\delta+h}V_{\delta+h}^\dagger$ (respectively), which have the same spectra and corresponding eigenvectors as the original operators, but are now both acting on the same Hilbert space $\mathcal{H}_D$. Now, schematically, we can solve for the spectrum and eigenvectors of $\tilde{\Delta}_{\delta+h}$ perturbatively in h_{ij},

$$\begin{aligned} \lambda &= \lambda^{(0)} + \lambda^{(1)} + \mathcal{O}(h^2) \\ |\lambda\rangle &= |\lambda^{(0)}\rangle + |\lambda^{(1)}\rangle + \mathcal{O}(h^2). \end{aligned}$$

The eigenvectors can then be mapped back to $\mathcal{H}_S(\delta+h)$ using $V_{\delta+h}^\dagger$. Note that this map can also be expanded in orders of h_{ij}, so that

$$V_{\delta+h}^\dagger |\lambda\rangle = V_\delta^\dagger |\lambda^{(0)}\rangle + \delta V_h^\dagger |\lambda^{(0)}\rangle + V_\delta^\dagger |\lambda^{(1)}\rangle + \mathcal{O}(h^2), \tag{6.15}$$

where $\delta V_h^\dagger := \int_{\mathcal{M}} dx\, \frac{1}{4} h(x)|x\rangle\langle x|$ with $h(x) := \delta^{ij}h_{ij}(x)$. Note that one has to be careful when working with position vectors $|x)$ in $\mathcal{H}_S(\delta+h)$ since their normalization and resolution of identity include factors of $\sqrt{|g|} = 1 + \frac{1}{2}h + \mathcal{O}(h^2)$. Thus, in the position representations, we have

$$(x|V_{\delta+h}^\dagger |\lambda\rangle = \left(1 - \tfrac{1}{4}h(x)\right) \langle x|\lambda^{(0)}\rangle + \langle x|\lambda^{(1)}\rangle + \mathcal{O}(h^2). \tag{6.16}$$

Now that we have a handle on the formulation of the problem, before proceeding with the calculation let us work out the explicit representations of the operator $\tilde{\Delta}_{\delta+h} = \tilde{\Delta}_\delta + \delta\tilde{\Delta}_h$ on $\mathcal{H}_D$. First, it is clear that in the coordinates we have chosen where the zeroth order metric is δ_{ij}, the zeroth order Laplacian is represented in the same way on $\mathcal{H}_D$ as on $\mathcal{H}_S(\delta)$. Namely, $\tilde{\Delta}_\delta = \partial^2$. For an arbitrary metric, g, in the position representation of $\tilde{\Delta}_g = V_g \Delta_g V_g^\dagger$ we have

$$\begin{aligned}\langle x|\tilde{\Delta}_g|x'\rangle &= |g(x)|^{1/4}(x|\Delta_g|x')|g(x')|^{1/4} \\ &= |g(x)|^{1/4}\left[\frac{1}{\sqrt{|g|}}\partial_i\left(\sqrt{|g|}g^{ij}\partial_j\cdot\right)\right]_x |g(x)|^{-1/4}\delta^{(n)}(x-x')\end{aligned}$$

Note that this representation of $\tilde{\Delta}_g$ is manifestly symmetric. Let us ignore the $\delta^{(n)}(x-x')$ and have the position representation of $\tilde{\Delta}_g$ be understood as a differential operator. Expanding the above expression, we find

$$\begin{aligned}(\tilde{\Delta}_g)_x = {} & g^{ij}\partial_i\partial_j + g^{ij}{}_{,i}\partial_j \\ & - \tfrac{1}{4}\left[\tfrac{1}{4}g^{ij}(\partial_i \ln|g|)(\partial_j \ln|g|) + g^{ij}{}_{,i}(\partial_j \ln|g|) + g^{ij}(\partial_i\partial_j \ln|g|)\right].\end{aligned}$$

Now writing $g_{ij} = \delta_{ij} + h_{ij}$, we find

$$(\tilde{\Delta}_{\delta+h})_x = \partial^2 - h^{ij}\partial_i\partial_j - h^{ij}{}_{,i}\partial_j - \tfrac{1}{4}(\partial^2 h) + \mathcal{O}(h^2). \tag{6.17}$$

Note that to first order the indices are raised and lowered with δ_{ij}. Let us write the first order perturbation as $(\delta\tilde{\Delta}_h)_x := -h^{ij}\partial_i\partial_j - h^{ij}{}_{,i}\partial_j - \frac{1}{4}(\partial^2 h)$. One can also write an arbitrary matrix element of $\delta\tilde{\Delta}_h$ as:

$$\langle\psi|\,\delta\tilde{\Delta}_h\,|\phi\rangle = \int dx\left[(\partial_i\psi^*)(\partial_j\phi) - \tfrac{1}{4}\delta_{ij}\partial^2(\psi^*\phi)\right]h^{ij}. \tag{6.18}$$

6.4 Spectrum and eigenvectors

Recall at zeroth order, we have $\tilde{\Delta}_\delta\,|k_m\rangle = \lambda_m\,|k_m\rangle$, with $\lambda_m = -(k_m)^2 = -\left(\frac{2\pi m}{L}\right)^2$ for $m \in \mathbb{Z}^n$, and $\langle x|k_m\rangle = \frac{1}{L^{n/2}}e^{ik_m\cdot x}$. The nonzero eigenvalues of $\tilde{\Delta}_\delta$ are degenerate. Let $E^{(0)}_\lambda \subset \mathcal{H}_D$ denote the eigenspace associated with some fixed eigenvalue λ of $\tilde{\Delta}_\delta$. It is guaranteed that this eigenspace is finite-dimensional (see, e.g., [28]). Let $\{|\psi^{(0)}_{\lambda,\zeta}\rangle\}_\zeta$ be a general orthonormal basis for this space, indexed by $\zeta = 1, \ldots, \dim E^{(0)}_\lambda$. The set $\{|k_m\rangle\}_{m:\lambda_m=\lambda}$ is of course a

basis for this eigenspace, but it is not necessarily the orientation in which any degeneracies are potentially resolved, so we need to consider a general basis.

Now we want to find some $|\psi_{\lambda,\zeta}\rangle \in \mathcal{H}_D$ which is an eigenvector of $\tilde{\Delta}_{\delta+h}$ such that $|\psi_{\lambda,\zeta}\rangle \to |\psi^{(0)}_{\lambda,\zeta}\rangle$ as $h_{ij} \to 0$. Expanding in a perturbation series, to first order we have

$$\left(\tilde{\Delta}_\delta + \delta\tilde{\Delta}_h + \cdots\right)\left(|\psi^{(0)}_{\lambda,\zeta}\rangle + |\psi^{(1)}_{\lambda,\zeta}\rangle + \cdots\right) = (\lambda + \delta\lambda_\zeta + \cdots)\left(|\psi^{(0)}_{\lambda,\zeta}\rangle + |\psi^{(1)}_{\lambda,\zeta}\rangle + \cdots\right)$$
$$(\lambda - \tilde{\Delta}_\delta)\,|\psi^{(1)}_{\lambda,\zeta}\rangle = (\delta\tilde{\Delta}_h - \delta\lambda_\zeta)\,|\psi^{(0)}_{\lambda,\zeta}\rangle + \mathcal{O}(h^2).$$

Contracting this last line with another basis vector $|\psi^{(0)}_{\lambda,\zeta'}\rangle \in E_\lambda$ with $\zeta' \neq \zeta$, one obtains the standard eigenvalue equation

$$\langle\psi^{(0)}_{\lambda,\zeta'}|\,\delta\tilde{\Delta}_h\,|\psi^{(0)}_{\lambda,\zeta}\rangle = \delta\lambda_\zeta\delta_{\zeta,\zeta'}. \tag{6.19}$$

This determines $\delta\lambda_\zeta$ and the parametrization ζ, giving the preferred basis in $E^{(0)}_\lambda$ for the perturbation problem. Explicitly solving this eigenvalue equation would be difficult in general, but we will see in a later section that one may not need to, provided h_{ij} (or, more precisely, $\delta\lambda_\zeta$) satisfies some appropriate condition.

Contracting instead with some $|\psi^{(0)}_{\lambda',\zeta'}\rangle \in E^{(0)}_{\lambda'}$ (where $\lambda' \neq \lambda$), one obtains

$$\langle\psi^{(0)}_{\lambda',\zeta'}|\psi^{(1)}_{\lambda,\zeta}\rangle = \frac{1}{\lambda - \lambda'}\,\langle\psi^{(0)}_{\lambda',\zeta'}|\,\delta\tilde{\Delta}_h\,|\psi^{(0)}_{\lambda,\zeta}\rangle\,. \tag{6.20}$$

This determines the components of the perturbed eigenstates $|\psi^{(1)}_{\lambda,\zeta}\rangle$ in directions orthogonal to $E^{(0)}_\lambda$. Notice that since $\{|\psi^{(0)}_{\lambda',\zeta'}\rangle\}_{\zeta'}$ forms an orthonormal basis of the eigenspace $E^{(0)}_{\lambda'}$, we can write:

$$\begin{aligned} P^{(0)}_{\lambda'}\,|\psi^{(1)}_{\lambda,\zeta}\rangle &= \sum_{\zeta'} |\psi^{(0)}_{\lambda',\zeta'}\rangle\,\langle\psi^{(0)}_{\lambda',\zeta'}|\psi^{(1)}_{\lambda,\zeta}\rangle \\ &= \sum_{\zeta'} |\psi^{(0)}_{\lambda',\zeta'}\rangle\,\frac{1}{\lambda - \lambda'}\,\langle\psi^{(0)}_{\lambda',\zeta'}|\,\delta\tilde{\Delta}_h\,|\psi^{(0)}_{\lambda,\zeta}\rangle \\ &= \frac{1}{\lambda - \lambda'} P^{(0)}_{\lambda'}\delta\tilde{\Delta}_h\,|\psi^{(0)}_{\lambda,\zeta}\rangle\,, \end{aligned}$$

where $P^{(0)}_{\lambda'}$ is the projector onto the subspace $E^{(0)}_{\lambda'} \subset \mathcal{H}_D$. Since the full set of eigenvectors of $\tilde{\Delta}_\delta$ resolve the identity on $\mathcal{H}_D$, $\sum_\lambda P^{(0)}_\lambda = 1$, let us write $P^{(0)\perp}_\lambda := 1 - P^{(0)}_\lambda = \sum_{\lambda'\neq\lambda} P^{(0)}_{\lambda'}$.

Then we see

$$\begin{aligned} P_\lambda^{(0)\perp} |\psi_{\lambda,\zeta}^{(1)}\rangle &= \sum_{\lambda' \neq \lambda} P_{\lambda'}^{(0)} |\psi_{\lambda,\zeta}^{(1)}\rangle \\ &= \frac{1}{\lambda - \tilde{\Delta}_\delta} P_\lambda^{(0)\perp} \delta\tilde{\Delta}_h |\psi_{\lambda,\zeta}^{(0)}\rangle , \end{aligned}$$

where we note that $(\lambda - \tilde{\Delta}_\delta)$ is invertible on $E_\lambda^{(0)\perp}$, and is bounded since the spectrum of $\tilde{\Delta}_\delta$ is discrete on $\mathcal{M} = T^n$. One may notice that this form for $P_\lambda^{(0)\perp} |\psi_{\lambda,\zeta}^{(1)}\rangle$ is a discrete analogy of the Lippmann-Schwinger equation, which is used in scattering theory for the perturbed eigenfunctions of an operator with a continuous spectrum (see, e.g., [90, 108]). Let us denote

$$\tilde{G}_\lambda := \frac{1}{\lambda - \tilde{\Delta}_\delta} P_\lambda^{(0)\perp} \delta\tilde{\Delta}_h, \tag{6.21}$$

in analogy with the Lippmann-Schwinger kernel. Therefore we can succinctly write

$$P_\lambda^{(0)\perp} |\psi_{\lambda,\zeta}^{(1)}\rangle = \tilde{G}_\lambda |\psi_{\lambda,\zeta}^{(0)}\rangle . \tag{6.22}$$

Note that $\tilde{G}_\lambda$ does not depend on ζ.

So far, we have identified (6.19) as the equation necessary to determine the appropriate basis $\{|\psi_{\lambda,\zeta}^{(0)}\rangle\}_\zeta$ in the subspace $E_\lambda^{(0)}$ for the perturbation problem (as well as the first order eigenvalue corrections $\delta\lambda_\zeta$). This is difficult to solve explicitly, but once this basis is obtained, then $|\psi_{\lambda,\zeta}^{(1)}\rangle$ is determined by $P_\lambda^{(0)\perp} |\psi_{\lambda,\zeta}^{(1)}\rangle = \tilde{G}_\lambda |\psi_{\lambda,\zeta}^{(0)}\rangle$ up to a component in $E_\lambda^{(0)}$. The vector $|\psi_{\lambda,\zeta}^{(1)}\rangle$ will typically have nonzero components within the subspace $E_\lambda^{(0)}$, but their determination (even to first order) requires going to higher order in perturbation theory [90].

Fortunately, we will not be required to explicitly determine either the parametrization ζ nor the components of $|\psi_{\lambda,\zeta}^{(1)}\rangle$ within $E_\lambda^{(0)}$. Recall that our current aim is to find the bandlimited projector P_Λ to first order. This is built from summing over projectors onto the eigenspaces associated with eigenvalues below some bandlimit. We will not need the actual eigenvectors, but only the projector onto the subspace they span. Why this is the case requires further discussion provided in the next section, but for now let us just demonstrate how these stated dependencies drop out. We have established that to first order, the eigenvector $|\psi_{\lambda,\zeta}\rangle$ that reduces to $|\psi_{\lambda,\zeta}^{(0)}\rangle$ as $h_{ij} \to 0$ is given by

$$|\psi_{\lambda,\zeta}\rangle = |\psi_{\lambda,\zeta}^{(0)}\rangle + P_\lambda^{(0)} |\psi_{\lambda,\zeta}^{(1)}\rangle + \tilde{G}_\lambda |\psi_{\lambda,\zeta}^{(0)}\rangle , \tag{6.23}$$

where $P_\lambda^{(0)} |\psi_{\lambda,\zeta}^{(1)}\rangle$ remains undetermined. Now let us write Π_λ as the projector onto the subspace spanned by the full eigenvectors $\{|\psi_{\lambda,\zeta}\rangle\}_\zeta$. Although at zeroth order $\{|\psi_{\lambda,\zeta}^{(0)}\rangle\}_\zeta$ spans the eigenspace $E_\lambda^{(0)}$ corresponding to eigenvalue λ of $\tilde{\Delta}_\delta$, the projector Π_λ is not projecting onto some eigenspace associated with a single eigenvalue of $\tilde{\Delta}_{\delta+h}$, since the eigenvalues $\{\lambda + \delta\lambda_\zeta\}_\zeta$ are generically different if some degeneracy is lifted. Nevertheless, we will see in the following section that this projector will still be useful. Now, to see the claims, to first order

$$\begin{aligned}\Pi_\lambda &= \sum_\zeta |\psi_{\lambda,\zeta}\rangle \langle\psi_{\lambda,\zeta}| \\ &= P_\lambda^{(0)} + P_\lambda^{(0)} \left(\sum_\zeta |\psi_{\lambda,\zeta}^{(1)}\rangle \langle\psi_{\lambda,\zeta}^{(0)}| \right) + \left(\sum_\zeta |\psi_{\lambda,\zeta}^{(0)}\rangle \langle\psi_{\lambda,\zeta}^{(1)}| \right) P_\lambda^{(0)} \\ &\quad + P_\lambda^{(0)} \tilde{G}_\lambda^\dagger + \tilde{G}_\lambda P_\lambda^{(0)} + \mathcal{O}(h^2).\end{aligned}$$

Note that the first three terms simply map $E_\lambda^{(0)}$ back into itself, whereas the last two involve maps between $E_\lambda^{(0)}$ and $E_\lambda^{(0)\perp}$, since this is the range of $\tilde{G}_\lambda$ (which can be seen from the definition). Since $P_\lambda^{(0)}$ is already a projector onto the subspace $E_\lambda^{(0)}$, the only possibility for the part of Π_λ mapping $E_\lambda^{(0)}$ back into itself is to project out a certain subspace of $E_\lambda^{(0)}$. However, we will see that this will not happen at first order. Because we know Π_λ should be a projector, it must satisfy $\Pi_\lambda^2 = \Pi_\lambda$. We find that

$$\begin{aligned}\Pi_\lambda^2 &= P_\lambda^{(0)} + 2P_\lambda^{(0)} \left(\sum_\zeta |\psi_{\lambda,\zeta}^{(1)}\rangle \langle\psi_{\lambda,\zeta}^{(0)}| \right) + 2 \left(\sum_\zeta |\psi_{\lambda,\zeta}^{(0)}\rangle \langle\psi_{\lambda,\zeta}^{(1)}| \right) P_\lambda^{(0)} \\ &\quad + P_\lambda^{(0)} \tilde{G}_\lambda^\dagger + \tilde{G}_\lambda P_\lambda^{(0)} + \mathcal{O}(h^2),\end{aligned}$$

using $P_\lambda^{(0)} \tilde{G}_\lambda = 0$. Comparing to the expression for Π_λ, we see that this implies

$$P_\lambda^{(0)} \left(\sum_\zeta |\psi_{\lambda,\zeta}^{(1)}\rangle \langle\psi_{\lambda,\zeta}^{(0)}| \right) + \left(\sum_\zeta |\psi_{\lambda,\zeta}^{(0)}\rangle \langle\psi_{\lambda,\zeta}^{(1)}| \right) P_\lambda^{(0)} = 0 + \mathcal{O}(h^2). \tag{6.24}$$

Therefore,

$$\begin{aligned}\Pi_\lambda &= \sum_\zeta |\psi_{\lambda,\zeta}\rangle \langle\psi_{\lambda,\zeta}| \\ &= P_\lambda^{(0)} + \tilde{G}_\lambda P_\lambda^{(0)} + P_\lambda^{(0)} \tilde{G}_\lambda^\dagger + \mathcal{O}(h^2).\end{aligned}$$

Notice that the contribution from the component $P_\lambda^{(0)} |\psi_{\lambda,\zeta}^{(1)}\rangle$ has dropped out. Also, there is no need to solve (6.19) to find the appropriate basis $\{|\psi_{\lambda,\zeta}^{(0)}\rangle\}_\zeta$ for the perturbation problem since we can write $P_\lambda^{(0)}$ in terms of the $|k_m\rangle$'s and $\tilde{G}_\lambda$ is independent of ζ:

$$P_\lambda^{(0)} = \sum_\zeta |\psi_{\lambda,\zeta}^{(0)}\rangle \langle\psi_{\lambda,\zeta}^{(0)}| = \sum_{m:-(k_m)^2=\lambda} |k_m\rangle \langle k_m| ,$$
$$\tilde{G}_\lambda = \frac{1}{\lambda - \tilde{\Delta}_\delta} P_\lambda^{(0)\perp} \delta\tilde{\Delta}_h .$$

Now we will see how to use the projectors Π_λ in order to construct the bandlimited projector of $\tilde{\Delta}_{\delta+h}$ to first order in h_{ij}.

6.5 Bandlimited projector

Now we want to construct the bandlimited projector $\tilde{P}_\Lambda$ onto the subspace of $\mathcal{H}_D$ spanned by eigenvectors of $\tilde{\Delta}_{\delta+h}$ whose corresponding eigenvalues have a magnitude smaller than Λ^2. To first order, we denoted the eigenvalues of $\tilde{\Delta}_{\delta+h}$ by $\lambda+\delta\lambda_\zeta$, where λ is some eigenvalue of $\tilde{\Delta}_\delta = \partial^2$ and $\{\delta\lambda_\zeta\}_\zeta$ are a set of solutions to (6.19). Ideally, we would like to determine which of these satisfy $|\lambda + \delta\lambda_\zeta| < \Lambda^2$. However, since we do not have a general solution to (6.19), let us simply consider the case where $|\lambda + \delta\lambda_\zeta| < \Lambda^2$ if and only if $|\lambda| < \Lambda^2$. (Note this is only possible since the operators we are considering have a discrete spectrum.)

Such an assumption will make it tractable, and in fact very simple, to determine which eigenvectors to include in the bandlimited projector, since it would simply be all of the solutions $|\psi_{\lambda,\zeta}\rangle$ to the perturbation problem which tend to $|\psi_{\lambda,\zeta}^{(0)}\rangle$ as $h_{ij} \to 0$ where $|\lambda| < \Lambda^2$. By making this assumption, it is possible to work out the bandlimited projector using Π_λ of the previous section,

$$\begin{aligned}
\tilde{P}_\Lambda &= \sum_{|\lambda|<\Lambda^2,\zeta} |\psi_{\lambda,\zeta}\rangle \langle\psi_{\lambda,\zeta}| \\
&= \sum_{|\lambda|<\Lambda^2} \Pi_\lambda \\
&= P_\Lambda^{(0)} + \sum_{|\lambda|<\Lambda^2} \left(\tilde{G}_\lambda P_\lambda^{(0)} + P_\lambda^{(0)} \tilde{G}_\lambda^\dagger \right).
\end{aligned}$$

This assumption is asserting that, for a fixed cutoff Λ^2, no eigenvectors enter or leave the bandlimited subspace. The eigenvectors can still change their form under the perturbation, even by acquiring components along directions which were outside of the bandlimit (encoded in the operator $\tilde{G}_\lambda$). The point is that no vector will be included if the unperturbed eigenvector lay outside of the bandlimited subspace, nor will one be excluded if the unperturbed vector lay inside this subspace.

Although it seems one must make this assumption to proceed on general grounds, it is not yet clear what kind of restriction this imposes on the perturbation h_{ij}. Recall at the beginning of this chapter we stated that the number of eigenvalues below a cutoff Λ^2 is $N = \frac{1}{(4\pi)^{n/2}}[\frac{\Lambda^n}{\Gamma(n/2+1)}V + \frac{\Lambda^{n-2}}{\Gamma(n/2)}\frac{V\langle R\rangle}{6} + \cdots]$. If we assume that nothing leaves or enters the bandlimited subspace under the perturbation, then its dimension will remain the same. Therefore, from this formula, we see that for our simplifying assumption it is necessary that $\langle R\rangle = 0$ (or at least $\langle R\rangle \ll \frac{1}{\Lambda^{n-2}V}$, which is very small in dimensions $n \geq 3$ with Λ at the Planck scale). Although this is a significant limitation, it would still allow us to investigate our question of how the local curvature affects the local sample density. That is, we can still look at whether the sample density increases or decreases for geometries where there are pockets of positive or negative scalar curvature, provided that the total curvature averaged over the manifold vanishes. Strictly speaking one would need to show that $\langle R\rangle = 0$ is also sufficient to allow for this assumption, although we will not attempt this here. We will leave it as future work to analyze this further, as well as attempting to push beyond these assumptions by studying examples where (6.19) can be solved explicitly.

Returning to the expression for $\tilde{P}_\Lambda$, we can simplify it slightly by using the definition of $\tilde{G}_\lambda$, and splitting the factor of $P_\lambda^{(0)\perp}$ contained in $\tilde{G}_\lambda$ into a sum over eigenvalues below and above the bandlimit:

$$\begin{aligned}\tilde{P}_\Lambda &= P_\Lambda^{(0)} + \sum_{|\lambda|<\Lambda^2}\left(\frac{1}{\lambda-\tilde{\Delta}_\delta}P_\lambda^{(0)\perp}\delta\tilde{\Delta}_h P_\lambda^{(0)} + h.c.\right)\\ &= P_\Lambda^{(0)} + \sum_{|\lambda|<\Lambda^2,\,|\lambda'|<\Lambda^2:\lambda'\neq\lambda}\left(\frac{1}{\lambda-\lambda'}P_{\lambda'}^{(0)}\delta\tilde{\Delta}_h P_\lambda^{(0)} + h.c.\right)\\ &\quad + \sum_{|\lambda|<\Lambda^2,\,|\lambda'|\geq\Lambda^2}\left(\frac{1}{\lambda-\lambda'}P_{\lambda'}^{(0)}\delta\tilde{\Delta}_h P_\lambda^{(0)} + h.c.\right).\end{aligned}$$

Notice that the term $\frac{1}{\lambda-\lambda'}$ for $|\lambda'|, |\lambda| < \Lambda^2$ and $\lambda' \neq \lambda$ maps the unperturbed bandlimited subspace back into itself. By the same argument used for Π_λ at the end of the last section,

we can conclude that these terms vanish to first order. In the end, we have

$$\tilde{P}_\Lambda = P_\Lambda^{(0)} + \sum_{|\lambda|<\Lambda^2\leq|\lambda'|} \left(\frac{1}{\lambda-\lambda'} P_{\lambda'}^{(0)} \delta\tilde{\Delta}_h P_\lambda^{(0)} + h.c. \right) \tag{6.25}$$

If desired, one can rewrite the first order corrections to $\tilde{P}_\Lambda$ using

$$\int_0^\infty d\tau\, e^{(\lambda'-\lambda)\tau} = \frac{1}{\lambda-\lambda'}, \tag{6.26}$$

given that $\lambda, \lambda' < 0$ and $|\lambda'| > |\lambda|$. Then

$$\begin{aligned}
&\sum_{|\lambda|<\Lambda^2} \sum_{|\lambda'|\geq\Lambda^2} \left(\frac{1}{\lambda-\lambda'} P_{\lambda'}^{(0)} \delta\tilde{\Delta}_h P_\lambda^{(0)} \right) \\
&\quad = \sum_{|\lambda|<\Lambda^2} \sum_{|\lambda'|\geq\Lambda^2} \left(\int_0^\infty d\tau\, e^{(\lambda'-\lambda)\tau} P_{\lambda'}^{(0)} \delta\tilde{\Delta}_h P_\lambda^{(0)} \right) \\
&\quad = \int_0^\infty d\tau \left(\sum_{|\lambda'|\geq\Lambda^2} e^{\lambda'\tau} P_{\lambda'}^{(0)} \right) \delta\tilde{\Delta}_h \left(\sum_{|\lambda|<\Lambda^2} e^{-\lambda\tau} P_\lambda^{(0)} \right) \\
&\quad =: \int_0^\infty d\tau\, K'_\Lambda(\tau) \delta\tilde{\Delta}_h K_\Lambda(-\tau),
\end{aligned}$$

where K_Λ is the heat kernel of the unperturbed operator ∂^2 with sum restricted to $|\lambda| < \Lambda^2$, and K'_Λ is restricted to $|\lambda'| \geq \Lambda^2$. In the position representation,

$$\begin{aligned}
K_\Lambda(x,x;\tau) &= \langle x|\, K_\Lambda(\tau)\, |x'\rangle \\
&= \sum_{|\lambda|<\Lambda^2} e^{\lambda\tau} \langle x|\, P_\lambda^{(0)}\, |x'\rangle \\
&= \frac{1}{L^n} \sum_{m\in M_\Lambda} e^{-(k_m)^2\tau + ik_m\cdot(x-x')},
\end{aligned}$$

where we recall $P_\lambda^{(0)} = \sum_{m:-(k_m)^2=\lambda} |k_m\rangle \langle k_m|$ and $\langle x|k_m\rangle = \frac{1}{L^{n/2}} e^{ik_m\cdot x}$, since these were the eigenvectors of $\tilde{\Delta}_\delta$ which were mapped from $\mathcal{H}_S(\delta)$ to $\mathcal{H}_D$ under V_δ. Recall also that M_Λ is defined as the set of $m \in \mathbb{Z}^n$ such that $(k_m)^2 = \left(\frac{2\pi m}{L}\right)^2 < \Lambda^2$. One can obtain an analogous expression for K'_Λ.

Now that we have the bandlimited projector on $\mathcal{H}_D$, let us map to $\mathcal{H}_S(\delta+h)$ using $V^\dagger_{\delta+h}$ to obtain the bandlimited projector for scalar functions. Recall that since $V^\dagger_{\delta+h}$ depends on the metric, we also pick up additional factors of h. Above we noted that for a state of the form $|\psi\rangle = |\psi^{(0)}\rangle + |\psi^{(1)}\rangle + \mathcal{O}(h^2)$, we have

$$(x|V^\dagger_{\delta+h}\,|\psi\rangle = (1-\tfrac{1}{4}h(x))\langle x|\psi^{(0)}\rangle + \langle x|\psi^{(1)}\rangle + \mathcal{O}(h^2). \tag{6.27}$$

Therefore, to first order, the position representation of the bandlimited projector $P_\Lambda := V^\dagger_{\delta+h}\tilde{P}_\Lambda V_{\delta+h}$ in $\mathcal{H}_S(\delta+h)$ is

$$\begin{aligned}(x|P_\Lambda|x') &= (x|V^\dagger_{\delta+h}P^{(0)}_\Lambda V_{\delta+h}|x') \\ &\quad + (x|V^\dagger_{\delta+h}\sum_{|\lambda|<\Lambda^2\le|\lambda'|}\frac{1}{\lambda-\lambda'}\left(P^{(0)}_{\lambda'}\delta\tilde{\Delta}_h P^{(0)}_\lambda + h.c.\right)V_{\delta+h}|x') \\ &= \left(1-\tfrac{1}{4}h(x)-\tfrac{1}{4}h(x')\right)\langle x|\,P^{(0)}_\Lambda\,|x'\rangle \\ &\quad + \sum_{|\lambda|<\Lambda^2\le|\lambda'|}\frac{1}{\lambda-\lambda'}\left(\langle x|\,P^{(0)}_{\lambda'}\delta\tilde{\Delta}_h P^{(0)}_\lambda\,|x'\rangle + \langle x|\,P^{(0)}_\lambda\delta\tilde{\Delta}_h P^{(0)}_{\lambda'}\,|x'\rangle\right)\end{aligned}$$

Inserting $\int dx\,|x\rangle\langle x| = 1$ for $\mathcal{H}_D$ on either side of the $\delta\tilde{\Delta}_h$'s, and recalling that

$$\begin{aligned}\langle x|\,\delta\tilde{\Delta}_h\,|x'\rangle &= (\delta\tilde{\Delta}_h)_x\delta^{(n)}(x-x') \\ (\delta\tilde{\Delta}_h)_x &= -h^{ij}\partial_i\partial_j - h^{ij}{}_{,i}\partial_j - \tfrac{1}{4}(\partial^2 h),\end{aligned}$$

we have

$$(x|P_\Lambda|x') = \frac{1}{|g(x)|^{1/4}|g(x')|^{1/4}}\,\langle x|\,P^{(0)}_\Lambda\,|x'\rangle + \langle x|\,P^{(1)}_\Lambda\,|x'\rangle + \mathcal{O}(h^2), \tag{6.28}$$

with

$$\langle x|\,P^{(0)}_\lambda\,|x'\rangle = \frac{1}{L^n}\sum_{m:-(k_m)^2=\lambda} e^{ik_m\cdot(x-x')}, \tag{6.29}$$

and $P^{(0)}_\Lambda = \sum_{|\lambda|<\Lambda^2}P^{(0)}_\lambda$, as well as

$$\begin{aligned}\langle x|\,P^{(1)}_\Lambda\,|x'\rangle := \sum_{|\lambda|<\Lambda^2\le|\lambda'|}\frac{1}{\lambda-\lambda'}\int dx''\Big[&\langle x|\,P^{(0)}_{\lambda'}\,|x''\rangle\,(\delta\tilde{\Delta}_h)_{x''}\,\langle x''|\,P^{(0)}_\lambda\,|x'\rangle \\ &+ \langle x|\,P^{(0)}_\lambda\,|x''\rangle\,(\delta\tilde{\Delta}_h)_{x''}\,\langle x''|\,P^{(0)}_{\lambda'}\,|x'\rangle\Big].\end{aligned}$$

In order to simplify the notation, we write $|g|^{-1/4} = 1-\frac{1}{4}h+\mathcal{O}(h^2)$. Although we are writing $P^{(1)}_\Lambda$ with the superscript 1, it clearly does not contain all of the first order influence of the

perturbation because of the factors of $|g|^{-1/4}$ in front of $\langle x|\, P_\Lambda^{(0)}\, |x'\rangle$. One can check that P_Λ is indeed a projector. However, one must be careful to use the appropriate resolutions of identity: $\int dx \sqrt{|g|}\, |x)(x| = 1$ and $\int dx\, |x\rangle\, \langle x| = 1$.

6.6 Local sample density

Using the position representation of the (first order) bandlimited projector in $\mathcal{H}_S(\delta + h)$, we can construct the subsystem projector associated with a finite subset of sample points as in Chapter 5. Let $\{x_n\}_{n=1}^N$ be a collection of sample points on T^n, then the projector onto the subsystem spanned by $\{P_\Lambda|x_n)\}_{n=1}^N$ is

$$P_N = \sum_{n,n'=1}^{N} (Q^{-1})_{nn'} P_\Lambda|x_n)(x_{n'}|P_\Lambda, \tag{6.30}$$

where $Q_{nn'} := (x_n|P_\Lambda|x_{n'})$.

In order to arrive at the local sample density, we will examine the associated probability distribution associated with a single sample point at x_0,

$$p(x) = \frac{\sqrt{|g(x)|}}{(x_0|P_\Lambda|x_0)} |(x|P_\Lambda|x_0)|^2, \tag{6.31}$$

where the factor of $\sqrt{|g(x)|}$ is included so that the distribution is normalized using the flat measure, $\int dx\, p(x) = 1$. Expanding to first order, we find

$$\begin{aligned}
(x_0|P_\Lambda|x_0) &= \frac{1}{\sqrt{|g(x_0)}} \langle x_0|\, P_\Lambda^{(0)}\, |x_0\rangle + \langle x_0|\, P_\Lambda^{(0)}\, |x_0\rangle \\
&= \frac{|M_\Lambda|}{\sqrt{|g(x_0)|} L^n} \left[1 + \frac{L^n}{|M_\Lambda|} \langle x_0|\, P_\Lambda^{(1)}\, |x_0\rangle\right] \\
|(x|P_\Lambda|x_0)|^2 &= \frac{1}{\sqrt{|g(x)|}\sqrt{|g(x_0)|}} |\, \langle x|\, P_\Lambda^{(0)}\, |x_0\rangle\, |^2 \\
&\quad + \langle x_0|\, P_\Lambda^{(0)}\, |x\rangle\, \langle x|\, P_\Lambda^{(1)}\, |x_0\rangle + \langle x_0|\, P_\Lambda^{(1)}\, |x\rangle\, \langle x|\, P_\Lambda^{(0)}\, |x_0\rangle
\end{aligned}$$

Then we find

$$\begin{aligned}
p(x) &= \sqrt{|g(x)|}\sqrt{|g(x_0)|}\frac{L^n}{|M_\Lambda|}\left[1 - \frac{L^n}{|M_\Lambda|}\langle x_0| P_\Lambda^{(1)} |x_0\rangle\right] \\
&\quad \times \left[\frac{1}{\sqrt{|g(x)|}\sqrt{|g(x_0)|}}|\langle x| P_\Lambda^{(0)} |x_0\rangle|^2 \right. \\
&\quad\quad \left. + \langle x_0| P_\Lambda^{(0)} |x\rangle \langle x| P_\Lambda^{(1)} |x_0\rangle + \langle x_0| P_\Lambda^{(1)} |x\rangle \langle x| P_\Lambda^{(0)} |x_0\rangle\right] \\
&= \frac{L^n}{|M_\Lambda|}|\langle x| P_\Lambda^{(0)} |x_0\rangle|^2 \\
&\quad + \frac{L^n}{|M_\Lambda|}\left[-\langle x_0| P_\Lambda^{(1)} |x_0\rangle \frac{L^n}{|M_\Lambda|}|\langle x| P_\Lambda^{(0)} |x_0\rangle|^2 \right. \\
&\quad\quad \left. + \langle x_0| P_\Lambda^{(0)} |x\rangle \langle x| P_\Lambda^{(1)} |x_0\rangle + \langle x_0| P_\Lambda^{(1)} |x\rangle \langle x| P_\Lambda^{(0)} |x_0\rangle\right].
\end{aligned}$$

We will write this as $p(x) = p^{(0)}(x) + p^{(1)}(x)$ with $p^{(0)}(x) := \frac{L^n}{|M_\Lambda|}|\langle x| P_\Lambda^{(0)} |x_0\rangle|^2$.

It is easy to show that $\int dx\, p^{(0)}(x) = 1$, and using the definition of $\langle x| P_\Lambda^{(1)} |x'\rangle$ one can show that

$$\int dx \left[\langle x_0| P_\Lambda^{(0)} |x\rangle \langle x| P_\Lambda^{(1)} |x_0\rangle + \langle x_0| P_\Lambda^{(1)} |x\rangle \langle x| P_\Lambda^{(0)} |x_0\rangle\right] = \langle x_0| P_\Lambda^{(1)} |x_0\rangle, \tag{6.32}$$

and subsequently, $\int dx\, p^{(1)}(x) = 0$. This verifies that $p(x)$ is appropriately normalized.

Now we want to calculate the mean and variance to determine the location and size of this subsystem. Once we have the variance σ^2, the linear size of the subsystem will be taken to be $\sigma^2/2L$, which is the inverse of our notion of local sample density. Given some distance function d_{T^n} on our manifold T^n, we recall from Chapter 4 that the mean and variance are defined by

$$\mu := \mathrm{argmin}_{\tilde{\mu}\in T^n}\langle d_{T^n}(x,\tilde{\mu})^2\rangle_x \tag{6.33}$$

$$\sigma^2 := \langle d_{T^n}(x,\mu)^2\rangle_x, \tag{6.34}$$

where we denote $\langle f(x)\rangle_x := \int dx\, p(x) f(x)$. Since our distribution $p(x)$ is split into zeroth and first order parts, let us denote

$$\langle f(x)\rangle_{x,0} := \int dx\, p^{(0)}(x) f(x), \quad \text{and } \langle f(x)\rangle_{x,1} := \int dx\, p^{(1)}(x) f(x), \tag{6.35}$$

so that $\langle f(x)\rangle_x = \langle f(x)\rangle_{x,0} + \langle f(x)\rangle_{x,1}$.

In order to calculate these quantities, according to the discussion of Chapter 4, we will use the isometric embedding of T^n into $\mathbb{R}^{2n^2}$ found in Section 4.3 and take d_{T^n} to be the distance function induced by the Euclidean distance in $\mathbb{R}^{2n^2}$. The first order embedding, modified for coordinates $x \in [0, L)^n$ rather than $\theta \in [0, 2\pi)^n$, is

$$\begin{aligned}\psi + \tilde{\psi} : (x^i)_{i=1}^n \mapsto \left(\frac{L}{2\pi}\right) \Bigg[& \bigoplus_{i=1}^n \left(\tfrac{1}{\sqrt{2n-1}} + \tfrac{\sqrt{2n-1}}{2} h_{ii}(x)\right) \begin{pmatrix} \cos(2\pi x^i/L) \\ \sin(2\pi x^i/L) \end{pmatrix}, \\ & \bigoplus_{j>i} \left(\tfrac{1}{\sqrt{2n-1}} - \tfrac{\sqrt{2n-1}}{4} h_{ij}(x)\right) \begin{pmatrix} \cos[2\pi(x^i - x^j)/L] \\ \sin[2\pi(x^i - x^j)/L] \end{pmatrix}, \\ & \bigoplus_{j>i} \left(\tfrac{1}{\sqrt{2n-1}} + \tfrac{\sqrt{2n-1}}{4} h_{ij}(x)\right) \begin{pmatrix} \cos[2\pi(x^i + x^j)/L] \\ \sin[2\pi(x^i + x^j)/L] \end{pmatrix} \Bigg] \end{aligned} \tag{6.36}$$

The expectation value we need to work with is, to first order,

$$\begin{aligned} & \left(\frac{2\pi}{L}\right)^2 \langle d_{\psi+\tilde{\psi}}(x,\mu)^2 \rangle_x = \\ & \quad \frac{2n^2}{2n-1} - \frac{2}{2n-1} \sum_{i=1}^n \Re\{\langle e^{\frac{2\pi i}{L} x^i} \rangle_x e^{-\frac{2\pi i}{L}\mu^i}\} \\ & \quad - \frac{2}{2n-1} \sum_{j>i} \Re\{\langle e^{\frac{2\pi i}{L}(x^i - x^j)} \rangle_x e^{-\frac{2\pi i}{L}(\mu^i - \mu^j)} + \langle e^{\frac{2\pi i}{L}(x^i + x^j)} \rangle_x e^{-\frac{2\pi i}{L}(\mu^i + \mu^j)}\} \\ & \quad + \langle h(x) \rangle_{x,0} + h(\mu) - \sum_{i=1}^n \Re\{\langle h_{ii}(x) e^{\frac{2\pi i}{L} x^i} \rangle_{x,0} e^{-\frac{2\pi i}{L}\mu^i} + h_{ii}(\mu) \langle e^{\frac{2\pi i}{L} x^i} \rangle_{x,0} e^{-\frac{2\pi i}{L}\mu^i}\} \\ & \quad + \frac{1}{2} \sum_{j>i} \Re\{\langle h_{ij}(x) e^{\frac{2\pi i}{L}(x^i - x^j)} \rangle_{x,0} e^{-\frac{2\pi i}{L}(\mu^i - \mu^j)} + h_{ij}(\mu) \langle e^{\frac{2\pi i}{L}(x^i - x^j)} \rangle_{x,0} e^{-\frac{2\pi i}{L}(\mu^i - \mu^j)} \\ & \quad - \langle h_{ij}(x) e^{\frac{2\pi i}{L}(x^i + x^j)} \rangle_{x,0} e^{-\frac{2\pi i}{L}(\mu^i + \mu^j)} - h_{ij}(\mu) \langle e^{\frac{2\pi i}{L}(x^i + x^j)} \rangle_{x,0} e^{-\frac{2\pi i}{L}(\mu^i + \mu^j)}\} \end{aligned}$$

which is a combination of simpler expectation values. Let us collect the objects one would need to proceed:

$$\langle x | \, P_\Lambda^{(0)} \, | x' \rangle = \sum_{|\lambda| < \Lambda^2} P_\lambda^{(0)} = \frac{1}{L^n} \sum_{m \in M_\Lambda} e^{i k_m \cdot (x - x')}$$

$$\langle x | \, P_\Lambda^{(1)} \, | x' \rangle = \sum_{|\lambda| < \Lambda^2 \leq |\lambda'|} \frac{1}{\lambda - \lambda'} \int dx'' \, \langle x | \left[P_{\lambda'}^{(0)} \, | x'' \rangle \, (\delta \tilde{\Delta}_h)_{x''} \, \langle x'' | \, P_\lambda^{(0)} + h.c. \right] | x' \rangle$$

with $(\delta\tilde{\Delta}_h)_x = -h^{ij}\partial_i\partial_j - h^{ij}{}_{,i}\partial_j - \frac{1}{4}(\partial^2 h)$, and

$$p^{(0)}(x) = \frac{L^n}{|M_\Lambda|} \left| \langle x| P_\Lambda^{(0)} |x_0\rangle \right|^2$$
$$p^{(1)}(x) = \frac{L^n}{|M_\Lambda|} \left[- \langle x_0| P_\Lambda^{(1)} |x_0\rangle p^{(0)}(x) + \langle x_0| P_\Lambda^{(0)} |x\rangle \langle x| P_\Lambda^{(1)} |x_0\rangle + \langle x_0| P_\Lambda^{(1)} |x\rangle \langle x| P_\Lambda^{(0)} |x_0\rangle \right].$$

Alas, this expression is somewhat intractable, so we will leave this here and try to push this further in future work, perhaps by reducing to some subclass of perturbations and working out some examples. At least we have worked out some tools and have taken some preliminary steps towards answering the questions posed at the beginning of this chapter.

Chapter 7

Lorentzian bandlimitation from Generalized Uncertainty Principles

Lorentzian bandlimitation was introduced in [69] by direct analogy with the Euclidean case. Formulating bandlimitation as a restriction to a subset of eigenspaces of a covariant differential operator generalizes naturally to pseudo-Riemannian manifolds. We discussed in Chapter 2 the nature of the sampling theory one obtains for the case of Minkowski spacetime.

The application of Euclidean bandlimitation to quantum field theory was originally motivated by the Generalized Uncertainty Principle (GUP). Before proceeding to further study Lorentzian-bandlimited QFT in the following chapters, here we ask whether Lorentzian bandlimitation can similarly be motivated from a kind of GUP. Schematically, the question is whether one would arrive at a similar conclusion through a different set of arguments?

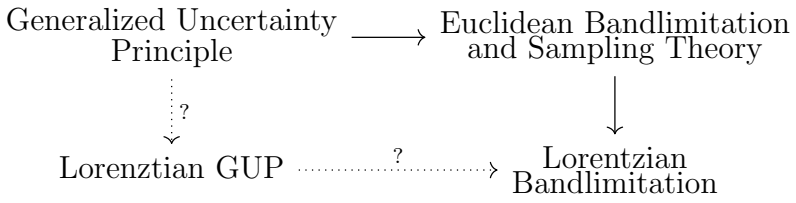

The purpose of such an endeavour is both to further support the motivation for such a generalization, as well as to expose and map out some other possibilities, by thinking about what assumptions are being made in order to arrive at this idea.

The work in this chapter and the next is based on the publication [101]. First, we will briefly review how one can think about employing GUPs in field theory, which requires a little consideration because the motivation for the GUP comes from thinking about the uncertainty principle between X and P, which are operators in nonrelativistic quantum mechanics, not quantum field theory. We will then present our Lorentzian analogue of the Generalized Uncertainty principle. Following this, we will show how one can obtain Lorentzian bandlimitation by a suitable change of representation of this Lorentzian GUP. Finally, we will conclude this chapter with some discussion.

7.1 GUPs and field theory

Recall that a Generalized Uncertainty Principle of the form $\Delta X \Delta P \geq \frac{1}{2}(1+\ell_P^2 \Delta P^2)$ (where ℓ_P is the Planck length) implies that the uncertainty in position has a finite minimum, $\Delta X \geq \ell_P$ [65, 73]. For purposes of simplicity, here we will discuss the one-dimensional version of the GUP, although it can be extended to higher dimensions. There are also many other modifications one can consider that yield similar qualitative behaviour, but we will consider this one explicitly since it is the simplest.

One can arrive at a GUP of the above form through a modification of the commutation relation between the operators X and P [65, 73]:

$$[X, P] = i(1 + \ell_P^2 P^2). \tag{7.1}$$

This implies an uncertainty principle of the above form (up to a term proportional to $\langle P \rangle^2$, although this does not significantly change the above conclusion). Hence, if we consider states in a representation of this modified Heisenberg algebra, they will automatically exhibit the feature of a minimum uncertainty in position. For example, one such representation is:

$$(X\tilde{\psi})(p) = i(1 + \ell_P^2 p^2)\frac{d}{dp}\tilde{\psi}(p), \qquad (P\tilde{\psi})(p) = p\tilde{\psi}(p), \tag{7.2}$$

with inner product, $\langle \tilde{\phi} | \tilde{\psi} \rangle = \int \frac{dp}{2\pi}(1 + \ell_P^2 p^2)^{-1} \tilde{\phi}^*(p)\tilde{\psi}(p)$. The physical states are those in a dense subset of this Hilbert space (typically the common domain of $[X, P]$ and various powers of X, P, and their products).

There have been many papers studying various implications of GUPs (e.g., see [23, 30, 56, 66, 99, 106, 107]), including extensions to relativistic quantum mechanics (with a noncommutative geometry) [123]. Our interest here is rather to study Lorentz-covariant

modifications of quantum field theory as one approaches the Planck scale. In order to apply the GUP to QFT, one must first identify how the ordinary uncertainty principle of nonrelativistic quantum mechanics manifests itself in QFT.

The classical space of field configurations (on flat spacetime) is taken to be a representation space of the Poincaré group. From the Poincaré generators $L_{\mu\nu}$ and P^{Λ}, one can build momentum space representations of the fields $\tilde{\phi}(p) \equiv (p|\phi)$, with $P^{\lambda}|p) = p^{\lambda}|p)$. The position or spacetime representation of the fields is then naturally obtained via a Fourier transform. The assumption that position and momentum space are Fourier-related presumes an underlying Heisenberg algebra structure, $[X_{\mu}, P^{\nu}] = i\delta_{\mu}{}^{\nu}$, with position representation $\phi(x) \equiv (x|\phi)$, where $X^{\mu}|x) = x^{\mu}|x)$. This is formally similar to the typical account in quantum mechanics. Naturally, this is the step at which one can introduce a modification of the Heisenberg algebra. That is, one can continue to build momentum space representations for the Poincaré group, but a modified Heisenberg algebra may alter the relationship between position and momentum space.

Notice that in the position representation, x is simply a label for an element in the joint spectrum of the X^{μ} operators. Hence, field configurations in the spacetime representation reside on the joint spectra of these operators. A modification of the Heisenberg algebra may change the structure of these spectra. For example, if the spectra become discrete after a modification, then these field configurations could be thought of as living on a lattice.

Let us first consider how our approach would apply using the one-dimensional version of the GUP at a fixed time, before moving on to arbitrary spacetime dimensions. Above we presented the momentum space representation of the GUP corresponding to $[X, P] = i(1+\ell_P^2 P^2)$. In order to find the position space representation, we must find the eigenvalues and eigenvectors of X. However, the finite minimum uncertainty, $\Delta X \geq \ell_P$, implies that X has no eigenvectors in the domain where the GUP is represented, since the uncertainty for an eigenvector would vanish (or in the case of a continuous spectrum could be made arbitrarily close to zero).

This situation can be made more clear by performing a momentum space diffeomorphism in the p-representation. Using the functional calculus of P, we define an operator,

$$K := \frac{1}{\ell_P} \arctan(\ell_P P), \tag{7.3}$$

which can be easily shown satisfies the canonical commutation relation with X: $[X, K] = i$. It may appear that this simply reverts the GUP to the ordinary uncertainty principle, with x-space and k-space being Fourier-related. However, because arctan has a finite range, the

fields in k-space have finite support, i.e., are bandlimited. The k-space representation consists of fields on the interval $[-\Lambda, \Lambda]$ with $\Lambda := \frac{\pi}{2\ell_P}$, obeying Dirichlet boundary conditions (and with the usual measure $dk/2\pi$). Therefore, by focusing solely on the x- and k-space representations, we can view the deformation as equivalent to simply restricting to a subset of k-space. In other words, we are restricting the spectrum of the K operator (ordinarily represented in position space as the derivative operator $-id/dx$). Note that one can also perform this diffeomorphism when considering the GUP for wavefunctions in quantum mechanics, and think of the resulting system as a particle in a box in momentum space.

Do we still have finite minimum uncertainty in position? Does the position operator continue to lack eigenvectors? Of course this should be the case, since we have not changed the abstract algebraic properties enforcing these features. Although the operators X and K are canonically related, the bandlimitation implies a maximum uncertainty in K. Therefore, the uncertainty in X continues to exhibit a finite minimum since $\Delta X \geq 1/2\Delta K \geq 1/2\Delta K_{\text{max}}$. As we reviewed in Chapter 2, after considering a family of the extensions of the domain of X, one obtains a discrete spectrum for each extension. From this, one can construct the sampling theorem for bandlimited functions.

Hence, we arrive at the conclusion that implementing the one-dimensional GUP to quantum fields yields the one-dimensional version of Euclidean-bandlimited quantum field theory. Indeed, this construction is another way to motivate the premise of applying bandlimitation to quantum field theory in the way discussed in Chapter 3. Now let us examine a Lorentzian version of the GUP, and see how one can arrive at Lorentzian-bandlimited QFT.

7.2 Lorentzian GUPs

The strategy of the GUP was to introduce a minimum length scale by modifying the commutation relation between X and P to give a finite minimum uncertainty in position. Now we will attempt to do this Lorentz-covariantly. By *Lorentz-covariant*, we mean that the coordinates, and not necessarily the momenta, transform appropriately under an infinitesimal Lorentz transformation. This is because we are primarily concerned with symmetries of spacetime, rather than the space described by the momenta. At the very least, we can begin with this level of generality to see what kind of structure we end up with.

We will continue to focus primarily on the kinematical structure of the fields, postponing a discussion of dynamics until Chapter 8. Indeed, if we are interested in a regulator for

the entanglement entropy, it should arise from the kinematics, as entanglement is typically thought of as between regions of space at a fixed time.

We will consider a somewhat general set of deformations of the Heisenberg algebra:

$$[X_I, P^\mu] = i\theta_I{}^\mu(P), \qquad [X_I, X_J] = 0, \qquad [P^\mu, P^\nu] = 0. \tag{7.4}$$

where we assume $\theta_I{}^\mu$ is a smooth function of the P^μ operators, and as a matrix is pointwise-invertible (i.e., $\det\theta \neq 0$). (Note that $\theta_I{}^\mu$ should be a function of the dimensionless quantity $\ell_P P^\mu$, however, to keep the notation compact, we will omit an explicit reference to ℓ_P.) We take $\theta_I{}^\mu$ to be a function of the P^μ operators and not the X_I operators for both simplicity and in analogy with the one-dimensional GUP (where X-dependence yields an infrared, rather than an ultraviolet, cutoff [65]). Both sets of indices traverse all spacetime dimensions, $I, \mu = 0, 1, 2, \ldots, n-1$. We label the X_I operators and P^μ operators differently since we only require the upper-case Latin indices to transform appropriately under Lorentz transformations.

The requirements of commuting coordinates and commuting momenta are made solely as simplifying assumptions in order to make conclusive statements. If this prevents the model from producing a suitable cutoff, then one could take this as an indication that these assumptions (such as the commutative geometry assumption) should be relaxed in order to obtain a cutoff in a model of this kind. Indeed, we are attempting to determine whether one can obtain a minimum length without resorting to non-commutative geometry.

Of course, we will also assume that the Jacobi identities are satisfied. This introduces the following restriction for θ: $[X_I, \theta_J{}^\mu(P)] = [X_J, \theta_I{}^\mu(P)]$. With this structure, it is simple to build a p-space representation for this algebra as:

$$(X_I\phi)(p) = i\theta_I{}^\mu(p)\frac{\partial}{\partial p^\mu}\phi(p), \qquad (P^\mu\phi)(p) = p^\mu\phi(p), \tag{7.5}$$

with inner product: $(\phi|\psi) = \int \frac{d^n p}{(2\pi)^n}(\det\theta(p))^{-1}\phi^*(p)\psi(p)$. Note that throughout we assume the summation convention. In this representation, the condition for the Jacobi identity becomes: $\theta_I{}^\nu\partial_\nu\theta_J{}^\mu = \theta_J{}^\nu\partial_\nu\theta_I{}^\mu$. This ensures that the coordinates commute and are symmetric operators. One can write the Lorentz generators in this representation as:

$$L_{IJ} := X_I\int^p dp'^\mu(\theta^{-1})_{\mu J}(p') - X_J\int^p dp'^\mu(\theta^{-1})_{\mu I}(p'), \tag{7.6}$$

where the upper-case Latin indices are lowered using the Minkowski metric,

$$\eta_{IJ} := \mathrm{diag}(+1, -1, -1, \ldots, -1). \tag{7.7}$$

It is straightforward to show that these indeed satisfy the Lorentz algebra, and that the X_I operators transform appropriately as: $[X_K, L_{IJ}] = i\eta_{JK}X_I - i\eta_{IK}X_J$. Note that the integration makes sense because $(\theta^{-1})_{\mu I}(p)dp^\mu$ is an exact one-form, which we will now see.

In the one-dimensional case, we made a simplification by enacting a coordinate change in momentum space to recover canonical commutation relations, but with a restriction of the spectrum of the new momentum operator. We can also establish such a diffeomorphism here for an arbitrary deformation ${\theta_I}^\mu(P)$ (with the already-mentioned assumptions). Notice that the operators $-iX_I$ provide a basis of vector fields on p-space. Because these vector fields commute with each other, they can be written as a coordinate basis after a suitable diffeomorphism (see, e.g., [80]). That is, there is some diffeomorphism $k^I(p)$ for which we can write $X_I\phi(k) = i(\partial/\partial k^I)\phi(k)$. The functions parametrizing the deformation of the Heisenberg algebra can then simply be associated with the (inverse) Jacobian of this diffeomorphism, ${\theta_I}^\mu(p) = (\partial k^I(p)/\partial p^\mu)^{-1}$. We can define multiplication operators in k-space as $K^I\phi(k) = k^I\phi(k)$ (or in p-space as $K^I\phi(p) = k^I(p)\phi(p)$), which satisfy: $[X_I, K^J] = i{\delta_I}^J$. Notice that with the K^I operators, the Lorentz generators take their familiar form: $L_{IJ} = X_IK_J - X_JK_I$.

7.3 From Lorentzian GUPs to bandlimitation

We have established that a deformation of the commutator between X_I and P^μ in the Heisenberg algebra can be reverted to the canonical commutation relations (provided the coordinate and momentum operators remain commuting among themselves). Therefore, with regards to the kinematical structure of the classical field configurations, we are only left with the possibility of modifying the global properties of momentum space. Can we restrict to a subset of k-space in order to achieve a kind of bandlimitation, as in the one-dimensional case?

Of course, we cannot make an arbitrary restriction. Because x- and k-space are Fourier-related, Lorentz transformations act on k-space in the usual way. Therefore, in order to maintain Lorentz-symmetry, the hypersurfaces $k^2 = \text{const}$ must remain unmodified. This leaves only the possibility of restricting k-space to a subset of these hypersurfaces, i.e., we can restrict the set of admissible mass shells. For example, we can constrain the quantity $|k^2| = |k_0^2 - \vec{k}^2| < 1/\ell_P^2$. This can be achieved, for example, by the following deformation (similar to [66]):

$$ {\theta_I}^J(p) = f(p^2){\delta_I}^J + p_I p^J \frac{2f(p^2)f'(p^2)}{f(p^2) - 2p^2 f'(p^2)}, \tag{7.8} $$

where $p^2 := p_0^2 - \vec{p}^2$, with diffeomorphism $k^I = p^I/f(p^2)$ and inverse denoted $p^I = b(k^2)k^I$. To achieve the desired restriction of k^2, we can choose $b(k^2) = \sum_{n=0}^{\infty}(\ell_P^2 k^2)^{2n}$. Due to the finite radius of convergence of this series, fields in the domain of P^I are confined to the region $|k^2| < 1/\ell_P^2$. One can check that this indeed defines a diffeomorphism in this region, and by writing $\theta_I{}^J(p(k)) = b(k^2)\delta_I{}^J + 2k_I k^J b'(k^2)$, that θ satisfies the required properties.

The result is of course the same as Lorentzian bandlimitation that we discussed in Chapter 2. Recall that this was introduced in previous works [27,69,72] as a restriction of the spectrum of the covariant d'Alembertian operator, in analogy with the restriction of the spectrum of $-id/dx$ in the one-dimensional case. Here we have shown that one is also led to covariant bandlimitation by a class of deformations of the Heisenberg algebra.

7.4 Discussion

Let us now review some of the assumptions that were made in order to arrive at Lorentzian bandlimitation, and where one might proceed to consider alternatives. We chose a GUP of the form,

$$[X_I, P^\mu] = i\theta_I{}^\mu(P), \qquad [X_I, X_J] = 0, \qquad [P^\mu, P^\nu] = 0, \tag{7.9}$$

with the only assumptions on $\theta_I{}^\mu$ being that the Jacobi identities are satisfied and $\det\theta \neq 0$. We saw that this leads to fields (i.e., elements in a representation space of this algebra) whose Fourier transforms have support on some subset of mass shells (possibly all of them). The simplest modification of the usual case is Lorentzian bandlimitation.

Of course, this GUP we chose to examine is not the most general one. First, we made a major assumption that the position and momenta are mutually commuting. In non-commutative geometry, there is the idea that non-commutativity is dual to curvature [83]. Since here we were simply looking at modifications for Minkowski spacetime, it was natural to choose the momenta to commute among themselves. We will not pursue this here, but it may be worth considering whether one recovers bandlimitation associated with the Laplace-Beltrami operator for some curved spacetime by introducing a GUP to an analogue of the Heisenberg algebra where the momenta do not commute.

The case of non-commuting coordinates is the subject of Non-Commutative Geometry [29,81]. This is a qualitatively different approach to considering Planck-scale modifications to the structure of spacetime. In bandlimitation and sampling theory, the idea is to restrict the space of functions one is considering while keeping the underlying manifold unchanged. Our investigation in this thesis is restricted to this perspective, but perhaps it is necessary

to move to non-commutative geometry if one insists on obtaining a stronger regulator for the degrees of freedom in QFT.

Another assumption we made is that ${\theta_I}^\mu$ is a function of P^μ and not X^I. This simplification was made since in the analogous one-dimensional case, P-dependence generically yields an ultraviolet cutoff, whereas X-dependence yields an infrared cutoff. It is not clear whether the same happens in this generalization of the GUP, hence this is possibly a line of further investigation.

We noted in Chapter 2 that the obstruction to obtaining discrete spacetime representations was due to the infinite volume of momentum space. If we consider restricting to a finite volume of momentum space (through whatever means), then in spacetime one obtains a space of analytic functions (see, e.g., [104]). Analytic functions exhibit a severe non-locality since all of the degrees of freedom are contained in a small volume around any point in spacetime (as the Taylor series can be evaluated in a neighborhood). Hence it seems that anything akin to ordinary sampling theory would allow for superluminal signalling, and thus would be inappropriate for the configuration space of a relativistic field theory. In practical applications of sampling theory (e.g., in communications engineering [93, 110, 111]) this non-locality does not appear as realistic signals are only approximately bandlimited. In any case, practically one could not fully evaluate the Taylor series coefficients to arbitrary precision. Therefore, instead of attempting to model the fundamental configuration space of the field theory, one could adopt these analytic functions as an approximation, and perhaps prevent superluminal effects in the model by introducing other practical limitations (such as finite precision of measurements).

Despite the infinite density of degrees of freedom one obtains under Lorentzian bandlimitation, we can still ask what implications this has for the structure of quantum field theory. We already saw how the Feynman propagator is modified in Chapter 3, but what other properties of these fields are changed? Does the bandlimit still provide a regulator for the field theory in some sense? We will now turn to these questions in the remaining two chapters of this thesis, with a brief discussion for free fields in Chapter 8, and then interacting theories in Chapter 9.

Chapter 8

Lorentzian bandlimitation in free field theory

In previous chapters, we saw how Lorentzian bandlimitation is a natural generalization of the Euclidean-signature case, as well as made some preliminary investigations as to how this modification would appear in quantum field theory. Now we will examine more thoroughly how Lorentzian bandlimitation can be integrated into the framework of QFT, in order to see what other impacts it might have. Naturally, we will begin with free theories, both to build up some intuition for interacting theories, but also because free theories are relevant for studies of entanglement, in the context of black hole physics, for example. Some of the observations in this chapter were discussed briefly in [101].

8.1 Classical solutions and Fock space

As we mentioned in the opening of Chapter 3, the simplest way of implementing bandlimitation in field theory is to simply restrict the space of fields one inserts into the action (for a classical field theory) or integrates over in the path integral (for a quantum field theory). However, first let us briefly discuss possibilities for modifications of the action itself. We will continue to focus on the case of a real scalar field theory, for which the simplest choice of action is the Klein-Gordon action,

$$S[\phi] = \tfrac{1}{2}(\phi|K_I K^I \phi) - \tfrac{1}{2}m^2(\phi|\phi), \tag{8.1}$$

where $K_I := -i\partial/\partial x^I$. In Chapter 7, we had two different sets of momentum operators, K^I and P^μ, which motivates one to consider using the P^μ operators in the action instead.

After arriving at the conclusion that the Lorentzian GUP is equivalent to Lorentzian bandlimitation, for kinematic considerations one can simply ignore the P^μ operators and focus on the k-space representations. However, now that we are considering dynamics, there is a choice of which of the K^I or P^μ operators should feature in the action. For example, one generalization could be

$$S[\phi] = (\phi|\sigma(P, p_0)\phi) - (\phi|\sigma(p_m, p_0)\phi), \tag{8.2}$$

where σ is the Synge world function in p-space (i.e., half of the squared geodesic distance), and we define p_0 and p_m as points in p-space that satisfy $k^I(p_0) = 0$ and $k_I(p_m)k^I(p_m) = m^2$. Due to the coordinate-invariance of σ, if we choose the p-space metric to be the pullback of the Minkowski metric on k-space, that is, $g_{\mu\nu}(p) = \eta_{IJ}(\theta^{-1})_\mu{}^I(\theta^{-1})_\nu{}^J$ (where $\theta_I{}^\mu$ is the GUP deformation from the previous chapter), then this simply reduces to the Klein-Gordon action. One could alternatively introduce another metric on p-space for this purpose. For example, with the deformation example used to arrive at Lorentzian bandlimitation, $p^I = b(k^2)k^I$ with $b(k^2) = \sum_{n=0}^{\infty}(\ell_P^2 k^2)^{2n}$, one could use η_{IJ} in p-space to obtain the action:

$$S[\phi] = \tfrac{1}{2}(\phi|P_I P^I\phi) - \tfrac{1}{2}b(m^2)^2 m^2(\phi|\phi). \tag{8.3}$$

This can be viewed as a replacement of the d'Alembertian operator $\Box \to \Box/(1 - \ell_P^4\Box^2)^2$ along with a re-scaling of the mass. However, regardless of the choice, to retain covariance in x-space one is restricted to using functions of the d'Alembertian operator in the action. A locally analytic function whose power series has a finite radius of convergence will yield Lorentzian bandlimitation [69]. One could entertain many possibilities here, many of which have been studied elsewhere under the name of *nonlocal theories* (see, e.g., [11, 19, 33, 34, 94, 112]). We are not aware of any of these references considering the property of Lorentzian bandlimitation. In the following, we will proceed by simply considering the ordinary Klein-Gordon action restricted to field configurations that are Lorentzian-bandlimited. We simply wanted to mention here the connection with these nonlocal theories, since, for example, certain deformations considered here could be viewed as equivalent to the nonlocal d'Alembertian operators arising from averaging over causal sets [10, 14].

Now let us consider the implications of Lorentzian bandlimitation in the classical field theory. With the Klein-Gordon action, the equation of motion for the fields is

$$(\Box + m^2)\phi(x) = 0. \tag{8.4}$$

We notice immediately that the solution space for this equation is simply the eigenspace of $\Box$ corresponding to the eigenvalue $\lambda = -m^2$. Because Lorentzian bandlimitation is

simply a restriction of these eigenspaces to those with eigenvalue $|\lambda| < \Lambda^2$, it does not make any difference whether or not we begin with the space of Lorentzian-bandlimited fields (provided that the mass is smaller than the Planck scale, otherwise the equation of motion has no nontrivial solutions in this space). Therefore, we see that the on-shell classical fields are already Lorentzian-bandlimited in ordinary field theory.

How then can we think about the corresponding reconstruction properties discussed in Chapter 2? Well, recall that one manner in which we framed the reconstruction property is that all fixed spatial modes, $\phi(x) = \psi(t)e^{i\vec{k}\cdot\vec{x}}$ ($\vec{k}$ fixed), have a sampling property in time. (Figure 2.1 is reproduced here for convenience.) Furthermore, there is a sampling lattice

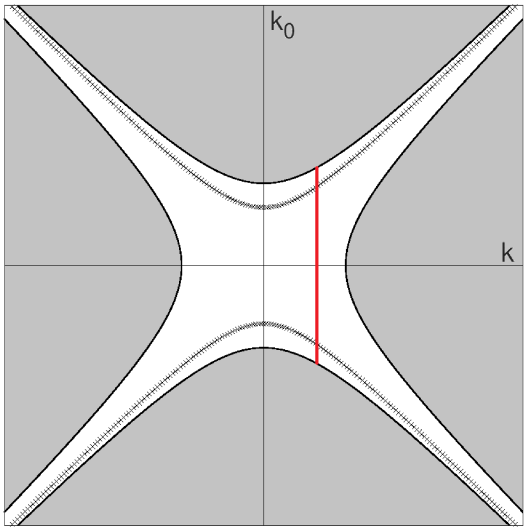

Figure 8.1: Illustration of the region $|k_0^2 - \vec{k}^2| < \Lambda^2$ in 1+1 dimensions. A mass shell is shown as a series of $\times$'s. The vertical red line indicates a surface of fixed $\vec{k}$.

in time with density $\sqrt{2}\Lambda/\pi$ which suffices to reconstruct all the spatial modes, although there is no restriction on the spatial configurations. However, a solution to the above equation of motion is completely specified by fixing the spatial field configuration at *two* different times, so in this sense it has a very simple sampling theory in time. What about sampling in space? Remember before we said that a fixed temporal mode, $\phi(x) = \psi(\vec{x})e^{ik^0t}$ ($k^0 = \text{const}$, fixed), has a sampling property in space, since it has finite spatial bandwidth, i.e., the region $\max\{0, (k^0)^2 - \Lambda^2\} < \vec{k}^2 < (k^0)^2 + \Lambda^2$ has a finite volume. (Although recall that for spatial dimensions greater than two, the volume as a function of k^0 is not bounded above; hence there is no sampling lattice that suffices for all k^0.) However, for

on-shell fields, there is no corresponding sampling theory in space because we are not fixing $k^0 = \text{const}$ in k-space, but rather $k^0 = \omega_k := \sqrt{\vec{k}^2 + m^2}$, and this region (the mass shell) has an infinite volume. (Using coordinates $\vec{k}$ on the mass shell, the hypersurface volume is $\int \frac{m}{\omega_k} \frac{d\vec{k}}{(2\pi)^{n-1}} = \infty$.)

Therefore, the Lorentzian bandlimit has no impact on the space of classical solutions, since fields obeying the equation of motion are already Lorentzian-bandlimited in ordinary field theory. This is also true for quantum field operators, since they also satisfy the Klein-Gordon equation, $(\Box + m^2)\phi(x) = 0$. For instance, using the expansions

$$\phi(x) = \int \frac{d\vec{k}}{(2\pi)^{n-1}} \frac{1}{\sqrt{2\omega_k}} \left(a_k e^{-ik\cdot x} + a_k^\dagger e^{ik\cdot x} \right)$$
$$\pi(x) = \int \frac{d\vec{k}}{(2\pi)^{n-1}} (-i) \sqrt{\frac{\omega_k}{2}} \left(a_k e^{-ik\cdot x} - a_k^\dagger e^{ik\cdot x} \right),$$

where $k = (k^0, \vec{k})$ and $k \cdot x = k^0 x^0 - \vec{k} \cdot \vec{x}$, we see that applying the bandlimited projector,

$$(x|P_\Lambda|x') = \int_{|k^2|<\Lambda^2} \frac{d^n k}{(2\pi)^n} e^{ik\cdot(x-x')}, \tag{8.5}$$

simply acts as the identity on these operators.

Because of this, the corresponding Fock space one constructs with the above creation and annihilation operators is also the same, which can be seen directly from the above expansions. Alternatively, in general the Fock space of a free field theory can be constructed using the (complexified) classical solution space [127] (see also [37]). The procedure is to first choose a space of positive frequency solutions inside the (complexified) classical solution space (corresponding to solutions with initial data having compact support). Upon completion, this gives a Hilbert space $\mathcal{H}$, which is identified with the single-particle subspace of the Fock space, $\mathcal{F}[\mathcal{H}]$, corresponding to the quantum state space of the field. From either perspective, we see that the Fock space of the field theory is unaffected by the Lorentzian bandlimit, due to the fact that the classical solution space is unchanged.

Note that because the Fock space is unmodified, it seems that we do not get issues associated with the construction of multiparticle states that occurs in other kinds of modifications of momentum space (the so-called "soccer-ball problem" [9, 54, 55]).

Therefore, we have seen that Lorentzian bandlimitation does not change the classical solution space, the field operators, nor the structure of the Hilbert space of quantum states. It seems then that everything in the quantum field theory is unmodified by the Lorentzian bandlimit. Then how can we understand the modification to the Feynman propagator that we obtained in Chapter 3?

8.2 Two-point functions

Typically the quantities one is interested in computing for a free field theory are two-point functions. These can be divided into two classes: homogeneous and inhomogeneous.

Examples of homogeneous two-point functions are the Wightman function, commutator, and covariance:

$$\langle 0|\,\phi(x)\phi(y)\,|0\rangle\,, \quad \langle[\phi(x),\pi(y)]\rangle, \quad \tfrac{1}{2}\langle\{\phi(x),\phi(y)\}\rangle. \tag{8.6}$$

These quantities are all on-shell, e.g., satisfy $(\Box + m^2)\langle\phi(x)\phi(y)\rangle = 0$. For example, if we write the Wightman function in the non-bandlimited theory as

$$\begin{aligned}\langle 0|\,\phi(x)\phi(y)\,|0\rangle &= \int \frac{d\vec{k}}{(2\pi)^{n-1}}\frac{1}{2\omega_k}e^{-i\omega_k(x^0-y^0)+i\vec{k}\cdot(\vec{x}-\vec{y})} \\ &= \int \frac{d^nk}{(2\pi)^{n-1}}\theta(k^0)\delta(k^2-m^2)e^{-ik\cdot(x-y)},\end{aligned}$$

we see that applying the bandlimited projector does nothing because of the $\delta(k^2 - m^2)$. Therefore, we can conclude that anything depending on these on-shell quantities is not modified by the Lorentzian bandlimit. This includes the entanglement entropy between spatial regions, since this can be calculated from only the commutator and covariance function [109], which are both on-shell. Hence, not only is the entanglement entropy not regulated, but it is completely unchanged. Note that if we were to use a nonlocal action to impose the Lorentzian bandlimit, as we discussed above, then this observation about the entanglement entropy is consistent with calculations for nonlocal theories and modified dispersion relations using the path integral approach [13, 92, 114].

What about the inhomogeneous two-point functions? These include the Feynman, advanced, and retarded propagators, which ordinarily satisfy

$$(\Box + m^2)G(x,y) = -i\delta^{(n)}(x-y). \tag{8.7}$$

Now $\delta^{(n)}(x-y)$ is not a bandlimited function, as can be seen by expressing it as:

$$\delta^{(n)}(x-y) = \int \frac{d^nk}{(2\pi)^n}e^{ik\cdot(x-y)}. \tag{8.8}$$

We saw in Chapter 3 that the modified Feynman propagator satisfies

$$(\Box + m^2)G_F(x-y) = -i(x|P_\Lambda|y). \tag{8.9}$$

That is, it is a (pseudo-)inverse of $(\Box + m^2)$ restricted to the bandlimited subspace, on which the identity is P_Λ.

Indeed, these propagators are not on-shell quantities. Recall that in order to obtain a more explicit form for the Feynman propagator in Chapter 3, we integrated over the usual k^0 contour and then subtracted a contribution coming from the region $|k^2| > \Lambda^2$. This gave us an expression which differs from the one in the non-bandlimited QFT. Therefore, we see that these propagators indeed do get modified by the Lorentzian bandlimit.

Typically one can also calculate these propagators from the homogeneous two-point functions as well. For example, in ordinary QFT, the Feynman propagator is simply the time-ordered Wightman function:

$$\begin{aligned} G_F(x,y) &= \langle 0| \mathcal{T}\phi(x)\phi(y) |0\rangle \\ &:= \theta(x^0 - y^0) \langle 0| \phi(x)\phi(y) |0\rangle + \theta(y^0 - x^0) \langle 0| \phi(y)\phi(x) |0\rangle . \end{aligned}$$

Clearly this can no longer be the case in the bandlimited theory, since the Feynman propagator is modified by the bandlimit, but the Wightman function is not. We will discuss this more thoroughly in the next chapter, but the fact is that when one multiplies the Wightman function by a step function in time, the resulting function is no longer bandlimited. Hence, we must modify the time-ordering operator in order to be consistent with the Lorentzian bandlimit.

Thus, one must be careful when assuming the ordinary relationships between the homogeneous and inhomogeneous two-point functions after applying the Lorentzian bandlimit. For example, in ordinary QFT, the Feynman propagator evaluated at equal times is equal to the (equal-time) covariance function (using $\theta(0) = 1/2$):

$$G_F(t = 0, \vec{x} - \vec{y}) = \tfrac{1}{2} \langle 0| \{\phi(\vec{x}), \phi(\vec{y})\} |0\rangle \qquad \text{(without bandlimit)}. \tag{8.10}$$

However, this is no longer the case with the Lorentzian bandlimit, since as we have seen, the equal-time Feynman propagator is modified by the bandlimit, but the covariance function is not.

One may recall that in the Wightman approach to axiomatic QFT, the Wightman reconstruction theorem tells us that any theory is distinguished by a specification of the n-point Wightman functions (see, e.g., [45]). More precisely, these functions determine the Hilbert space of the theory as well as the action of the field operators on this space. As we have shown, the Wightman functions of the QFT with a Lorentzian bandlimit are unchanged from the ordinary case without the bandlimit (as they are on-shell). Consistent with the reconstruction theorem, the Hilbert space and mode expansion of the fields are also

unchanged. The manner in which Lorentzian-bandlimited QFT differs from the ordinary case can be seen as a modification of the time-ordering operator, which is an ingredient that one does not typically consider deforming.

By thinking of the effect of the Lorentzian bandlimit in terms of which quantities are on- or off-shell, it is also possible to extrapolate the conclusions to the case of curved spacetime. On a general pseudo-Riemannian manifold, recall from Chapter 2 that bandlimitation can be analogously defined in terms of cutting off the spectrum of a covariant differential operator, such as the Laplace-Beltrami operator, $\Box_g = |g|^{-1/2}\partial_\mu(|g|^{1/2}g^{\mu\nu}\partial_\nu\cdot)$. However, even in this case, the eigenvalues correspond to allowable masses in the Klein-Gordon equation, $\Box_g\phi = -m^2\phi$. Therefore, restricting the allowable masses has no effect on the homogeneous solutions to the Klein-Gordon equation here as well. One would then not expect the entanglement entropy to be modified either (for example, between the interior and exterior regions of a black hole). Despite this, perhaps it would be interesting to examine field theories with different equations of motion, for example if we included a direct curvature coupling: $(\Box_g + m^2 + \xi R)\phi = 0$.

We have seen that the Lorentzian bandlimit only appears as changes to the propagators of the field theory. Therefore, we expect that any modifications will primarily be featured in interacting theories, where the propagators play a central role. Considering the bandlimit as a restriction of the set of allowable mass shells can give us some preliminary intuition for which interaction processes one should look at in order to see effects of the bandlimit. For example, a simple interacting theory one could consider is a field operator linearly coupled to an accelerated detector, through which one can study the Unruh effect [124]. However, because the Unruh effect corresponds to a first-order response, there are no internal field lines (i.e., factors of the Feynman propagator) which could be affected by the covariant bandlimit (drawn schematically below, reading the figure left to right).

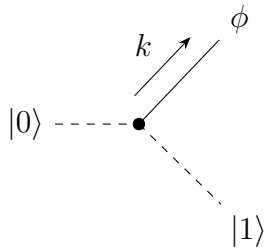

Therefore, it seems that there would be no modification to the usual leading-order thermal response of an accelerated detector.

Suppose we instead considered the s-channel of a $\phi\phi \to \phi\phi$ scattering process at tree-level in a ϕ^3 theory:

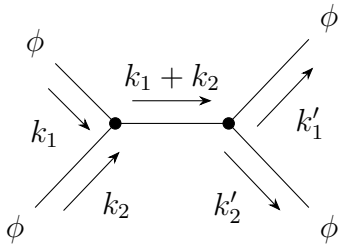

The matrix element for this diagram is:

$$i\mathcal{M} = \frac{-ig^2}{(k_1 + k_2)^2 - m^2 + i\epsilon}, \tag{8.11}$$

where g is the coupling constant. If the momenta of the incoming particles are localized in momentum space far from the Planck scale (which would be the case in realistic collision experiments), then one would expect the corrections to this amplitude due to the bandlimit to be very small. Even though we saw that there are corrections to the Feynman propagator (shown in Figure 3.1), there we looked at $\tilde{G}_F(t = 0, \vec{k})$, which is highly delocalized in the k^0 direction. This is in contrast with the above matrix element, which is evaluated at the point $k_1 + k_2$ in momentum space. Even if we were to consider localized wavepackets for the incoming particles, one would expect that the truncation which occurs at the Planck scale to contribute very little in realistic scenarios.

Therefore, from these examples we see that we expect significant contributions from the Lorentzian bandlimit in processes where the corresponding Feynman diagram contains internal field lines (i.e., factors of the Feynman propagator) which venture far off-shell, and hence have the possibility of running into the bandlimit, $|k^2| < \Lambda^2$. This leads us to the investigation of what happens to loop diagrams, in which one typically integrates over all of k-space. In the next chapter we will take some first steps in this pursuit. In particular, we will examine whether the Lorentzian bandlimit helps to tame the divergences occuring in these loop integrals.

Chapter 9

Interactions with Lorentzian bandlimitation

At the end of the last chapter, we argued that one would expect to see contributions of the Lorentzian bandlimit primarily for loop integrals in interacting field theories. Here we will take some preliminary steps in examining this.

How do we expect these integrals to be affected? Each loop in a diagram comes with an undetermined momentum that must be integrated over, $d^n\ell$, and each internal line comes with a propagator, $1/(\ell^2 - m^2)$. For a diagram with L loops and I internal lines, the superficial degree of divergence is $D = nL - 2I$, with an expected divergence when $D \geq 0$. However, with the covariant bandlimit, we are restricting the momentum space. Recall, for fixed $\vec{k}$, we have k^0 restricted to the interval $I(\vec{k})$, where

$$I(\vec{k}) := \begin{cases} [-r_+(\vec{k}), r_+(\vec{k})] & \text{if } \vec{k}^2 \leq \Lambda^2 \\ [-r_+(\vec{k}), -r_-(\vec{k})] \cup [r_-(\vec{k}), r_+(\vec{k})] & \text{if } \vec{k}^2 > \Lambda^2 \end{cases} \tag{9.1}$$

with $r_\pm(\vec{k}) := \sqrt{\vec{k}^2 \pm \Lambda^2}$. If we assume this applies to the loop integrals (we will demonstrate this later), we see that this is restricting one of the dimensions of the $d^n\ell$ integral to a finite interval, while leaving the remaining integral ranges the same. Naively, one would expect this to change the power counting, to something like $D = (n-1)L - 2I$, thus suppressing some of the divergences. For example, perhaps the quadratic divergences become linear, linear divergences become logarithmic, logarithmic divergences become finite. Our goal here is to carefully investigate what happens, since it would be interesting to know if it improves the renormalizability of a theory.

We saw briefly in the previous chapter that the Lorentzian bandlimit interacts with the time-ordering operator in a nontrivial way. We will begin by showing how the bandlimit can be interpreted as a deformation of the time-ordering operator appearing in the propagators for the Klein-Gordon equation. Because the time-ordering operator is ubiquitous in deriving the Feynman rules for scattering amplitudes, we will revisit the arguments to see how the rules should be modified. It turns out to be rather simple in the end; we argue that it basically amounts to replacing the propagators with the bandlimited ones. However, we will examine this closely, as it needs to be justified. Note that we did not give any background on these kinds of calculations at the beginning of the thesis. This is because we will be following the usual derivations very closely here, highlighting any differences along the way. We will then proceed to examine loop integrals, in order to determine whether the power counting changes in the way described above.

9.1 Off-shellness and bandlimited time-ordering

We begin by examining how time-ordering is affected by the Lorentzian bandlimit. We will begin with the Feynman propagator,

$$\begin{aligned} G_F(x,y) &= \langle 0|\, \mathcal{T}\phi(x)\phi(y)\, |0\rangle \\ &= \theta(x^0-y^0)\, \langle 0|\, \phi(x)\phi(y)\, |0\rangle + \theta(y^0-x^0)\, \langle 0|\, \phi(y)\phi(x)\, |0\rangle\,. \end{aligned}$$

Recall that $\langle 0|\, \phi(x)\phi(y)\, |0\rangle$ is on-shell, hence already Lorentzian-bandlimited. Then the reason that G_F has off-shell components is simply due to the presence of the step functions implementing the time-ordering. After all, since bandlimitation affects localizability, it may not make sense to try and localize a function at a $t = t_0$ hypersurface. (Although this may be true, it certainly does not prevent us from evaluating a function at a particular time, at least in principle.)

One would then expect a similar effect on the retarded and advanced Greens' functions, which are also combinations of the on-shell Wightman function with step functions in time. We see that, although one can intuitively think of the covariant bandlimit as projecting out certain off-shell fluctuations, the effect will appear throughout calculations as a modification of the propagators.

How exactly is the time-ordering modified by the bandlimit? It is straightforward to project the step function $\theta(t)$ onto the bandlimited subspace and arrive at $(P_\Lambda\theta)(t) = \frac{1}{2} + \frac{1}{\pi}\,\mathrm{Si}(\Lambda t)$, where $\mathrm{Si}(\Lambda t) := \int_0^{\Lambda t} \frac{dy}{y}\sin(y)$ is the sine integral. However, if we multiply this bandlimited step function by another covariantly bandlimited function, $f(x)$, the

product $(P_\Lambda\theta)(t)f(x)$ will generally not be bandlimited, since in Fourier space it would be the convolution of $\tilde{f}(k)$ and $\left(\frac{1}{ik^0}\chi_{[-\Lambda,\Lambda]}(k^0)+\pi\delta(k^0)\right)(2\pi)^{n-1}\delta^{(n-1)}(\vec{k})$, which generally has support outside of the bandlimited region. Note that $\chi_I(k^0)$ is defined as 1 if $k^0\in I$ and 0 if $k^0\notin I$. Therefore, in order to obtain a bandlimited $\theta(t)f(x)$, we must apply the bandlimited projector after the multiplication. Using the following integral representation for $\theta(t)$,

$$\theta(t)=\lim_{\epsilon\to 0^+}\frac{1}{2\pi i}\int\frac{d\nu}{\nu-i\epsilon}e^{i\nu t}, \tag{9.2}$$

and the bandlimited projector (signature $+---\cdots-$)

$$P_\Lambda(x-x'):=\int_{|k^2|<\Lambda^2}\frac{d^nk}{(2\pi)^n}e^{ik\cdot(x-x')}, \tag{9.3}$$

we find that the projection of $\theta(x^0-\tau)f(x)$ for arbitrary $f(x)$ and some fixed τ can be implemented by multiplying the function $f(x)$ in Fourier space by an appropriate momentum-dependent modification of the step function:

$$\int d^nx'\;P_\Lambda(x-x')\theta(x'^0-t_0)f(x')=\int\frac{d^nk}{(2\pi)^n}\tilde{f}(k)e^{ik\cdot x}\theta_{I(\vec{k})-k^0}(x^0-t_0). \tag{9.4}$$

Here, $I(\vec{k})$ is the temporal bandwidth for mode $\vec{k}$, given by (9.1), and $\theta_{[a,b]}$ for an arbitrary interval $[a,b]\subset\mathbb{R}$ is defined to be

$$\theta_{[a,b]}(t):=\lim_{\epsilon\to 0^+}\frac{1}{2\pi i}\int_a^b\frac{d\nu}{\nu-i\epsilon}e^{i\nu t},$$

which can be written in terms of exponential integrals, if desired. We see that if $[a,b]\to\mathbb{R}$, then we recover the usual step function. One can also show that $\lim_{t\to\infty}\theta_{[a,b]}(t)=1$ and $\lim_{t\to-\infty}\theta_{[a,b]}(t)=0$, hence the corrections due to the bandlimit vanish at asymptotic times. This will be useful when we examine scattering.

Now let us apply this to the Feynman propagator. Recall that the Fourier transform of $\langle 0|\,\phi(x)\phi(y)\,|0\rangle$ is $(2\pi)\theta(-k^0)\delta(k^2-m^2)=(2\pi)\frac{1}{2\omega_k}\delta(k^0+\omega_k)$ (with $\omega_k:=\sqrt{\vec{k}^2+m^2}$), so

$$\theta(x^0-y^0)\,\langle 0|\,\phi(x)\phi(y)\,|0\rangle\overset{P_\Lambda}{\mapsto}\int\frac{d\vec{k}}{(2\pi)^{n-1}}\frac{1}{2\omega_k}e^{-i\omega_k(x^0-y^0)+i\vec{k}\cdot(\vec{x}-\vec{y})}\theta_{I(\vec{k})+\omega_k}(x^0-y^0). \tag{9.5}$$

Then the spatial Fourier transform of the projected Feynman propagator is, with $\tau:=x^0-y^0$,

$$\tilde{G}_F^\Lambda(\vec{k},\tau)=\frac{1}{2\omega_k}\left[e^{-i\omega_k\tau}\theta_{I(\vec{k})+\omega_k}(\tau)+e^{i\omega_k\tau}\theta_{I(\vec{k})+\omega_k}(-\tau)\right]. \tag{9.6}$$

In the limit $\tau = 0$, we can recover the formula (3.37) we discussed in Chapter 3.

The advanced and retarded propagators differ from the Feynman propagator by additions of homogeneous solutions (this can be seen by examining the k^0 integral contours). Since the homogeneous solutions are already within the bandlimited subspace, they are not affected by the projection. Therefore, the modification due to the bandlimit will be the same for all of these propagators.

The particular form for the bandlimited time ordering will not be used much in the following. The message here is that the Lorentzian bandlimit manifests itself through a modification of time ordering. Since the time-ordering operator is used extensively in quantum field theory derivations, these must be carefully reexamined in light of this modification. We will begin with the LSZ reduction formula.

9.2 S-matrix and LSZ reduction formula

In this section we will derive the LSZ (Lehmann-Symanzik-Zimmermann) reduction formula for Lorentzian-bandlimited QFT. Our treatment is based on [108, 118], with some details taken from [122]. First we will review how it works in ordinary field theory, and then we will consider what might change in the bandlimited field theory. We will find that the usual formula applies as-is also to the bandlimited case, so most of the content of this section is simply a review of background material.

Consider a real scalar field theory,

$$\mathcal{L} = -\tfrac{1}{2}\phi(\Box + m^2)\phi + \mathcal{L}_{int}(\phi). \tag{9.7}$$

Let us write a quantum field $\phi(x)$ as

$$\phi(x) = \int \frac{d\vec{k}}{(2\pi)^3}\frac{1}{\sqrt{2\omega_k}}\left(a_k(t)e^{-ik\cdot x} + a_k^\dagger(t)e^{ik\cdot x}\right), \tag{9.8}$$

where at any fixed time, $[a_k(t), a_{k'}^\dagger(t)] = (2\pi)^3\delta^{(3)}(\vec{k}-\vec{k}')$, so we get the usual Fock space at any fixed time. The time dependence is from evolving the fields in the Heisenberg picture under the full interacting Hamiltonian. Rearranging the above expression,

$$\sqrt{2\omega_k}a_k(t) = i\int d\vec{x}\, e^{ik\cdot x}(\partial_t - i\omega_k)\phi(x). \tag{9.9}$$

For simplicity of notation, for this section, let us absorb the factor of $\sqrt{2\omega_k}$ into the $a_k(t)$ operators.

One can therefore obtain,

$$a_k(+\infty) - a_k(-\infty) = \int_{-\infty}^{\infty} dt\, \frac{d}{dt} a_k(t) = i \int d^n x\, e^{ik\cdot x}(\Box + m^2)\phi(x) \tag{9.10}$$

and

$$a_k^\dagger(+\infty) - a_k^\dagger(-\infty) = \int_{-\infty}^{\infty} dt\, \frac{d}{dt} a_k^\dagger(t) = -i \int d^n x\, e^{-ik\cdot x}(\Box + m^2)\phi(x). \tag{9.11}$$

Note that for a free theory, we have $(\Box + m^2)\phi(x) = 0$ in the Heisenberg picture, and consequently $a_k(t)$ and $a_k^\dagger(t)$ are time-independent.

Now let us consider the S-matrix for an example of $\phi\phi \to \phi\phi$ scattering. Generalizations of the following are striaghtforward. We begin with,

$$\langle f|\, S\, |i\rangle = \langle 0|\, a_{p_1'}(+\infty) a_{p_2'}(+\infty) a_{p_1}^\dagger(-\infty) a_{p_2}^\dagger(-\infty)\, |0\rangle \tag{9.12}$$

Note that for the derivation, we will only consider cases where the incoming and outgoing momenta are different (no forward scattering), although the resulting formula still applies to those cases [108, 118]. Now since these are time-ordered, we can introduce $\mathcal{T}$ without changing anything,

$$\begin{aligned}
\langle f|\, S\, |i\rangle &= \langle 0|\, \mathcal{T}\{a_{p_1'}(+\infty) a_{p_2'}(+\infty) a_{p_1}^\dagger(-\infty) a_{p_2}^\dagger(-\infty)\}\, |0\rangle \\
&= \langle 0|\, \mathcal{T}\{[a_{p_1'}(+\infty) - a_{p_1'}(-\infty)][a_{p_2'}(+\infty) - a_{p_2'}(-\infty)] \\
&\qquad\qquad [a_{p_1}^\dagger(-\infty) - a_{p_1}^\dagger(+\infty)][a_{p_2}^\dagger(-\infty) - a_{p_2}^\dagger(+\infty)]\}\, |0\rangle \\
&= \langle 0|\, \mathcal{T} \left[i \int dx_1'\, e^{ip_1'\cdot x_1'}(\Box_{1'} + m^2)\phi(x_1') \right] \left[i \int dx_2'\, e^{ip_2'\cdot x_2'}(\Box_{2'} + m^2)\phi(x_2') \right] \\
&\qquad\qquad \left[i \int dx_1\, e^{-ip_1\cdot x_1}(\Box_1 + m^2)\phi(x_1) \right] \left[i \int dx_2\, e^{-ip_2\cdot x_2}(\Box_2 + m^2)\phi(x_2) \right] |0\rangle
\end{aligned}$$

In the first step, the operators introduced vanish acting on $\langle 0|$ or $|0\rangle$ because of the presence of $\mathcal{T}$. Now we want to show

$$\begin{aligned}
\langle f|\, S\, |i\rangle = &\left[i \int dx_1'\, e^{ip_1'\cdot x_1'}(\Box_{1'} + m^2) \right] \left[i \int dx_2'\, e^{ip_2'\cdot x_2'}(\Box_{2'} + m^2) \right] \\
&\left[i \int dx_1\, e^{-ip_1\cdot x_1}(\Box_1 + m^2) \right] \left[i \int dx_2\, e^{-ip_2\cdot x_2}(\Box_2 + m^2) \right] \\
&\times \langle 0|\, \mathcal{T}\{\phi(x_1')\phi(x_2')\phi(x_1)\phi(x_2)\}\, |0\rangle\,.
\end{aligned}$$

The issue with doing this is that $\mathcal{T}$ does not commute with either $(\Box + m^2)$ or $\int dx^0$, however, as shown in [122], these problems cancel out. Because the formula depends intricately on the nature of the time-ordering operator, it is worth going through the details in order to expose any points that may change when replaced with the bandlimited time-ordering.

The key is to consider one $\phi(x)$ and the corresponding derivatives and integrals involving x. Let $t_N > t_{N-1} > \cdots > t_1$ and $B_j(t_j)$ some operator at t_j. Then for arbitrary x, we have

$$\mathcal{T}\{\phi(x)B_N(t_N)\cdots B_1(t_1)\} = \sum_{j=0}^{N} B_N(t_N)\cdots B_{j+1}(t_{j+1})\theta(t_{j+1}-x^0)\phi(x)\theta(x^0-t_j)B_j(t_j)\cdots B_1(t_1), \tag{9.13}$$

where we identify $t_{N+1} = +\infty$ and $t_0 = -\infty$, as well as $B_{N+1}(t_{N+1}) = B_0(t_0) = 1$. In these cases, we simply omit the step functions by identifying $\theta(t_{N+1}-x^0) \equiv 1$ and $\theta(x^0-t_0) \equiv 1$. For example, in our above problem, if we identify $x = x_2$, then for fixed x_1, x_1', and x_2', the $B_j(t_j)$'s will correpond to $\phi(x_1)$, $\phi(x_1')$, and $\phi(x_2')$ in the appropriate temporal ordering. However, let us keep the formula general.

Now we will apply $i\int dx e^{\pm ip\cdot x}(\Box + m^2)$ to $\mathcal{T}\{\phi(x)B_N(t_N)\cdots B_1(t_1)\}$. Start with

$$\begin{aligned}(\Box + m^2)[\theta(t_{j+1}-x^0)\phi(x)\theta(x^0-t_j)] = \theta(t_{j+1}-x^0)\theta(x^0-t_j)(\Box+m^2)\phi(x)\\ - 2[\delta(t_{j+1}-x^0)-\delta(x^0-t_j)]\partial_{x^0}\phi(x)\\ + [\delta'(t_{j+1}-x^0)+\delta'(x^0-t_j)]\phi(x).\end{aligned}$$

Note that the delta functions involving t_{N+1} and t_0 are dropped. Now apply the integral. We get, using the above relations for $a_p(t)$

$$\begin{aligned}&i\int dx e^{ip\cdot x}\theta(t_{j+1}-x^0)\theta(x^0-t_j)(\Box+m^2)\phi(x)\\ &\qquad = \int_{t_j}^{t_{j+1}} dx^0\,\frac{d}{dx^0}a_p(x^0) = a_p(t_{j+1}) - a_p(t_j)\\ &i\int dx e^{ip\cdot x}[\delta'(t_{j+1}-x^0)\phi(x) - 2\delta(t_{j+1}-x^0)\partial_{x^0}\phi(x)]\\ &\qquad = i\int dx e^{ip\cdot x}\delta(t_{j+1}-x^0)(i\omega_p - \partial_{x^0})\phi(x) = -a_p(t_{j+1})\\ &i\int dx e^{ip\cdot x}[\delta'(x^0-t_j)\phi(x) + 2\delta(x^0-t_j)\partial_{x^0}\phi(x)]\\ &\qquad = i\int dx e^{ip\cdot x}\delta(x^0-t_j)(-i\omega_p + \partial_{x^0})\phi(x) = a_p(t_j)\end{aligned}$$

Therefore, the sum of these cancel, except for the cases t_{N+1} and t_0 where the delta functions are dropped and we do not get the latter two terms.

$$i\int dxe^{ip\cdot x}(\Box+m^2)[\theta(t_{j+1}-x^0)\phi(x)\theta(x^0-t_j)]=\begin{cases}-a_p(-\infty) & \text{if } j=0\\ a_p(+\infty) & \text{if } j=N\\ 0 & \text{if } 0<j<N.\end{cases} \tag{9.14}$$

Then

$$\begin{aligned}
&i\int dxe^{ip\cdot x}(\Box+m^2)\mathcal{T}\{\phi(x)B_N(t_N)\cdots B_1(t_1)\}\\
&\quad=i\int dxe^{ip\cdot x}(\Box+m^2)\sum_{j=0}^{N}B_N(t_N)\cdots B_{j+1}(t_{j+1})\theta(t_{j+1}-x^0)\phi(x)\theta(x^0-t_j)B_j(t_j)\cdots B_1(t_1)\\
&\quad=a_p(+\infty)B_N(t_N)\cdots B_1(t_1)-B_N(t_N)\cdots B_1(t_1)a_p(-\infty)
\end{aligned}$$

Similarly, for the opposite sign in the exponential,

$$\begin{aligned}
&i\int dxe^{-ip\cdot x}(\Box+m^2)\mathcal{T}\{\phi(x)B_N(t_N)\cdots B_1(t_1)\}\\
&\qquad=-a_p^\dagger(+\infty)B_N(t_N)\cdots B_1(t_1)+B_N(t_N)\cdots B_1(t_1)a_p^\dagger(-\infty).
\end{aligned}$$

Take vacuum expectation values,

$$i\int dxe^{ip\cdot x}(\Box+m^2)\left\langle 0\right|\mathcal{T}\{\phi(x)B_N(t_N)\cdots B_1(t_1)\}\left|0\right\rangle=\left\langle 0\right|a_p(+\infty)B_N(t_N)\cdots B_1(t_1)\left|0\right\rangle \tag{9.15}$$

$$i\int dxe^{-ip\cdot x}(\Box+m^2)\left\langle 0\right|\mathcal{T}\{\phi(x)B_N(t_N)\cdots B_1(t_1)\}\left|0\right\rangle=\left\langle 0\right|B_N(t_N)\cdots B_1(t_1)a_p^\dagger(-\infty)\left|0\right\rangle \tag{9.16}$$

Then for the LSZ formula, we apply these in turn, keeping the other coordinates fixed:

$$\begin{aligned}
&\left[i\int dx_1'\, e^{ip_1'\cdot x_1'}(\Box_{1'}+m^2)\right]\left[i\int dx_2'\, e^{ip_2'\cdot x_2'}(\Box_{2'}+m^2)\right]\\
&\qquad\left[i\int dx_1\, e^{-ip_1\cdot x_1}(\Box_1+m^2)\right]\left[i\int dx_2\, e^{-ip_2\cdot x_2}(\Box_2+m^2)\right]\\
&\qquad\times\langle 0|\,\mathcal{T}\{\phi(x_1')\phi(x_2')\phi(x_1)\phi(x_2)\}\,|0\rangle\\
&=\left[i\int dx_1'\, e^{ip_1'\cdot x_1'}(\Box_{1'}+m^2)\right]\left[i\int dx_2'\, e^{ip_2'\cdot x_2'}(\Box_{2'}+m^2)\right]\\
&\qquad\left[i\int dx_1\, e^{-ip_1\cdot x_1}(\Box_1+m^2)\right]\times\langle 0|\,\mathcal{T}\{\phi(x_1')\phi(x_2')\phi(x_1)\}a^\dagger_{p_2}(-\infty)\,|0\rangle\\
&=\left[i\int dx_1'\, e^{ip_1'\cdot x_1'}(\Box_{1'}+m^2)\right]\left[i\int dx_2'\, e^{ip_2'\cdot x_2'}(\Box_{2'}+m^2)\right]\\
&\qquad\times\langle 0|\,\mathcal{T}\{\phi(x_1')\phi(x_2')\}a^\dagger_{p_1}(-\infty)a^\dagger_{p_2}(-\infty)\,|0\rangle\\
&=\langle 0|\,a_{p_1'}(+\infty)a_{p_2'}(+\infty)a^\dagger_{p_1}(-\infty)a^\dagger_{p_2}(-\infty)\,|0\rangle\,.
\end{aligned}$$

We end up directly with the S-matrix element $\langle f|\,S\,|i\rangle$. It is straightforward to generalize this to different numbers of incoming and outgoing particles.

For bandlimited fields, the expression

$$\phi(x)=\int\frac{d\vec{k}}{(2\pi)^3}\frac{1}{\sqrt{2\omega_k}}\left(a_k(t)e^{-ik\cdot x}+a_k^\dagger(t)e^{ik\cdot x}\right), \tag{9.17}$$

will be covariantly bandlimited provided the temporal Fourier transform of $a_k(t)$ has support in $I(\vec{k})+\omega_k$ and $a_k^\dagger(t)$ has support in $I(\vec{k})-\omega_k$, where $I(\vec{k})$ is the bandlimited interval defined in (9.1). We can still write

$$\sqrt{2\omega_k}a_k(t)=\int d\vec{x}\, e^{ik\cdot x}(\partial_t-i\omega_k)\phi(x). \tag{9.18}$$

Naturally this obeys the appropriate bandlimitation condition as long as $\phi(x)$ is bandlimited. Recall that we argued commutation relations of ϕ and π do not change after the bandlimit, so we also have that the creation and annihilation commutation relations at fixed times are unchanged. Hence we still have a Fock space structure at each fixed time. Therefore, the S-matrix element should still be identified with

$$\langle f|\,S\,|i\rangle=\sqrt{2\omega_1}\sqrt{2\omega_2}\sqrt{2\omega_{1'}}\sqrt{2\omega_{2'}}\,\langle 0|\,a_{p_1'}(+\infty)a_{p_2'}(+\infty)a^\dagger_{p_1}(-\infty)a^\dagger_{p_2}(-\infty)\,|0\rangle\,. \tag{9.19}$$

Now what about the LSZ formula? We expect that one should replace

$$\langle 0|\,\mathcal{T}\{\phi(x_1')\phi(x_2')\phi(x_1)\phi(x_2)\}\,|0\rangle$$

with the bandlimited version, where the bandlimited projector P_Λ is applied to each of the four coordinates. However, this is already applied in the ordinary case. To see this, let us write $(p|x) = e^{ip\cdot x}$ with $\int dx|x)(x| = 1$, where we write round brackets because these are functions in the space of classical field configurations, not quantum states in the Fock space. Then for some function $f(x)$, we can write

$$i\int dx\, e^{ip\cdot x}(\Box+m^2)f(x) = i\int dxdx'\,(p|x)(x|(\Box+m^2)|x')(x'|f) = i(p|(\Box+m^2)|f). \quad (9.20)$$

Let us also write

$$\begin{aligned}\langle 0|\,\mathcal{T}\{\phi(x_1')\phi(x_2')\phi(x_1)\phi(x_2)\}\,|0\rangle &=: G^{(4)}(x_1', x_2', x_1, x_2)\\ &= (x_1'|\otimes(x_2'|\,G^{(4)}\,|x_1)\otimes|x_2).\end{aligned}$$

Then the right-hand side of the LSZ formula can be written

$$\begin{aligned}&\left[i\int dx_1'\, e^{ip_1'\cdot x_1'}(\Box_{1'}+m^2)\right]\left[i\int dx_2'\, e^{ip_2'\cdot x_2'}(\Box_{2'}+m^2)\right]\\ &\qquad\left[i\int dx_1\, e^{-ip_1\cdot x_1}(\Box_1+m^2)\right]\left[i\int dx_2\, e^{-ip_2\cdot x_2}(\Box_2+m^2)\right]\\ &\qquad\times\langle 0|\,\mathcal{T}\{\phi(x_1')\phi(x_2')\phi(x_1)\phi(x_2)\}\,|0\rangle\\ &= [i(p_1'|(\Box+m^2)]\otimes[i(p_1'|(\Box+m^2)]\,G^{(4)}\,[i(\Box+m^2)|p_1)]\otimes[i(\Box+m^2)|p_2)]\end{aligned}$$

Therefore, if we applied the projectors to the Greens' function, $G^{(4)}\mapsto(P_\Lambda\otimes P_\Lambda)G^{(4)}(P_\Lambda\otimes P_\Lambda)$, they commute past $(\Box+m^2)$ and hit the external momentum states, $P_\Lambda|p)$. Of course the external momenta are on-shell, and so the projectors are simply absorbed $P_\Lambda|p) = |p)$. Therefore, in Lorentzian-bandlimited case, this expression is mathematically equivalent to the ordinary case where there is no bandlimit. Hence the above derivation to obtain the S-matrix element (which also takes the same form in both cases) from this expression still holds. Even though at the intermediate stages, we use objects such at step functions in time, which are not bandlimited, we can simply delay applying the bandlimited projectors and absorb them into the external momentum states.

All of that is to say that the LSZ reduction formula with the Lorentzian bandlimit is the same as that without the bandlimit, despite the fact that time-ordering is a prominent

ingredient in the formula and is different in the bandlimited and non-bandlimited cases. Once the S-matrix element is calculated, it is clear that proceeding to calculate a cross-section or decay rate would proceed as usual, since all of the external particles are on-shell, hence not affected by the projecting out of off-shell field configurations.

The effect of the bandlimit will appear in the evaluation of $G^{(4)}$. Now let us figure out how the calculation of these using Feynman rules is modified with the bandlimit. The next step is to perturbatively examine the classical time evolution of the interacting field theory, before proceeding to the quantum time evolution.

9.3 Classical time evolution and field algebra

Let us consider the following Lagrangian for a real scalar field

$$\mathcal{L} = -\tfrac{1}{2}\phi(\Box + m^2)\phi + \mathcal{L}_{int}(\phi). \tag{9.21}$$

The classical equation of motion is:

$$(\Box + m^2)\phi = \mathcal{L}'_{int}(\phi), \tag{9.22}$$

where $\mathcal{L}'_{int}(\phi) := \frac{d}{d\phi}\mathcal{L}_{int}(\phi)$.

In order to solve this equation perturbatively, we set up an iteration by first defining a Greens' function,

$$(\Box_x + m^2)G(x, x') = -i\delta^n(x - x'). \tag{9.23}$$

(We will not specify retarded, advanced, Feynman, etc. at this point, but keep it general.) Of course, this is only a right inverse and we have a choice of how G should map into the kernel of the operator $\Box + m^2$. This corresponds to a choice of how to navigate around the poles of $1/(\Box + m^2)$ in the complexified k^0 direction. Later, we will be dealing with the Feynman contour.

Dealing with the kernel of $(\Box + m^2)$ is well-understood in ordinary quantum field theory. But now that we are projecting out eigenspaces of $\Box$, we have an analogous situation where we can choose how G should act on these directions we have projected out. Perhaps the natural thing to do is to just simply have G project these out, but we want to examine what physical assumption one is making by doing this. Such an assumption would correspond to $G \mapsto P_\Lambda G P_\Lambda$, where P_Λ is the projector onto the covariantly bandlimited subspace. Indeed, this is exactly what we did in the previous section. Consider splitting G into four components $P_\Lambda G P_\Lambda$, $P_\Lambda G(1 - P_\Lambda)$, $(1 - P_\Lambda)G P_\Lambda$, and $(1 - P_\Lambda)G(1 - P_\Lambda)$.

Since our differential operator is not the ordinary full $(\Box + m^2)$, but projected onto the bandlimited subspace, $P_\Lambda(\Box + m^2)P_\Lambda$, we cannot find an inverse on the full space, but only on this bandlimited subspace:

$$(\Box + m^2)G = -iP_\Lambda \tag{9.24}$$

This condition implies that $P_\Lambda G(1 - P_\Lambda) = 0$. Note that we only require G to be a right-inverse, so it does not need to be hermitian.

We set up the iteration for the interacting theory,

$$\phi = \phi_0 + iG\mathcal{L}'_{int}(\phi) \tag{9.25}$$

where ϕ_0 is some free solution $(\Box + m^2)\phi_0 = 0$. Now ϕ and ϕ_0 are bandlimited. If we plug these back into the equation, then the input to $\mathcal{L}'_{int}$ is covariantly bandlimited. What about the output?

The issue is that pointwise multiplication does not preserve bandlimitation. For example, if $\mathcal{L}_{int}(\phi) = \frac{g_n}{n!}\phi^n$, then the output of $\mathcal{L}'_{int}(\phi)$ will generally not be bandlimited for $n \geq 3$, since in Fourier space it is the convolution of two or more fields. Therefore, in order to ensure that the output of G is bandlimited, so that ϕ in the iteration remains in the bandlimited subspace, we must set $(1 - P_\Lambda)G = 0$. Hence, we are required to choose G of the form $P_\Lambda G P_\Lambda$. By choosing this way of doing it, just constantly projecting things out, i.e., the assumption is that the Planck scale becomes a sink for modes that venture past it. Intuitively, this indicates that the theory might not be unitary.

Is there a way we can have modes outside of the bandlimit enter into the bandlimited subspace? In the context of this model, it does not make sense for these modes to be dynamical. One can put a non-dynamical source at the Planck boundary, but this would involve a modification of the equations of motion and Lagrangian to include such a source. However, there is no clear guidance for how this should be chosen anyway, so we will not consider it here.

Another option is to keep G acting as the zero operator on the modes above the bandlimit, but deform the field multiplication to some star product $\phi * \phi$ in such a way that the output of $\mathcal{L}'_{int}$ remains bandlimited. In this way, the iteration process is not continually projecting things out that venture beyond the bandlimit, but rather the modes are prevented from leaving the bandlimited subspace. For example, one could do it in such a way that the modes are squeezed up against the boundary, in analogy with velocity addition in special relativity.

9.4 Feynman rules

Now that we have the machinery in place, generating the Feynman rules proceeds very closely to usual. We will follow the approach using the Schwinger-Dyson equations, because it is manifestly covariant and directly written in terms of propagators. Also, it is more closely related to classical equations of motion just discussed.

The first step is to determine the equation of motion for the time-ordered n-point functions. I.e., we want to evaluate $(\Box_x + m^2) \langle 0| \mathcal{T}\{\phi(x)\phi(x_N)\cdots\phi(x_1)\} |0\rangle$. Since the bandlimited time-ordered n-point functions are equal to the bandlimited projectors applied to each component of the non-bandlimited one, let us first consider the non-bandlimited case, and then argue that one can retrieve the bandlimited case by applying the projectors at the end. The proof is similar to the proof of the LSZ formula we showed above, except without the integrals. Suppose $x_1^0 > x_2^0 > \cdots > x_N^0$, then for arbitrary x,

$$\mathcal{T}\{\phi(x)\phi(x_N)\cdots\phi(x_1)\} = \sum_{j=0}^{N} \phi(x_N)\cdots\phi(x_{j+1})\theta(x_{j+1}^0 - x^0)\phi(x)\theta(x^0 - x_j^0)\phi(x_j)\cdots\phi(x_1). \tag{9.26}$$

As before, we identify $t_{N+1} = +\infty$ and $t_0 = -\infty$. First, the time derivative is,

$$\begin{aligned}\partial_{x^0}[\theta(x_{j+1}^0 - x^0)\phi(x)\theta(x^0 - x_j^0)] = \theta(x_{j+1}^0 - x^0)\theta(x^0 - x_j^0)\partial_{x^0}\phi(x) \\ + [-\delta(x_{j+1}^0 - x^0) + \delta(x^0 - x_j^0)]\phi(x).\end{aligned}$$

Then (still with $x_N^0 > \cdots > x_1^0$),

$$\begin{aligned}&\partial_{x^0} \langle 0| \mathcal{T}\{\phi(x)\phi(x_N)\cdots\phi(x_1)\} |0\rangle \\ &\quad= \sum_{j=0}^{N} \langle 0| \phi(x_N)\cdots\phi(x_{j+1})\theta(x_{j+1}^0 - x^0)[\partial_{x^0}\phi(x)]\theta(x^0 - x_j^0)\phi(x_j)\cdots\phi(x_1) |0\rangle \\ &\qquad+ \sum_{j=0}^{N} \langle 0| \phi(x_N)\cdots\phi(x_{j+1})[-\delta(x_{j+1}^0 - x^0)\phi(x) + \delta(x^0 - x_j^0)\phi(x)]\phi(x_j)\cdots\phi(x_1) |0\rangle .\end{aligned}$$

The last term vanishes, since

$$\begin{aligned}
&\sum_{j=0}^{N} \langle 0| \, \phi(x_N) \cdots \phi(x_{j+1})[-\delta(x^0_{j+1} - x^0)\phi(x) + \delta(x^0 - x^0_j)\phi(x)]\phi(x_j) \cdots \phi(x_1) \, |0\rangle \\
&\quad = \sum_{j=0}^{N} \langle 0| \, \phi(x_N) \cdots \phi(x_{j+1})[\delta(x^0 - x^0_j)\phi(x^0_j, \vec{x})]\phi(x_j) \cdots \phi(x_1) \, |0\rangle \\
&\qquad + \sum_{j=1}^{N+1} \langle 0| \, \phi(x_N) \cdots \phi(x_j)[-\delta(x^0_j - x^0)\phi(x^0_j, \vec{x})]\phi(x_{j-1}) \cdots \phi(x_1) \, |0\rangle \\
&= \sum_{j=1}^{N} \delta(x^0 - x^0_j) \, \langle 0| \, \phi(x_N) \cdots \phi(x_{j+1})[\phi(x^0_j, \vec{x}), \phi(x^0_j, \vec{x}_j)]\phi(x_{j-1}) \cdots \phi(x_1) \, |0\rangle \\
&= 0
\end{aligned}$$

due to the equal-time commutation relations $[\phi(x^0_j, \vec{x}), \phi(x^0_j, \vec{x}_j)] = 0$. The terms $j = 0$ and $j = N + 1$ at the ends vanish identically, since we have $x^0_0 = -\infty$ and $x^0_{N+1} = +\infty$ and so the delta functions vanish with these arguments (alternatively, recall that we said to omit the theta functions at the beginning, which would give rise to these). Thus, we arrive at a simplified formula (without delta functions),

$$\begin{aligned}
&\partial_{x^0} \, \langle 0| \, \mathcal{T}\{\phi(x)\phi(x_N) \cdots \phi(x_1)\} \, |0\rangle \\
&\quad = \sum_{j=0}^{N} \langle 0| \, \phi(x_N) \cdots \phi(x_{j+1})\theta(x^0_{j+1} - x^0)[\partial_{x^0}\phi(x)]\theta(x^0 - x^0_j)\phi(x_j) \cdots \phi(x_1) \, |0\rangle
\end{aligned}$$

Take another time derivative,

$$\begin{aligned}
&\partial^2_{x^0} \, \langle 0| \, \mathcal{T}\{\phi(x)\phi(x_N) \cdots \phi(x_1)\} \, |0\rangle \\
&\quad = \sum_{j=0}^{N} \langle 0| \, \phi(x_N) \cdots \phi(x_{j+1})\theta(x^0_{j+1} - x^0)[\partial^2_{x^0}\phi(x)]\theta(x^0 - x^0_j)\phi(x_j) \cdots \phi(x_1) \, |0\rangle \\
&\qquad + \sum_{j=0}^{N} \langle 0| \, \phi(x_N) \cdots \phi(x_{j+1})[-\delta(x^0_{j+1} - x^0)\partial_{x^0}\phi(x) + \delta(x^0 - x^0_j)\partial_{x^0}\phi(x)]\phi(x_j) \cdots \phi(x_1) \, |0\rangle \, .
\end{aligned}$$

but now, we use $[\phi(x_j^0,\vec{x}_j),\partial_{x^0}\phi(x_j^0,\vec{x})] = i\delta^{(3)}(\vec{x}-\vec{x}_j)$ to obtain

$$\begin{aligned}
&\sum_{j=0}^{N}\langle 0|\,\phi(x_N)\cdots\phi(x_{j+1})[-\delta(x_{j+1}^0-x^0)\partial_{x^0}\phi(x)+\delta(x^0-x_j^0)\partial_{x^0}\phi(x)]\phi(x_j)\cdots\phi(x_1)\,|0\rangle\\
&=\sum_{j=1}^{N}\delta(x^0-x_j^0)\,\langle 0|\,\phi(x_N)\cdots\phi(x_{j+1})[\partial_{x_j^0}\phi(x_j^0,\vec{x}),\phi(x_j^0,\vec{x}_j)]\phi(x_{j-1})\cdots\phi(x_1)\,|0\rangle\\
&=\sum_{j=1}^{N}(-i)\delta^{(4)}(x-x_j)\,\langle 0|\,\phi(x_N)\cdots\phi(x_{j+1})\phi(x_{j-1})\cdots\phi(x_1)\,|0\rangle
\end{aligned}$$

Applying $-\nabla_x^2+m^2$ to the n-point function is simple because it commutes with the time-ordering. Relaxing $x_N^0>\cdots>x_1^0$ and combining these results, we have the Schwinger-Dyson equations

$$\begin{aligned}
&(\Box_x+m^2)\,\langle 0|\,\mathcal{T}\{\phi(x)\phi(x_1)\cdots\phi(x_N)\}\,|0\rangle\\
&\quad=\langle 0|\,\mathcal{T}\{(\Box_x+m^2)\phi(x)\phi(x_1)\cdots\phi(x_N)\}\,|0\rangle\\
&\qquad+\sum_{j=1}^{N}(-i)\delta^{(4)}(x-x_j)\,\langle 0|\,\mathcal{T}\{\phi(x_1)\cdots\phi(x_{j-1})\phi(x_{j+1})\cdots\phi(x_N)\}\,|0\rangle\,.
\end{aligned}$$

Proceeding, we will simplify the notation to $\phi_x\equiv\phi(x)$, $D_x\equiv\Box_x+m^2$, $\delta_{xx'}\equiv\delta^{(4)}(x-x')$, and $\langle\phi_1\cdots\phi_N\rangle\equiv\langle 0|\,\mathcal{T}\{\phi(x)\phi(x_1)\cdots\phi(x_N)\}\,|0\rangle$. The Schwinger-Dyson equations are then

$$D_x\langle\phi_x\phi_1\cdots\phi_N\rangle=\langle D_x\phi_x\phi_1\cdots\phi_N\rangle+\sum_{j=1}^{N}(-i)\delta_{xj}\langle\phi_1\cdots\phi_{j-1}\phi_{j+1}\cdots\phi_N\rangle. \tag{9.27}$$

If we want the Schwinger-Dyson equations adapted to the bandlimited field theory, we see that one can simply apply projectors $P_{xx'}:=P_\Lambda(x-x')$ to each component. For the bandlimited version, let us first write $P_{xx'}:=P_\Lambda(x-x')$. To obtain the bandlimited time-ordered n-point function, one applies these bandlimited projectors to each component. Let us write this as:

$$\langle\phi_1\phi_2\cdots\phi_N\rangle_\Lambda:=P_{11'}P_{22'}\cdots P_{NN'}\langle\phi_{1'}\phi_{2'}\cdots\phi_{N'}\rangle, \tag{9.28}$$

leaving sums over repeated indices implicit. Then the left-hand side of the Schwinger-Dyson equation for the bandlimited case is

$$D_xP_{xx'}P_{11'}\cdots P_{NN'}\langle\phi_{x'}\phi_{1'}\cdots\phi_{N'}\rangle=P_{xx'}P_{11'}\cdots P_{NN'}D_{x'}\langle\phi_{x'}\phi_{1'}\cdots\phi_{N'}\rangle \tag{9.29}$$

since the projectors commute with the operator $(\Box_x + m^2)$. Therefore, we see that we can simply apply the Schwinger-Dyson equation to the ordinary n-point function, and project the components onto the bandlimited subspace after. Hence we arrive at

$$D_x\langle\phi_x\phi_1\cdots\phi_N\rangle_\Lambda = \langle D_x\phi_x\phi_1\cdots\phi_N\rangle_\Lambda + \sum_{j=1}^{N}(-i)P_{xj}\langle\phi_1\cdots\phi_{j-1}\phi_{j+1}\cdots\phi_N\rangle_\Lambda. \tag{9.30}$$

Thus are essentially unchanged, with $\delta \mapsto P$ since P is the identity on the bandlimited subspace.

We use these equations to produce an iteration to perturbatively evaluate a time-ordered n-point function (which can be inserted into the LSZ formula) in terms of combinations of free Feynman propagators. These will yield the position-space Feynman rules. The key is to use the Heisenberg equation of motion $D_x\phi_x \equiv (\Box_x + m^2)\phi_x = \mathcal{L}'_{int}(\phi_x)$, and the Feynman propagator $G_{xx'} := G_F(x-x')$ of the free theory, which satisfies $D_xG_{xx'} = -iP_{xx'}$ (or $P \mapsto \delta$ in the non-bandlimited theory).

At zeroth order, with $D_x\phi_x = \mathcal{L}'_{int}(\phi_x) = 0$,

$$\begin{aligned}
\langle\phi_1\phi_2\rangle &= \int dx\ P_{1x}\langle\phi_x\phi_2\rangle \\
&= \int dx\ i(D_xG_{x1})\langle\phi_x\phi_2\rangle \\
&= \int dx\ iG_{x1}D_x\langle\phi_x\phi_2\rangle \\
&= \int dx\ iG_{x1}\left(\langle D_x\phi_x\phi_2\rangle - iP_{x2}\right) \\
&= G_{12}.
\end{aligned}$$

For illustration, let us consider $\mathcal{L}_{int}(\phi) = \frac{g}{3!}\phi^3$. Of course, this theory does not have a ground state, but this will not be apparent in perturbation theory, so we will just use it as

a simple example to illustrate the method. Let us evaluate $\langle\phi_1\phi_2\rangle$ to second order in g.

$$\begin{aligned}
\langle\phi_1\phi_2\rangle &= \int dx\ P_{1x}\langle\phi_x\phi_2\rangle \\
&= \int dx\ iG_{1x}D_x\langle\phi_x\phi_2\rangle \\
&= \int dx\ iG_{1x}\left(\frac{g}{2}\langle\phi_x^2\phi_2\rangle - iP_{x2}\right) \\
&= G_{12} + \frac{g}{2}\int dxdy\ iG_{1x}P_{2y}\langle\phi_x^2\phi_y\rangle \\
&= G_{12} + \frac{g}{2}\int dxdy\ i^2G_{1x}G_{2y}D_y\langle\phi_x^2\phi_y\rangle \\
&= G_{12} + \frac{g}{2}\int dxdy\ i^2G_{1x}G_{2y}\left(\frac{g}{2}\langle\phi_x^2\phi_y^2\rangle - 2iP_{xy}\langle\phi_x\rangle\right).
\end{aligned}$$

Now, to first order

$$\langle\phi_x\rangle = \int dy\ P_{xy}\langle\phi_y\rangle = \int dy\ iG_{xy}D_y\langle\phi_y\rangle = \int dy\ iG_{xy}\frac{g}{2}\langle\phi_y^2\rangle = \frac{ig}{2}\int dy\ G_{xy}G_{yy}, \quad (9.31)$$

and to zeroth order

$$\begin{aligned}
\langle\phi_1\phi_2\phi_3\phi_4\rangle &= \int dx\ iG_{1x}D_x\langle\phi_x\phi_2\phi_3\phi_4\rangle \\
&= \int dx\ iG_{1x}\left(-iP_{x2}\langle\phi_3\phi_4\rangle - iP_{x3}\langle\phi_2\phi_4\rangle - iP_{x4}\langle\phi_2\phi_3\rangle\right) \\
&= G_{12}G_{34} + G_{13}G_{24} + G_{14}G_{23}.
\end{aligned}$$

Then, to second order,

$$\langle\phi_1\phi_2\rangle = G_{12} + (ig)^2\int dxdy\ \left(\tfrac{1}{2}G_{1x}G_{2y}(G_{xy})^2 + \tfrac{1}{4}G_{1x}G_{2y}G_{xx}G_{yy} + \tfrac{1}{2}G_{1x}G_{2x}G_{xy}G_{yy}\right) \quad (9.32)$$

These terms correspond to the Feynman diagrams below. The first will be the one-loop contribution to the ϕ^3 propagator, and the last two are tadpole diagrams that will be cancelled by a linear counterterm in the renormalization procedure.

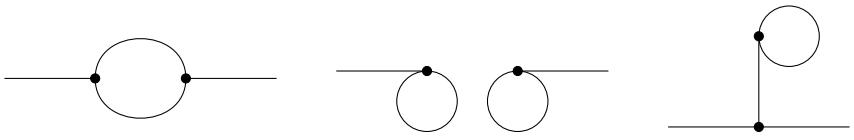

This is identical to the typical derivation of the Feynman rules, but now with bandlimited propagators. Conversion to obtaining momentum space Feynman rules for the S-matrix element after inserting into the LSZ formula proceeds similarly to the usual case as well. Namely, they are:

- Internal lines get factors of the propagator: $\frac{i}{p^2-m^2+i\epsilon}$.
- Vertices get factors of i times the coupling constant.
- Lines connected to external points get factors of 1, since their propagators are cancelled in the LSZ formula.
- 4-momentum is conserved at each vertex.
- Integrate over undetermined 4-momenta.
- Sum over all diagrams with relevant number of incoming and outgoing particles.

The only difference is that, since the Feynman propagators are covariantly bandlimited, integration over internal momenta will be restricted to the region $|k^2| < \Lambda^2$. Therefore, we have carefully justified our intuitive guess in the introduction to this chapter that applying Lorentzian bandlimitation to interacting field theory simply amounts to cutting off the internal momenta of the propagators in the corresponding Feynman graphs.

It is reasonably clear that a path integral approach would yield the same result we have found here, through

$$\langle 0|\,\mathcal{T}\{\phi(x_1)\cdots\phi(x_N)\}\,|0\rangle = \frac{1}{Z[0]}\,\frac{1}{i}\frac{\delta}{\delta J(x_1)}\cdots\frac{1}{i}\frac{\delta}{\delta J(x_N)}\bigg|_{J=0} Z[J] \tag{9.33}$$

with

$$Z[J] = \exp\left[i\int dx\;\mathcal{L}_{int}\left(\frac{1}{i}\frac{\delta}{\delta J(x)}\right)\right]\exp\left[\tfrac{1}{2}\int dx dx' J(x)G_F(x,x')J(x')\right] \tag{9.34}$$

Because of the issues with time-ordering, it seems a Hamiltonian approach would be awkward. The time-ordered n-point functions are given by

$$\langle 0|\,\mathcal{T}\{\phi(x_1)\cdots\phi(x_N)\}\,|0\rangle = \frac{\langle\emptyset|\,\mathcal{T}\{\phi_0(x_1)\cdots\phi_0(x_N)e^{i\int dx\mathcal{L}_{int}(\phi_0(x))}\}\,|\emptyset\rangle}{\langle\emptyset|\,\mathcal{T}\{e^{i\int dx\mathcal{L}_{int}(\phi_0(x))}\}\,|\emptyset\rangle}, \tag{9.35}$$

where $\phi_0(x_i)$ are free fields (i.e., evolved under the free Hamiltonian), and we use $|\emptyset\rangle$ to denote the vacuum of the free theory. One would have to carefully consider the use of time-ordering here, as well as the use of Wick's theorem to rewrite the time-ordered correlation function in terms of two-point Feynman propagators. Presumably one would arrive at the same answer, since we can just project everything after, although we will not check this explicitly here.

Now we want to see how it affects the loop integrals, and whether the cutoff aids in regulating the diagrams.

9.5 Lorentzian-bandlimited loop integrals

Let us now examine some loop integrals, in order to determine how the divergences are affected by the Lorentzian bandlimit. First, we will look at the following integral,

$$\int_{|\ell^2|<\Lambda^2} \frac{d^n\ell}{(2\pi)^n} \frac{1}{\ell^2 - m^2 + i\epsilon}. \tag{9.36}$$

This appears, for example, in the tadpole diagrams of ϕ^3 theory, such as

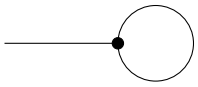

and the one-loop correction to the propagator of ϕ^4 theory.

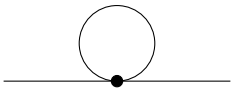

Typically (see, e.g., [98, 118]) one would evaluate this integral by first performing a Wick rotation of $\ell^0 \mapsto i\ell^0$, to get a Euclidean vector $q := (i\ell^0, \vec{\ell})$. That is, we rotate the ℓ^0 contour counterclockwise:

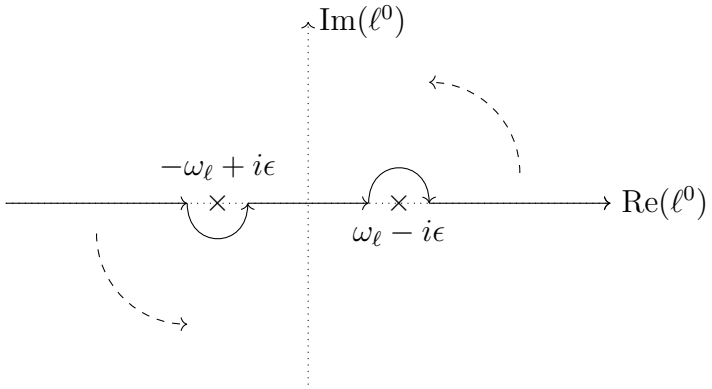

Then one can use dimensional regularization, by analytically continuing the spacetime dimension n. For arbitrary n, we have

$$\int \frac{d^n q}{(2\pi)^n} \frac{-1}{q^2 + m^2} = -\frac{\Gamma(1 - n/2)}{(4\pi)^{n/2} (m^2)^{(1-n/2)}}. \tag{9.37}$$

Since $\Gamma(z)$ diverges for z at nonpositive integers, this integral diverges for even dimensions with $n \geq 2$. If one is particularly interested in $n = 4$, for example, then set $n = 4 - \varepsilon$ and expand in orders of ε to get

$$\begin{aligned} \int \frac{d^n q}{(2\pi)^n} &= -\Gamma(-1 + \varepsilon/2) \frac{m^2}{(4\pi)^2} \left(\frac{4\pi}{m^2} \right)^{\varepsilon/2} \\ &= \frac{m^2}{(4\pi)^2} \left(\frac{2}{\varepsilon} - \gamma + 1 + \ln \left(\frac{4\pi}{m^2} \right) + \mathcal{O}(\varepsilon) \right). \end{aligned}$$

One can then subtract only the piece diverging as $\varepsilon \to 0$ or the entire quantity depending on which theory one is considering as well as the chosen renormalization scheme (on-shell, minimal subtraction, etc.). Generally, an integral of the form,

$$\int \frac{d^n q}{(2\pi)^n} \frac{(q^2)^a}{(q^2 + m^2)^b} = \frac{\Gamma(b - a - n/2)\Gamma(a + n/2)}{(4\pi)^{n/2} \Gamma(b) \Gamma(n/2)} (m^2)^{-(b-a-n/2)}, \tag{9.38}$$

diverges for even $n \geq 2(b - a)$ from $\Gamma(b - a - n/2)$. We see that a simple counting of the powers of q suffices to determine whether the integral will diverge.

Now let us return to the bandlimited version of this integral. Recall that one can decompose the integration as

$$\int \frac{d\vec{\ell}}{(2\pi)^{n-1}} \int_{I(\vec{\ell})} \frac{d\ell^0}{2\pi} \frac{1}{(\ell^0)^2 - \omega_\ell^2 + i\epsilon}, \tag{9.39}$$

where

$$I(\vec{\ell}) := \begin{cases} [-r_+(\vec{\ell}), r_+(\vec{\ell})] & \text{if } \vec{\ell}^2 \leq \Lambda^2 \\ [-r_+(\vec{\ell}), -r_-(\vec{\ell})] \cup [r_-(\vec{\ell}), r_+(\vec{\ell})] & \text{if } \vec{\ell}^2 > \Lambda^2 \end{cases} \tag{9.40}$$

and $r_\pm(\vec{\ell}) := \sqrt{\vec{\ell}^2 \pm \Lambda^2}$. For some $|\vec{\ell}| \leq \Lambda$, the contour in the complex ℓ^0 plane looks like:

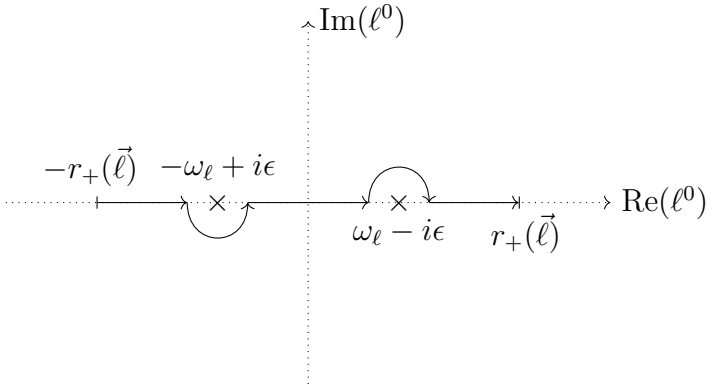

Can this contour be Wick-rotated as before? Of course we can deform the contour (provided we do not pass through the poles), but the endpoints of the contour are fixed on the real axis, so at best we can achieve something like:

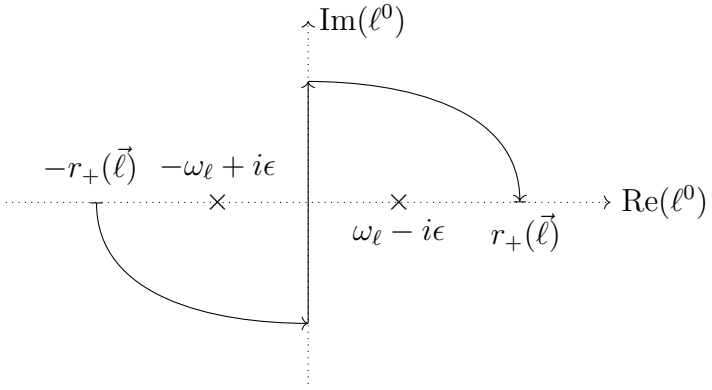

Therefore, as opposed to the ordinary case, the contributions from the arcs do not vanish, and so Wick rotation does not help us to evaluate the integral. Also, this means that the usual tricks for evaluating such integrals, such as dimensional or Pauli-Villars regularization, will no longer work, as they both involve a Wick rotation at some stage.

Let us then attempt a more direct evaluation. Note that the ℓ^0 integral is the same as the one we evaluated in Chapter 3 for the equal-time Fourier-transformed Feynman propagator. There, we saw that

$$i\int_{I(\vec{\ell})}\frac{d\ell^0}{2\pi}\frac{1}{\ell^2-m^2+i\epsilon}=\begin{cases}\frac{1}{2\omega_\ell}+\frac{1}{2\pi i}\frac{1}{\omega_\ell}\ln\left|\frac{r_+(\vec{\ell})+\omega_\ell}{r_+(\vec{\ell})-\omega_\ell}\right|, & \text{if } |\vec{\ell}|\leq\Lambda\\ \frac{1}{2\omega_\ell}+\frac{1}{2\pi i}\frac{1}{\omega_\ell}\left(\ln\left|\frac{r_+(\vec{\ell})+\omega_\ell}{r_+(\vec{\ell})-\omega_\ell}\right|-\ln\left|\frac{\omega_\ell+r_-(\vec{\ell})}{\omega_\ell-r_-(\vec{\ell})}\right|\right), & \text{if } |\vec{\ell}|>\Lambda\end{cases} \tag{9.41}$$

Now we want to integrate this over all $\vec{\ell}$, i.e.,

$$\begin{aligned}&\int_{|\ell^2|<\Lambda^2}\frac{d^n\ell}{(2\pi)^n}\frac{1}{\ell^2-m^2+i\epsilon}\\&\quad=\int_{|\vec{\ell}|\leq\Lambda}\frac{d\vec{\ell}}{(2\pi)^n}\frac{1}{\omega_\ell}\left[-i\pi-\ln\left|\frac{r_+(\vec{\ell})+\omega_\ell}{r_+(\vec{\ell})-\omega_\ell}\right|\right]\\&\qquad+\int_{|\vec{\ell}|>\Lambda}\frac{d\vec{\ell}}{(2\pi)^n}\frac{1}{\omega_\ell}\left[-i\pi-\left(\ln\left|\frac{r_+(\vec{\ell})+\omega_\ell}{r_+(\vec{\ell})-\omega_\ell}\right|-\ln\left|\frac{\omega_\ell+r_-(\vec{\ell})}{\omega_\ell-r_-(\vec{\ell})}\right|\right)\right].\end{aligned}$$

The first integral is finite, due to the ultraviolet cutoff $|\vec{\ell}|<\Lambda$. Therefore, in order to determine whether the full integral converges, let us focus on the second term. Specifically, we will examine the behaviour of the integrand for large $|\vec{\ell}|$ by expanding in $\Lambda/|\vec{\ell}|$. We find this gives

$$\begin{aligned}&\int_{|\vec{\ell}|>\Lambda}\frac{d\vec{\ell}}{(2\pi)^n}\frac{1}{\omega_\ell}\left[-i\pi-\left(\ln\left|\frac{r_+(\vec{\ell})+\omega_\ell}{r_+(\vec{\ell})-\omega_\ell}\right|-\ln\left|\frac{\omega_\ell+r_-(\vec{\ell})}{\omega_\ell-r_-(\vec{\ell})}\right|\right)\right]\\&\quad=\frac{\Omega_{n-1}}{(2\pi)^n}\int_\Lambda^\infty d|\vec{\ell}|\frac{|\vec{\ell}|^{n-2}}{\omega_\ell}\left[-i\pi+\ln\left(\frac{1-m^2/\Lambda^2}{1+m^2/\Lambda^2}\right)-\frac{\Lambda^2}{|\vec{\ell}|^2}+\frac{m^2}{4\Lambda^2}\frac{\Lambda^4}{|\vec{\ell}|^4}+\mathcal{O}\left(\frac{\Lambda^6}{|\vec{\ell}|^6}\right)\right].\end{aligned}$$

where $\Omega_{n-1}=2\pi^{n/2}/\Gamma(n/2)$ is the surface area of the unit $(n-1)$-sphere, and recall $\omega_\ell:=\sqrt{\vec{\ell}^2+m^2}$. The first two terms in this expansion diverge for $n\geq 2$, similar to the case without the bandlimit. Hence, we see that the Lorentzian bandlimit does not help to tame the divergences in this integral.

Does the power counting argument still hold? For example, in the ordinary case we would find that the integral

$$\int\frac{d^n\ell}{(2\pi)^n}\frac{1}{(\ell^2-m^2+i\epsilon)^2} \tag{9.42}$$

diverges only for $n \geq 4$. Instead of evaluating a new integral, we can simply use the standard trick,

$$\frac{\partial}{\partial m^2}\int_{|\ell^2|<\Lambda}\frac{d^n\ell}{(2\pi)^n}\frac{1}{\ell^2-m^2+i\epsilon}=\int_{|\ell^2|<\Lambda}\frac{d^n\ell}{(2\pi)^n}\frac{1}{(\ell^2-m^2+i\epsilon)^2}, \tag{9.43}$$

and apply it to the above expansion. We find this gives

$$\frac{\Omega_{n-1}}{(2\pi)^n}\int_\Lambda^\infty d|\vec{\ell}|\,|\vec{\ell}|^{n-2}\left\{\frac{-1}{2\omega_\ell^3}\left[-i\pi+\ln\left(\frac{1-m^2/\Lambda^2}{1+m^2/\Lambda^2}\right)-\frac{\Lambda^2}{|\vec{\ell}|^2}+\frac{m^2}{4\Lambda^2}\frac{\Lambda^4}{|\vec{\ell}|^4}+\mathcal{O}\left(\frac{\Lambda^6}{|\vec{\ell}|^6}\right)\right]\right.$$
$$\left.+\frac{1}{\omega_\ell}\left[\frac{-2}{\Lambda^2}\frac{1}{1-m^4/\Lambda^4}+\frac{1}{4\Lambda^2}\frac{\Lambda^4}{|\vec{\ell}|^4}+\mathcal{O}\left(\frac{\Lambda^6}{|\vec{\ell}|^6}\right)\right]\right\}.$$

The convergence of the first set of terms is improved, occuring for $n \geq 4$. However, the first of the second set of terms still diverges for $n \geq 2$. This term came from the logarithm which is only a function of m^2/Λ^2. Indeed, we see that taking even higher derivatives of m^2 will not improve the convergence of this integral, since we will always have a term of the form $\omega_\ell^{-1}f(m^2/\Lambda^2)$, which produces another term of this form (plus one with better convergence) after applying $\partial/\partial m^2$.

We see then that the simple power-counting argument no longer holds for these integrals that are Lorentzian-bandlimited. This is counterintuitive, since then it would seem that in the ordinary (non-bandlimited) field theory, the far off-shell loop momenta are actually helping in the convergence of some of these integrals.

How about other loop integrals? The next that one would naturally consider would be:

$$\int_{|\ell^2|,|(\ell-k)^2|<\Lambda^2}\frac{d\ell}{(2\pi)^n}\frac{1}{\ell^2-m^2+i\epsilon}\frac{1}{(\ell-k)^2-m^2+i\epsilon} \tag{9.44}$$

This appears, for example, in the one-loop correction to the ϕ^3 propagator,

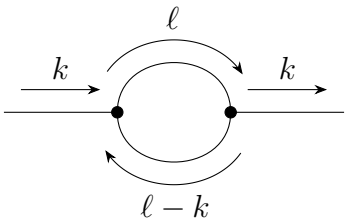

as well as the one-loop correction to the ϕ^4 4-vertex.

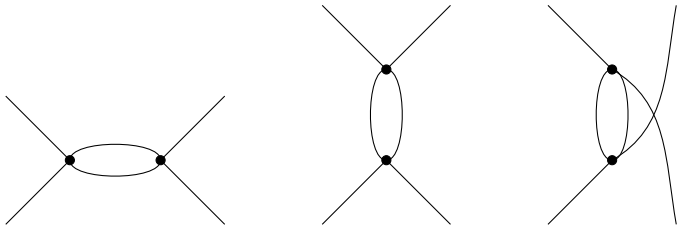

We will only give an overview of this calculation, as it becomes quite tedious. For later convenience, we will shift the integration variable by $k/2$, then

$$\int_{|(\ell+k/2)^2|,|(\ell-k/2)^2|<\Lambda^2} \frac{d\ell}{(2\pi)^n} \frac{1}{(\ell+k/2)^2 - m^2 + i\epsilon} \frac{1}{(\ell-k/2)^2 - m^2 + i\epsilon}. \tag{9.45}$$

Performing a calculation of this integral is very difficult in general, since it requires integrating over the intersection of the regions $|(\ell + k/2)^2| < \Lambda^2$ and $|(\ell - k/2)^2| < \Lambda^2$, for some arbitrary 4-momentum k. Recall that each of these are regions bounded by four hyperbolas. One can gain a little traction by assuming each component of k^μ is much smaller than Λ. This is reasonable for considering the one-loop correction to a $\phi\phi \to \phi\phi$ scattering process in either the ϕ^3 or ϕ^4 theories, where k in the above diagrams would consist of sums or differences of the momenta of the external particles. In this case, these two regions are slightly shifted from one another. In fact, the tails of the hyperbolas can intersect one another, yielding an ultraviolet cutoff for $|\vec{\ell}|$.

Calculating all the points of intersection of the boundaries of these two regions is tedious, but one can approximate where the ultraviolet cutoff occurs by considering the intersection of the boundaries $\ell^0 = -\frac{k^0}{2} + r_\pm(\vec{\ell} + \vec{k}/2)$ and $\ell^0 = \frac{k^0}{2} + r_\mp(\vec{\ell} - \vec{k}/2)$. The cutoff occurs in the tails of the hyperbolas, i.e., for $|\vec{\ell}| \gg \Lambda \gg |\vec{k}|$, so we will neglect any occurrences of $|\vec{k}|/|\vec{\ell}|$. We find that the cutoff occurs roughly at

$$|\vec{\ell}| = \frac{\Lambda^2}{|k^0 - |\vec{k}| \cos\theta|}, \tag{9.46}$$

where θ is the angle between $\vec{\ell}$ and $\vec{k}$. This is finite provided $k^0 \neq |\vec{k}| \cos\theta$. If k is timelike, then $k^0 \neq |\vec{k}| \cos\theta$ for all θ, and the loop integral will be finite. If k is spacelike, it is possible that this vanishes, and hence the ultraviolet cutoff for $|\vec{\ell}|$ disappears. Since we are integrating over θ in the loop integral, it is possible that this singularity is integrable, so let us try to evaluate it.

Let us focus on the region $\ell^0 \in [r_-(\vec{\ell}), r_+(\vec{\ell})]$ and $|\vec{\ell}| > \Lambda$. We find that

$$\begin{aligned}
&\int_{|\vec{\ell}|>\Lambda} \frac{d\vec{\ell}}{(2\pi)^n} \int_{r_-(\vec{\ell})}^{r_+(\vec{\ell})} d\ell^0 \frac{1}{(\ell + k/2)^2 - m^2 + i\epsilon} \frac{1}{(\ell - k/2)^2 - m^2 + i\epsilon} \\
&= \int_{\Lambda}^{(\Lambda^2 - m^2)/2|k^0 - |\vec{k}|\cos\theta|} \frac{d\vec{\ell}}{(2\pi)^n} \left[-i\pi F(\omega_+, \omega_-) + i\pi F(-\omega_-, \omega_+) \right] \\
&+ \int_{\Lambda}^{\Lambda^2/|k^0 - |\vec{k}|\cos\theta} \frac{d\vec{\ell}}{(2\pi)^n} \left\{ F(\omega_+, \omega_-) \ln \left| \frac{r_+(\vec{\ell}) + k^0/2 - \omega_+}{r_-(\vec{\ell}) + k^0/2 - \omega_+} \right| \right. \\
&- F(-\omega_-, \omega_+) \ln \left| \frac{r_+(\vec{\ell}) - k^0/2 - \omega_-}{r_-(\vec{\ell}) - k^0/2 - \omega_-} \right| + F(-\omega_+, \omega_-) \ln \left| \frac{r_+(\vec{\ell}) + k^0/2 + \omega_+}{r_-(\vec{\ell}) + k^0/2 + \omega_+} \right| \\
&\left. - F(\omega_-, \omega_+) \ln \left| \frac{r_+(\vec{\ell}) - k^0/2 + \omega_-}{r_-(\vec{\ell}) - k^0/2 + \omega_-} \right| \right\},
\end{aligned}$$

where $\omega_\pm := \sqrt{(\vec{\ell} \pm \vec{k}/2)^2 + m^2}$, and

$$F(\omega_+, \omega_-) := \frac{1}{2\omega_+} \frac{1}{(k^0 - \omega_+)^2 - \omega_-^2}. \tag{9.47}$$

In $n = 4$ dimensions, the first integral gives a finite value

$$\begin{aligned}
&\int_{\Lambda}^{(\Lambda^2 - m^2)/2|k^0 - |\vec{k}|\cos\theta|} \frac{d\vec{\ell}}{(2\pi)^n} \left[-i\pi F(\omega_+, \omega_-) + i\pi F(-\omega_-, \omega_+) \right] \\
&= \frac{i}{32\pi^2} \left(2 + \ln \left| \frac{(\Lambda^2 - m^2)^2}{4\Lambda^2 |k^2|} \right| + \frac{k^0}{|\vec{k}|} \ln \left| \frac{k^0 - |\vec{k}|}{k^0 + |\vec{k}|} \right| \right).
\end{aligned}$$

However, we find the second integral, to leading order, behaves as

$$\begin{aligned}
&\sim \int_{\Lambda}^{\Lambda^2/|k^0 - |\vec{k}|\cos\theta|} \frac{d^3\vec{\ell}}{(2\pi)^4} \frac{-\Lambda^2}{|\vec{\ell}|^3 (k^0 - |\vec{k}|\cos\theta)^2} \\
&= \frac{-\Lambda^2}{(2\pi)^3} \int_{-1}^{1} d\cos\theta \frac{1}{(k^0 - |\vec{k}|\cos\theta)^2} \ln \left| \frac{\Lambda}{k^0 - |\vec{k}|\cos\theta} \right| \\
&\to \infty \qquad \text{if } k \text{ spacelike.}
\end{aligned}$$

So we find the peculiar situation where this loop integral, for $|k^\mu| \ll \Lambda$, is finite if k is timelike, and diverges if k is spacelike. If this were included in the one-loop correction to the ϕ^4 4-vertex, for a $\phi\phi \to \phi\phi$ scattering process, we would find that the one-loop correction to the s-channel requires only a finite renormalization, whereas the t- and u-channels require an infinite renormalization. However, because of the issues with Wick rotation of these Lorentzian-bandlimited integrals, it is not apparent how this renormalization should be done, unless one introduces a simple non-covariant ultraviolet cutoff for $\vec{\ell}$. We leave such an investigation as future work.

There are also many other questions regarding loop integrals with the Lorentzian bandlimit. For example, the next loop integral one would consider after those we saw here would be the one-loop integral with three propagators, as occuring in the correction to the ϕ^3 3-vertex. This would involve the intersection of three hyperbolic regions, which seems would be even more tedious. Furthermore, in order to use these corrections in other scenarios, one should consider how they should be calculated for arbitrary k, not only $|k^\mu| \ll \Lambda$.

Chapter 10

Conclusion

In this thesis, we have examined various aspects of the application of Euclidean- and Lorentzian-bandlimitation to quantum field theory. For Euclidean-bandlimited fields, we investigated a notion of subsystem localization and developed some tools to help study this idea further. For Lorentzian-bandlimited fields, we developed some understanding of which quantities of these field theories are modified from the usual case and which are not.

We have seen that the entanglement in quantum fields is not affected by the Lorentzian bandlimit, and therefore cannot be used to address some of the motivations stated in the introduction. It would be interesting to flip this problem to get an idea of what kinds of conditions one would have to impose in order to regulate the entanglement entropy while preserving some aspects of the underlying spacetime structure. For example, one could simply assume that the formula from Gaussian state quantum mechanics that one uses to calculate the entropy holds, and determine conditions for the two-point functions so that the symplectic spectrum of the covariance matrix yields a finite entropy. Perhaps there is another kind of restriction of the ordinary function space which would produce this.

There are also many further aspects of interacting theories with a Lorentzian bandlimit which should be studied further, some of which we mentioned in the text. One should especially work towards finding low-energy manifestations of the Lorentzian bandlimit.

It would also be interesting to consider non-perturbative effects of the Lorentzian bandlimit in interacting theories. In this work, we gave intuitive interpretations of the Lorentzian bandlimit in terms of either cutting out modes which are highly off-shell, or as a modification of the time-ordering operator. This led us to consider interacting theories, since these are concepts which occur in perturbation theory. However, the discovery of

non-perturbative consequences of the bandlimit could provide a different perspective on the effect it has on the structure of QFT.

We also left many open questions in the text in regards to developing our notion of subsystem localization for Euclidean-bandlimited fields. Even in the case of a flat geometry, the variance of the distributions we considered seems to have some properties which do not match our intuition from the visualizations. Also, clearly more work needs to be done to further proceed with the calculation for nontrivial geometry. Some aspects of the calculation may be simpler in cases of a non-compact manifold, however the point was that we did not have a good notion of variance for the heavy-tailed distributions one obtains in these cases. Perhaps there is some other way of dealing with this issue.

It would also be interesting to perform the calculation to second order in the perturbation. For geometries which are Ricci-flat and only have nontrivial Weyl curvature, the effects of the geometry on the local sample density would only appear at this order.

References

[1] V. A. Acciari et al. Bounds on lorentz invariance violation from magic observation of grb 190114c. *Phys. Rev. Lett.*, 125:021301, Jul 2020.

[2] N I Akhiezer and I M Glazman. *Theory of Linear Operators in Hilbert Space*. Dover Publications, Inc., 1993.

[3] A. Albert et al. Constraints on lorentz invariance violation from hawc observations of gamma rays above 100 tev. *Phys. Rev. Lett.*, 124:131101, Mar 2020.

[4] Ahmed Almheiri, Netta Engelhardt, Donald Marolf, and Henry Maxfield. The entropy of bulk quantum fields and the entanglement wedge of an evaporating black hole. *Journal of High Energy Physics*, 2019(12):63, 2019.

[5] Ahmed Almheiri, Thomas Hartman, Juan Maldacena, Edgar Shaghoulian, and Amirhossein Tajdini. The entropy of hawking radiation. *arXiv preprint arXiv:2006.06872*, 2020.

[6] Ahmed Almheiri, Donald Marolf, Joseph Polchinski, and James Sully. Black holes: complementarity or firewalls? *Journal of High Energy Physics*, 2013(2):62, 2013.

[7] G Amelino-Camelia. Doubly special relativity. *Nature*, 418:34–35, 2002.

[8] Giovanni Amelino-Camelia, Laurent Freidel, Jerzy Kowalski-Glikman, and Lee Smolin. Principle of relative locality. *Physical Review D*, 84(8):084010, 2011.

[9] Giovanni Amelino-Camelia, Laurent Freidel, Jerzy Kowalski-Glikman, and Lee Smolin. Relative locality and the soccer ball problem. *Physical Review D*, 84(8):087702, 2011.

[10] Siavash Aslanbeigi, Mehdi Saravani, and Rafael D Sorkin. Generalized causal set d'alembertians. *J. High Energy Phys.*, 2014(6):24, 2014.

[11] DG Barci, LE Oxman, and M Rocca. Canonical quantization of nonlocal field equations. *International Journal of Modern Physics A*, 11(12):2111–2126, 1996.

[12] Jacob D Bekenstein. Black holes and entropy. *Physical Review D*, 7(8):2333, 1973.

[13] Alessio Belenchia, Dionigi MT Benincasa, Marco Letizia, and Stefano Liberati. On the entanglement entropy of quantum fields in causal sets. *Classical and Quantum Gravity*, 35(7):074002, 2018.

[14] Alessio Belenchia, Dionigi MT Benincasa, and Stefano Liberati. Nonlocal scalar quantum field theory from causal sets. *J. High Energy Phys.*, 2015(3):36, 2015.

[15] John J Benedetto and Paulo J S G Ferreira. *Modern sampling theory: mathematics and applications*. Birkhäuser, 2001.

[16] Rabi Bhattacharya and Vic Patrangenaru. Large sample theory of intrinsic and extrinsic sample means on manifolds. i. *The Annals of Statistics*, 31(1):1–29, 2003.

[17] Rabi Bhattacharya and Vic Patrangenaru. Large sample theory of intrinsic and extrinsic sample means on manifolds—ii. *Annals of Statistics*, 33(3):1225–1259, 2005.

[18] Eugenio Bianchi and Robert C Myers. On the architecture of spacetime geometry. *Classical and Quantum Gravity*, 31(21):214002, 2014.

[19] CG Bollini and JJ Giambiagi. Lagrangian procedures for higher order field equations. *Revista Brasileira de Fisica*, 17(1):14–30, 1987.

[20] Luca Bombelli, Joe Henson, and Rafael D Sorkin. Discreteness without symmetry breaking: a theorem. *Modern Physics Letters A*, 24(32):2579–2587, 2009.

[21] Luca Bombelli, Rabinder K. Koul, Joohan Lee, and Rafael D. Sorkin. Quantum source of entropy for black holes. *Phys. Rev. D*, 34(2):373–383, 1986.

[22] Luca Bombelli, Joohan Lee, David Meyer, and Rafael D Sorkin. Space-time as a causal set. *Physical review letters*, 59(5):521, 1987.

[23] Fabian Brau. Minimal length uncertainty relation and the hydrogen atom. *J. Phys. A*, 32(44):7691, 1999.

[24] Matvei Bronstein. Republication of: Quantum theory of weak gravitational fields. *Gen. Rel. and Grav.*, 44(1):267–283, 2012.

[25] Matvei P Bronstein. Quantentheorie schwacher gravitationsfelder. *Phys. Z. Sowjetunion*, 9(2–3):140–157, 1936. (Republished in [24]).

[26] ChunJun Cao, Sean M Carroll, and Spyridon Michalakis. Space from hilbert space: recovering geometry from bulk entanglement. *Physical Review D*, 95(2):024031, 2017.

[27] Aidan Chatwin-Davies, Achim Kempf, and Robert TW Martin. Natural covariant planck scale cutoffs and the cosmic microwave background spectrum. *Physical Review Letters*, 119(3):031301, 2017.

[28] Isaac Chavel. *Eigenvalues in Riemannian geometry*. Academic press, 1984.

[29] Alain Connes. *Noncommutative geometry*. Academic Press, 1994.

[30] Saurya Das and Elias C Vagenas. Universality of quantum gravity corrections. *Phys. Rev. Lett.*, 101(22):221301, 2008.

[31] Stanley Deser. General relativity and the divergence problem in quantum field theory. *Reviews of Modern Physics*, 29(3):417, 1957.

[32] Bryce S DeWitt. Gravity: a universal regulator? *Physical Review Letters*, 13(3):114, 1964.

[33] RLPG Do Amaral and EC Marino. Canonical quantization of theories containing fractional powers of the d'alembertian operator. *Journal of Physics A: Mathematical and General*, 25(19):5183, 1992.

[34] DA Eliezer and RP Woodard. The problem of nonlocality in string theory. *Nuclear Physics B*, 325(2):389–469, 1989.

[35] James MG Fell. The dual spaces of c*-algebras. *Transactions of the American Mathematical Society*, 94(3):365–403, 1960.

[36] William Feller. *An Introduction to Probability Theory and Its Applications*, volume 2. John Wiley & Sons, Inc., 1971.

[37] Christopher J Fewster and Kasia Rejzner. Algebraic quantum field theory. In *Progress and Visions in Quantum Theory in View of Gravity*, pages 1–61. Springer, 2020.

[38] Maurice Fréchet. Les éléments aléatoires de nature quelconque dans un espace distancié. In *Annales de l'institut Henri Poincaré*, volume 10, pages 215–310, 1948.

[39] Stephen A Fulling. *Aspects of quantum field theory in curved spacetime*. Cambridge university press, 1989.

[40] Dmitri Fursaev and Dmitri Vassilevich. *Operators, geometry and quanta: methods of spectral geometry in quantum field theory*. Springer, 2011.

[41] Luis J Garay. Quantum gravity and minimum length. *International Journal of Modern Physics A*, 10(02):145–165, 1995.

[42] Peter B Gilkey. *Asymptotic formulae in spectral geometry*. CRC press, 2003.

[43] Peter B Gilkey et al. The spectral geometry of a riemannian manifold. *Journal of Differential Geometry*, 10(4):601–618, 1975.

[44] Florian Girelli and Etera R Livine. Physics of deformed special relativity: relativity principle revisited. *Brazilian journal of physics*, 35(2B):432–438, 2005.

[45] Rudolf Haag. *Local quantum physics: Fields, particles, algebras*. Springer, 1992.

[46] Rudolf Haag and Daniel Kastler. An algebraic approach to quantum field theory. *Journal of Mathematical Physics*, 5(7):848–861, 1964.

[47] Qing Han and Jia-Xing Hong. *Isometric Embedding of Riemannian Manifolds in Euclidean Spaces*, volume 130 of *Mathematical Surveys and Monographs*. American Mathematical Society, 2006.

[48] Stephen W Hawking. Particle creation by black holes. *Communications in mathematical physics*, 43(3):199–220, 1975.

[49] Stephen W Hawking. Quantum gravity and path integrals. *Physical Review D*, 18(6):1747, 1978.

[50] Harrie Hendriks and Zinoviy Landsman. Asymptotic behavior of sample mean location for manifolds. *Statistics & probability letters*, 26(2):169–178, 1996.

[51] Harrie Hendriks and Zinoviy Landsman. Mean location and sample mean location on manifolds: asymptotics, tests, confidence regions. *Journal of Multivariate Analysis*, 67(2):227–243, 1998.

[52] Philipp Andres Höhn. Reflections on the information paradigm in quantum and gravitational physics. In *J. Phys. Conf. Ser*, volume 880, page 012014, 2017.

[53] Christoph Holzhey, Finn Larsen, and Frank Wilczek. Geometric and renormalized entropy in conformal field theory. *Nuclear Physics B*, 424(3):443–467, 1994.

[54] Sabine Hossenfelder. Minimal length scale scenarios for quantum gravity. *Liv. Rev. Rel.*, 16(1):2, 2013.

[55] Sabine Hossenfelder. The soccer-ball problem. *SIGMA*, 10(074):8, 2014.

[56] Sabine Hossenfelder, Marcus Bleicher, Stefan Hofmann, Jörg Ruppert, Stefan Scherer, and Horst Stöcker. Signatures in the planck regime. *Phys. Lett. B*, 575(1-2):85–99, 2003.

[57] Stephan Huckemann and Thomas Hotz. Nonparametric statistics on manifolds and beyond. In *Rabi N. Bhattacharya*, pages 599–609. Springer, 2016.

[58] C J Isham and N Linden. Continuous histories and the history group in generalized quantum theory. *Journal of Mathematical Physics*, 36(10):5392–5408, 1995.

[59] Christopher J Isham, Noah Linden, Konstantina Savvidou, and Steven Schreckenberg. Continuous time and consistent histories. *Journal of Mathematical Physics*, 39(4):1818–1834, 1998.

[60] Ted Jacobson. Thermodynamics of spacetime: The einstein equation of state. *Phys. Rev. Lett.*, 75:1260–1263, Aug 1995.

[61] Ted Jacobson. Entanglement equilibrium and the einstein equation. *Phys. Rev. Lett.*, 116:201101, May 2016.

[62] Ted Jacobson and Aron C Wall. Black hole thermodynamics and lorentz symmetry. *Foundations of Physics*, 40(8):1076–1080, 2010.

[63] S Rao Jammalamadaka and A SenGupta. *Topics in Circular Statistics*, volume 5 of *Multivariate Analysis*. World Scientific, 2001.

[64] Abdul J Jerri. The shannon sampling theorem—its various extensions and applications: A tutorial review. *Proceedings of the IEEE*, 65(11):1565–1596, 1977.

[65] Achim Kempf. Uncertainty relation in quantum mechanics with quantum group symmetry. *Journal of Mathematical Physics*, 35(9):4483–4496, 1994.

[66] Achim Kempf. Non-pointlike particles in harmonic oscillators. *Journal of Physics A: Mathematical and General*, 30(6):2093, 1997.

[67] Achim Kempf. Black holes, bandwidths and beethoven. *Journal of Mathematical Physics*, 41(4):2360–2374, 2000.

[68] Achim Kempf. Fields over unsharp coordinates. *Physical review letters*, 85(14):2873, 2000.

[69] Achim Kempf. Covariant information-density cutoff in curved space-time. *Physical review letters*, 92(22):221301, 2004.

[70] Achim Kempf. Fields with finite information density. *Physical Review D*, 69(12):124014, 2004.

[71] Achim Kempf. Information-theoretic natural ultraviolet cutoff for spacetime. *Physical review letters*, 103(23):231301, 2009.

[72] Achim Kempf, Aidan Chatwin-Davies, and Robert TW Martin. A fully covariant information-theoretic ultraviolet cutoff for scalar fields in expanding friedmann robertson walker spacetimes. *Journal of Mathematical Physics*, 54(2):022301, 2013.

[73] Achim Kempf, Gianpiero Mangano, and Robert B Mann. Hilbert space representation of the minimal length uncertainty relation. *Physical Review D*, 52(2):1108, 1995.

[74] Achim Kempf and Robert Martin. Information theory, spectral geometry, and quantum gravity. *Physical review letters*, 100(2):021304, 2008.

[75] John R Klauder. Exponential hilbert space: Fock space revisited. *Journal of Mathematical Physics*, 11(2):609–630, 1970.

[76] Shoshichi Kobayashi and Katsumi Nomizu. *Foundations of Differential Geometry*, volume 2. John Wiley & Sons, Inc., 1969.

[77] V. Alan Kostelecký and Neil Russell. Data tables for lorentz and *cpt* violation. *Rev. Mod. Phys.*, 83:11–31, Mar 2011.

[78] E Kreyszig. *Introductory Functional Analysis with Applications*. John Wiley & Sons, 1989.

[79] HJ Landau. Necessary density conditions for sampling and interpolation of certain entire functions. *Acta Math.*, 117(1):37–52, 1967.

[80] John M Lee. *Introduction to Smooth Manifolds*, volume 218 of *Graduate Texts in Mathematics*. Springer, 2002.

[81] J Madore. An introduction to non-commutative differential geometry. *London Mathematical Society Lecture Note Series*, 206, 1995.

[82] Joao Magueijo and Lee Smolin. Lorentz invariance with an invariant energy scale. *Physical Review Letters*, 88(19):190403, 2002.

[83] Shahn Majid. Meaning of noncommutative geometry and the planck-scale quantum group. In *Towards Quantum Gravity*, pages 227–276. Springer, 2000.

[84] K V Mardia. *Statistics of Directional Data*. Academic Press Inc., London, 1972.

[85] Kanti V Mardia and Peter E Jupp. *Directional Statistics*. Probability and Statistics. John Wiley & Sons, Ltd., 1999.

[86] R Martin and A Kempf. Approximation of bandlimited functions on a non-compact manifold by bandlimited functions on compact submanifolds. *Sampling Theory in Signal and Image Processing*, 7(3):281–293, 2008.

[87] Robert Martin. *Bandlimited functions, curved manifolds, and self-adjoint extensions of symmetric operators*. PhD thesis, University of Waterloo, 2008.

[88] David Mattingly. Modern tests of lorentz invariance. *Living Reviews in relativity*, 8(1):5, 2005.

[89] C Alden Mead. Possible connection between gravitation and fundamental length. *Phys. Rev.*, 135(3B):B849, 1964.

[90] Albert Messiah. *Quantum mechanics: volume II*. North-Holland Publishing Company Amsterdam, 1962.

[91] Viatcheslav Mukhanov and Sergei Winitzki. *Introduction to quantum effects in gravity*. Cambridge university press, 2007.

[92] Dmitry Nesterov and Sergey N Solodukhin. Gravitational effective action and entanglement entropy in uv modified theories with and without lorentz symmetry. *Nucl. Phys. B*, 842(2):141–171, 2011.

[93] Harry Nyquist. Certain topics in telegraph transmission theory. *Trans. IEEE*, 47(2):617–644, 1928.

[94] A Pais and GE Uhlenbeck. On field theories with non-localized action. *Physical Review*, 79(1):145, 1950.

[95] Mikhail Panine and Achim Kempf. A convexity result in the spectral geometry of conformally equivalent metrics on surfaces. *International Journal of Geometric Methods in Modern Physics*, 14(11):1750157, 2017.

[96] Maria Papageorgiou and Jason Pye. Impact of relativity on particle localizability and ground state entanglement. *Journal of Physics A: Mathematical and Theoretical*, 52(37):375304, 2019.

[97] Geoffrey Penington. Entanglement wedge reconstruction and the information paradox. *arXiv preprint arXiv:1905.08255*, 2019.

[98] Michael E Peskin and Daniel V Schroeder. *Introduction to Quantum Field Theory*. Perseus Books Publishing, 1995.

[99] Igor Pikovski, Michael R Vanner, Markus Aspelmeyer, MS Kim, and Časlav Brukner. Probing planck-scale physics with quantum optics. *Nature Phys.*, 8(5):393, 2012.

[100] Jason Pye. Localising information in bandlimited quantum field theory. Master's thesis, University of Waterloo, 2015.

[101] Jason Pye. Covariant bandlimitation from generalized uncertainty principles. In *Journal of Physics: Conference Series*, volume 1275, page 012025. IOP Publishing, 2019.

[102] Jason Pye, William Donnelly, and Achim Kempf. Locality and entanglement in bandlimited quantum field theory. *Physical Review D*, 92(10):105022, 2015.

[103] P L Robinson. The sphere is not flat. *The American Mathematical Monthly*, 113(2):171–173, 2006.

[104] Walter Rudin. *Real and Complex Analysis*. McGraw-Hill, 3 edition, 1987.

[105] Laura Ruetsche. *Interpreting quantum theories*. Oxford University Press, 2011.

[106] Fabio Scardigli, Massimo Blasone, Gaetano Luciano, and Roberto Casadio. Modified unruh effect from generalized uncertainty principle. *Eur. Phys. J. C*, 78(9):728, 2018.

[107] Fabio Scardigli and Roberto Casadio. Gravitational tests of the generalized uncertainty principle. *Eur. Phys. J. C*, 75(9):425, 2015.

[108] Matthew D Schwartz. *Quantum field theory and the standard model*. Cambridge University Press, 2014.

[109] Alessio Serafini. *Quantum continuous variables: a primer of theoretical methods*. CRC press, 2017.

[110] C. E. Shannon. Communication in the presence of noise. *Proc. IRE*, 37(1):10–21, 1949.

[111] Claude Elwood Shannon. A mathematical theory of communication. *Bell Sys. Tech. J.*, 27(3):379–423, 1948.

[112] Jonathan Z Simon. Higher-derivative lagrangians, nonlocality, problems, and solutions. *Physical Review D*, 41(12):3720, 1990.

[113] Hartland S Snyder. Quantized space-time. *Physical Review*, 71(1):38, 1947.

[114] Sergey N Solodukhin. Entanglement entropy of black holes. *Liv. Rev. Rel.*, 14(1):8, 2011.

[115] Rafael D Sorkin. On the entropy of the vacuum outside a horizon. In *Tenth International Conference on General Relativity and Gravitation (held Padova, 4-9 July, 1983), Contributed Papers*, volume 2, pages 734–736, 1983.

[116] Michael Spivak. *A Comprehensive Introduction to Differential Geometry*, volume 5. Publish or Perish, Inc., Berkeley, 2 edition, 1979.

[117] Mark Srednicki. Entropy and area. *Phys. Rev. Lett.*, 71:666–669, 1993.

[118] Mark Srednicki. *Quantum field theory*. Cambridge University Press, 2007.

[119] R F Streater. Current commutation relations, continuous tensor products and infinitely divisible group representations. In R Jost, editor, *Proceedings of the International School of Physics E. Fermi, Local Quantum Theory*, pages 247–263, 1969.

[120] Raymond F Streater and Arthur S Wightman. *PCT, spin and statistics, and all that*. W. A. Benjamin, Inc., 1964.

[121] Leonard Susskind and James Lindesay. *An introduction to black holes, information and the string theory revolution: The holographic universe*. World Scientific, 2005.

[122] Robin Ticciati. *Quantum field theory for mathematicians*, volume 72. Cambridge University Press, 1999.

[123] Vasil Todorinov, Pasquale Bosso, and Saurya Das. Relativistic generalized uncertainty principle. *Annals of Physics*, 405:92–100, 2019.

[124] William G Unruh. Notes on black-hole evaporation. *Phys. Rev. D*, 14(4):870, 1976.

[125] Mark Van Raamsdonk. Building up spacetime with quantum entanglement. *General Relativity and Gravitation*, 42(10):2323–2329, 2010.

[126] John von Neumann. On infinite direct products. *Compositio mathematica*, 6:1–77, 1939.

[127] Robert M Wald. *Quantum field theory in curved spacetime and black hole thermodynamics*. University of Chicago Press, 1994.

[128] E Witten. Reflections on the fate of spacetime. *Physics Today*, 49(4):24–30, 1996.

[129] Ahmed I Zayed. *Advances in Shannon's Sampling Theory*. CRC Press, 1993.

[130] Herbert Ziezold. On expected figures and a strong law of large numbers for random elements in quasi-metric spaces. In *Transactions of the Seventh Prague Conference on Information Theory, Statistical Decision Functions, Random Processes and of the 1974 European Meeting of Statisticians*, pages 591–602. Springer, 1977.